PHARMACOKINETICS-PHARMACODYNAMICS DRIVEN APPROACH FOR LEAD OPTIMIZATION IN ANTI-MYCOBACTERIAL AND ANTI-MALARIAL DRUG DISCOVERY

SURESH BANGALORE LAKSHMINARAYANA

(M.Pharm., Rajiv Gandhi University of Health Sciences, Karnataka)

A THESIS SUBMITTED

FOR THE DEGREE OF DOCTOR OF PHILOSOPHY

DEPARTMENT OF PHARMACY

NATIONAL UNIVERSITY OF SINGAPORE

2015

DECLARATION

I hereby declare that the thesis is my original work and it has been written by me in its entirety. I have duly acknowledged all the sources of information which have been used in the thesis.

This thesis has also not been submitted for any degree in any university previously.

B. L. Suresh

Suresh Bangalore Lakshminarayana

8 May 2015

ACKNOWLEDGEMENTS

I would like to express my sincere gratitude to my supervisor, Prof. Paul Ho for his constant guidance, suggestions and advices throughout the whole course of this project and thesis write-up. I would also like to thank thesis committee members, Dr. Koh Hwee Ling and Dr. Yau Wai Ping, for their valuable comments, discussions and advices during the entire course of this project, especially during qualifying examinations. I am grateful to the Novartis Institute for Tropical Diseases (NITD) for providing the opportunity to do this research work from in-house projects and for financial support. I would like to express my heartfelt gratitude to Dr. Francesca Blasco, my current supervisor at NITD, for her helpful guidance, ideas and continuous support. Dr. Veronique Dartois's valuable advice, suggestions and guidance during the initial part of the project is highly appreciated.

My deepest thanks are due to past and present animal pharmacology and bio-analytical team members for their technical help during *in vivo* pharmacokinetic and pharmacodynamic studies and also to MAP colleagues, NIBR and Cyprotex, UK team for generating *in vitro* PK data. I also convey my gratitude to Ujjini Manjunatha, Srinivasa Rao, Paul Smith and Thomas Dick for their valuable comments, discussions and critical feedback towards tuberculosis research. My humble thanks go to Matthias Rottmann, Thomas Bouillon, Xingting Wang, Jay Prakash Jain and Thierry Diagana for enlightening discussions towards malaria research. I also wish to thank everyone at NITD who has helped me in one way or another towards this thesis.

A special thanks to Dr. Shahul Nilar and Dr. Kantharaj Ethirajulu for providing philosophical views, critical feedback and guidance; Parind Desai, Ramesh Jayaram, Sam and Prakash Vachaspati for their moral support and helpful discussions. Last but not least, I would like to thank my family members, V. Nagarathna, P. Murthy, Deepu and Dhruv for their understanding and continuous support.

Suresh B. Lakshminarayana

January 2015

LIST OF PUBLICATIONS AND CONFERENCE

PRESENTATIONS

Publications

1. **Lakshminarayana SB**, Haut TB, Ho PC, Manjunatha UH, Dartois V, Dick T and Rao SPS. Comprehensive physicochemical, pharmacokinetic and activity profiling of anti-TB agents. ***J. Antimicrob. Chemother***, November 11, 2014. doi: 10.1093/jac/dku457

2. **Lakshminarayana SB**, Boshoff HI, Cherian J, Ravindran S, Goh A, Jiricek J, Nanjundappa M, Nayyar A, Gurumurthy M, Singh R, Dick T, Blasco F, Barry CE 3rd, Ho PC, Manjunatha UH. Pharmacokinetics-pharmacodynamics analysis of bicyclic 4-nitroimidazole analogs in a murine model of tuberculosis. ***PLoS One***. 2014 Aug 20; 9(8):e105222. doi: 10.1371/journal.pone.0105222. eCollection 2014.

3. **Lakshminarayana SB**, Freymond C, Fischli C, Yu J, Weber S, Goh A, Yeung BK, Ho PC, Dartois V, Diagana TT, Rottmann M, Blasco F. Pharmacokinetics-pharmacodynamics analysis of spiroindolone analogs and KAE609 in a murine malaria model. ***Antimicrob Agents Chemothera***. 2014 Dec 8. Pii: AAC.03274-14.

Conference presentations

1. **Lakshminarayana SB et al.,** "Evaluation of Pharmacokinetics-Pharmacodynamics of bicyclic nitroimidazole analogues in a Murine Model of Tuberculosis". Tuberculosis Drug Development, Gordon Research Conference, July 3-8, 2011, II Ciocco Hotel and Resort, Lucca (Barga), Italy.

2. **Lakshminarayana SB et al.,** "Evaluation of Physicochemical, *in vitro* potency, *in vivo* Pharmacokinetics and Pharmacodynamic properties of Anti-mycobacterial compounds". AAPS-NUS, 2nd PharmSci@India, 3rd & 4th September 2011, National Institute of Pharmaceutical Education and Research, Balanagar, Hyderabad-500037, India.

3. **Lakshminarayana SB.** "Evaluation of Pharmacokinetics-Pharmacodynamics of bicyclic nitroimidazole analogues in a Murine Model of Tuberculosis". National University of Singapore, 7th December 2011.

4. **Lakshminarayana SB.** Pharmacokinetics and pharmacodynamics of NITD609 and spiroindolone analogs in a murine malaria model. Metabolism and Pharmacokinetics Global Meeting, October 2nd – 5th 2012 at Colmar, France.

5. **Lakshminarayana SB et al.,** Pharmacokinetics and pharmacodynamics of NITD609 and spiroindolone analogs in a murine malaria model. American Association of Pharmaceutical Scientists, October 14-18, 2012 at McCormick place in Chicago, IL, USA.

6. **Lakshminarayana SB.** Pharmacokinetics and pharmacodynamics of anti-infective drugs: approaches and challenges in drug discovery and development. International conference on Pharmacology and Drug Development, 9^{th} – 11^{th} December, 2013, Singapore.

TABLE OF CONTENTS

SUMMARY

Due to the high attrition rates in drug development and lengthy and resource intensive animal pharmacology studies, there is a need for expedited cost-effective selection of the leading drug candidates to progress into development. This objective could be accomplished by establishing *in silico* – *in vitro* – *in vivo* correlations (ISIVIVC) and pharmacokinetic-pharmacodynamic (PK-PD) relationships for the drug candidates as early as possible during the discovery phase.

The ISIVIVC have been extensively studied and empirical rules established for a diverse set of compounds from different therapeutic areas. Further, PK-PD relationships have been established for several classes of therapeutic compounds, particularly for the anti-infective agents. However, the corresponding ISIVIVC analysis is lacking for anti-mycobacterial compounds and PK-PD relationship analysis is limited to individual anti-mycobacterial and anti-malarial drugs. Hence, to fill up the information gap in these areas, ISIVIVC for the standard anti-mycobacterial compounds was investigated in this thesis; further, the PK-PD relationships for the compound classes of nitroimidazoles and spiroindolones, respectively from tuberculosis and malaria programs, were examined.

The objectives of the research work presented in this thesis can be broadly divided into two categories: tuberculosis (under Part 1 and 2) and malaria (under Part 3). In Part 1, the ISIVIVC of anti-mycobacterials are described. Tuberculosis (TB) drug discovery and development have met limited success with only two new drugs approved over the last 40 years. The problem is partly due to the lack of well-established relationship between *in*

vitro physicochemical properties and pharmacokinetic parameters of anti-tuberculosis (anti-TB) drugs. In an attempt to benchmark and compare such physicochemical properties for anti-TB agents, these parameters derived from standard assays were compiled for 36 anti-TB compounds, thus ensuring direct comparability across drugs and drug classes. Correlations between the *in vitro* physicochemical properties and the *in vivo* pharmacokinetic parameters were then evaluated. Such correlations will be useful for guiding the drug development of future drugs. In our study, it was found that most of the current anti-TB drugs exhibited favorable solubility, permeability and metabolic stability. Analysis of human PK parameters revealed associations between lipophilicity and volume of distribution, clearance, plasma protein binding and oral bioavailability. Not surprisingly, most compounds with favorable pharmacokinetic properties complied with various empirical rules. This work will provide a reference dataset for the TB drug discovery community with a focus on comparative *in vitro* properties and pharmacokinetics.

The second part of this thesis describes the PK-PD relationship for nitroimidazoles. PA-824 is a bicyclic 4-nitroimidazole, currently in phase II clinical trials for the treatment of tuberculosis. Dose fractionation PK-PD studies in mice indicated that the driver of PA-824 *in vivo* efficacy is the time during which the free plasma drug concentrations are above the MIC ($fT_{>MIC}$). In this study, a panel of closely related potent bicyclic 4-nitroimidazoles was profiled in both *in vivo* PK and efficacy studies. A retrospective analysis was performed for a set of seven nitroimidazole analogs to identify the PK parameters that correlate with the *in vivo* efficacy. It was found that the *in vivo*

efficacy of bicyclic 4-nitroimidazoles correlated better with the lung PK than with the plasma PK. Further, moderate-to-high volumes of distribution and lung to plasma ratios of > 2 related to good efficacy. Among all the PK-PD indices, total lung $T_{>MIC}$ correlated the best with the *in vivo* efficacy (r_s = 0.88) followed by lung C_{max}/MIC and AUC/MIC. Thus, lung drug distribution studies could potentially be exploited to guide the selection of new nitroimidazole analogs for efficacy studies.

Limited information is available on PK-PD parameters driving the efficacy of antimalarial class of compounds. The third part of this thesis describes the PK-PD relationship for compounds belonging to the class of spiroindolones analogs. The objective in this study was to determine dose-response relationships for a panel of related spiroindolone analogs and further identify the PK-PD index that correlates best with the efficacy of KAE609 using a dose fractionation approach. All spiroindolone analogs studied displayed a maximum reduction in parasitemia, with 90% effective dose (ED_{90}) values ranging between 6 and 38 mg/kg of body weight. KAE609 was identified as the most potent analog. Further, the dose fractionation study revealed that the percentage of the time in which KAE609 plasma concentrations remained above 2*IC_{99} (TRE) within 48 h (%$T_{>TRE}$) and the AUC_{0-48}/TRE correlated well with parasite reduction (R^2=0.97 and 0.95, respectively), but less so for the C_{max}/TRE (R^2=0.88). For KAE609, (and supposedly for its analogs) the dosing regimens covering $T_{>TRE}$ of 100%, AUC_{0-48}/TRE of 587 and a C_{max}/TRE of 30 result in maximum reduction in parasitemia in the *P. berghei* malaria mouse model.

The outcome of this work could serve as guidance to prioritize new drug candidates against tuberculosis and malaria, thereby facilitating the lead optimization and possibly expediting the drug discovery process.

LIST OF TABLES

LIST OF FIGURES

LIST OF ABBREVIATIONS

µg/g	Microgram per gram of tissue
µg/mL	Microgram per milliliter
µg·h/g	Microgram-hour per gram of tissue
µg·h/mL	Microgram-hour per milliliter
cm/s	Centimeter per second
h	Hour
L/kg	Liters per kilogram of body weight
mg/kg	Milligram per kilogram of bodyweight
mg/L	Milligram per liter
mL/min/kg	Milliliter per minute per kilogram of body weight
ng·h/mL	Nanogram-hour per milliliter
nM	Nanomolar
uL/min/mg	Microliter per minute per milligram of protein
uM	Micromolar
ACTs	Artemisinin-based combination therapies
ADME	Absorption Distribution Metabolism Elimination
AIDS	Acquired Immuno Deficiency Syndrome
ATO	Atovaquone
AUC	Area under the curve
BHK21	Baby Hamster Kidney cell line
Caco-2	Colon carcinoma cell line
CC_{50}	Cytotoxicity
CFU	Colony Forming Units
CHQ	Chloroquine
CL	Clearance
Cl_{int}	Intrinsic clearance
CM-2	Cyclodextrin complexation
C_{max}	Maximum concentration
CRT	Chloroquine resistance transporter
CYC	Cycloguanil
CYTB	Cytochrome bc1 complex
DHFR	Dihydrofolate reductase
DHPS	Dihydropteroate synthetase
DOTS	Directly Observed Therapy Short Course
DV	Observed data
ED_{90}	Effective does in lowering 90% of parasitemia
F	Oral bioavailability
G6PD	Glucose-6-phosphate dehydrogenase
Gm-	Gram-negative bacteria
Gm+	Gram-positive bacteria
HBA	Hydrogen Bond Acceptor
HBD	Hydrogen Bond Donor
HepG2	Hepatocyte cell line
HIV	Human Immuno Deficiency Virus
HPLC	High performance liquid chromatography
i.v.	intravenous
IACUC	Institutional animal care and use committee
IC_{50}	50% inhibitory concentration

IC_{99}	99% inhibitory concentration
ISIVIVC	*In silico - in vitro - in vivo* correlations
K_a	Absorption rate constant
L/P	Lung-to-plasma ratio
LC-MS	Liquid chromatography mass spectrometry
LLOQ	Lower limit of quantification
LO	Lead Optimization
MDR	Multi Drug Resistant
MDR1	Multidrug resistance protein-1
MIC	Minimum Inhibitory Concentration
MMV	Medicines for Malaria Venture
MRM	Multiple reaction monitoring
Mtb	Mycobactaerium tuberculosis
MW	Molecular Weight
NCE's	New chemical entities
NI	Nitroimidazoles
NITD	Novartis Institute for Tropical Diseases
NONMEM	Nonlinear mixed effect modeling
NP	Natural product
P. berghei	*Plasmodium berghei*
P. falciparum	*Plasmodium falciparum*
P. knowlesi	*Plasmodium knowlesi*
P. ovale	*Plasmodium ovale*
P. vivax	*Plasmodium vivax*
P.malarie	*Plasmodium malariae*
p.o.	per oral
PAMPA	Parallel Artificial Membrane Permeability Assay
P_{app}	Apparent Permeability
PAS	Para aminosalicylic acid
PBS	Phosphate Buffer Saline
PD	Pharmacodynamics
PfATP4	P-type sodium transporter ATPase 4
Pfcarl	*Plasmodium falciparum* cyclic amine resistance locus
PK	Pharmacokinetics
PK-PD	Pharmacokinetics-pharmacodynamics
P_{max}	Maximum parasitemia
P_{min}	Minimum parasitemia
PPB	Plasma protein binding
pRBCs	parasitized red blood cells
PRED	Predicted data
PSA	Polar Surface Area
PYR	Pyrimethamine
Q	Inter compartmental clearance
RB	Rotatable Bond
r_s	Spearman's rank correlations coefficient
SAR	Structure Activity Relationship
SD	Standard deviation
SDX	Sulphadoxine
SEM	Standard error of mean
SM	Synthetic molecule

SPR	Structure Property Relationship
$T_{>MIC}$	Time during which plasma concentration remains above MIC
$T_{>TRE}$	Time during which plasma concentration remains above threshold
$t_{1/2}$	Half-life
TB	Tuberculosis
THP1	Human acute monocytic leukemia cell line
T_{max}	Time to reach maximum concentration
TPP	Target Product Profile
TRE	Threshold
V_c	Central volume of distribution
V_d	Volume of distribution
V_p	Peripheral volume of distribution
V_{ss}	Volume of distribution at steady state
WHO	World Health Organization
WRES	Weighted residuals
XDR	Extremely Drug Resistant

Chapter 1. Introduction

1.1 Infectious diseases

Infectious diseases are caused by pathogenic microorganisms, such as bacteria, viruses, parasites or fungi; the diseases can spread directly or indirectly from one person to another. Three major infectious diseases namely acquired immune deficiency syndrome (AIDS), tuberculosis (TB) and malaria are related to increased number of deaths every year. Hence there is an urgent need to develop effective medicines to treat successfully such diseases (WHO, 2014a).

The Novartis Institute for Tropical Diseases (NITD) is dedicated to the discovery and development of new drugs to treat neglected infectious diseases and efforts are ongoing in the fields of Dengue fever, Human African Trypanosomiasis, Malaria and Tuberculosis (NITD, 2014). The research work presented in this thesis is focused on two infectious diseases namely, tuberculosis (Part 1 - *In silico – in vitro – in vivo* correlations for standard anti-TB drugs and Part 2 - Pharmacokinetic-Pharmacodynamic relationships for nitroimidazoles) and malaria (Part 3 - Pharmacokinetic-Pharmacodynamic relationships for spiroindolones).

1.2 Tuberculosis

TB is a contagious disease affecting about one third of the world population. It is caused by the bacteria, mycobacterium tuberculosis (Mtb) and is spread through the air by coughing, sneezing, or even talking. Due to its unique lipid cell wall, the bacillus can remain in dormant state for many years. Some people with the latent form of infection will never develop active TB, however, 5 to 10 percent of carriers may develop active TB and will become

sick in their lifetime (Dye and Williams, 2010). Every year nearly 8 million new cases of TB are reported globally resulting in 1.4 million deaths. In 2012, around 8.6 million people developed TB, [including ~450,000 multi drug resistant (MDR) TB cases] resulting in 1.3 million deaths (WHO, 2012a). Approximately 80% of reported TB cases are from 22 different countries with the largest number of new TB cases occurring in Asia and the greatest proportion of new cases per population are from sub-Saharan Africa (Figure 1).

Common symptoms of active lung TB are cough with sputum and blood at times, chest pains, weakness, weight loss, fever and night sweats. Treatment for active, drug-sensitive TB consists of 4 medicines known as first-line drugs and is administered for a period of 6 months [a combination of 4 drugs (rifampicin, isoniazid, ethambutol and pyrazinamide) for 2 months, followed by rifampicin and isoniazid for 4 months]. The long duration and complex regimen is burdensome for patients. World Health Organization (WHO) recommended Directly Observed Therapy Short Course (DOTS), aiding TB patients to take medicines under direct observation by healthcare worker. Poor treatment compliance as well as the use of inadequate regimens has led to the emergence of multi-drug-resistant and extensively-drug-resistant (MDR-TB and XDR-TB) TB strains. Today, treatment for drug-resistant TB relies on the second-line drugs [aminoglycosides (kanamycin and amikacin), cycloserine, ethionamide, protionamide, capreomycin, aminosalicylic acid, and fluoroquinolones (including ofloxacin, levofloxacin, gatifloxacin and moxifloxacin)], and is commonly administered for 2 years or longer including daily injections for six months. This treatment is complex, expensive, and

often causes severe side effects. MDR-TB is resistant to at least isoniazid and rifampicin, and XDR-TB is resistant to isoniazid, rifampicin, fluoroquinolones and at least one of the three injectable second-line drugs (capreomycin, kanamycin and amikacin) (WHO, 2012b). Currently, drug-resistant TB is quite common in India and China — the two countries with the highest MDR-TB burdens.

One-third of the more than 33 million people living with AIDS are also infected with tuberculosis. TB is a serious threat for people with human immuno deficiency virus (HIV), especially in sub-Saharan Africa, where it causes up to half of all AIDS deaths. TB-HIV co-infections are also on the rise in other areas of the world, particularly Western Asia, including China, and Eastern Europe. TB control programs are further complicated in settings where the incidence of co-infection with HIV is high, because drug-drug interactions with anti-retroviral therapy are difficult to avoid (Balganesh et al., 2008; WHO, 2012b). To make the landscape even more complex, there are recent reports of totally drug resistant TB cases (Udwadia et al., 2012). Needless to say, there is an urgent need to discover new TB drugs active against all drug-resistant forms of TB and compatible with treatment against HIV.

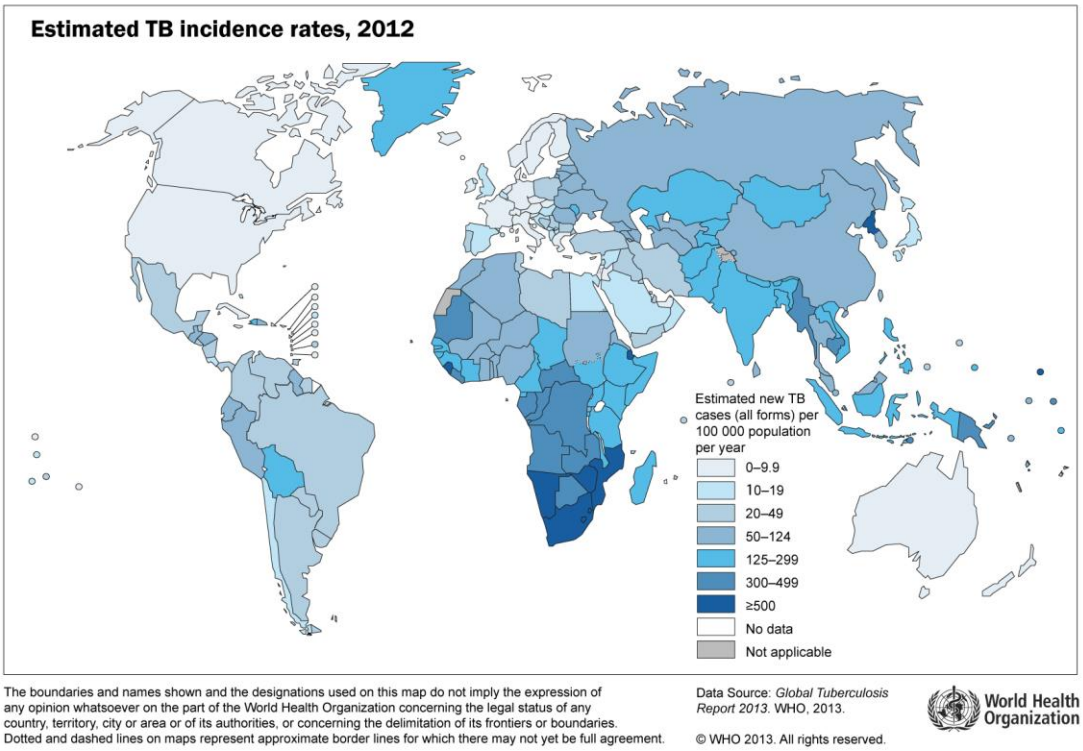

Figure 1. Estimated TB incidence rates during 2012. Data Source from WHO (2013)

1.2.1 Discovery of anti-mycobacterial drugs

In 1946 streptomycin was discovered to be active against Mtb and since then it has been extensively used as monotherapy, as a consequence, arising undesired resistance to the treatment. The need for multidrug therapy of TB to prevent the rapid development of drug resistance was then widely recognized. Later on, para aminosalicylic acid (PAS) and isoniazid were found to be active against TB. The first combination regimen was given in 1952 and consisted of streptomycin, aminosalicylic acid and isoniazid for a period of 24 months. Several other drugs were discovered to be active against Mtb (e.g. pyrazinamide, cycloserine, kanamycin, ethionamide and ethambutol) in the following years. During 1960's, streptomycin, isoniazid and ethambutol were given for a period of 18 months (Figure 2).

The discovery of rifampicin in 1963 and its addition to the combination therapy during 1970's led to a significant reduction of the treatment duration from 18 months to 9-12 months. In 1980's streptomycin was replaced with pyrazinamide and the new four drug combination (i.e. pyrazinamide, rifampicin, isoniazid and ethambutol) led to further reduction of the treatment to 6-8 months. Since then this combination has been used to treat TB (Ma et al., 2010). Although rifampicin is a cornerstone of the current TB regimen, it induces the enzyme cytochrome P450. These enzymes cause some antiretroviral drugs to be metabolized rapidly, inhibiting effective anti-retro viral therapy. Hence, drug-drug interactions are a major concern with combination of drug treatment for therapeutic area like anti-HIV or other chronic disease medications such as those used in diabetics (Koul et al., 2011).

All four 1st-line anti-TB agents in use today were launched in the 50's and 60's before the era of pharmacokinetics (PK) and pharmacodynamics (PD). In the case of rifampicin, financial considerations came before clinical pharmacology evaluation to support dose selection (van et al., 2011). Since there is a rapid emergence of resistance against standard TB drug regimen, new drug candidates with novel mechanisms of action are needed urgently.

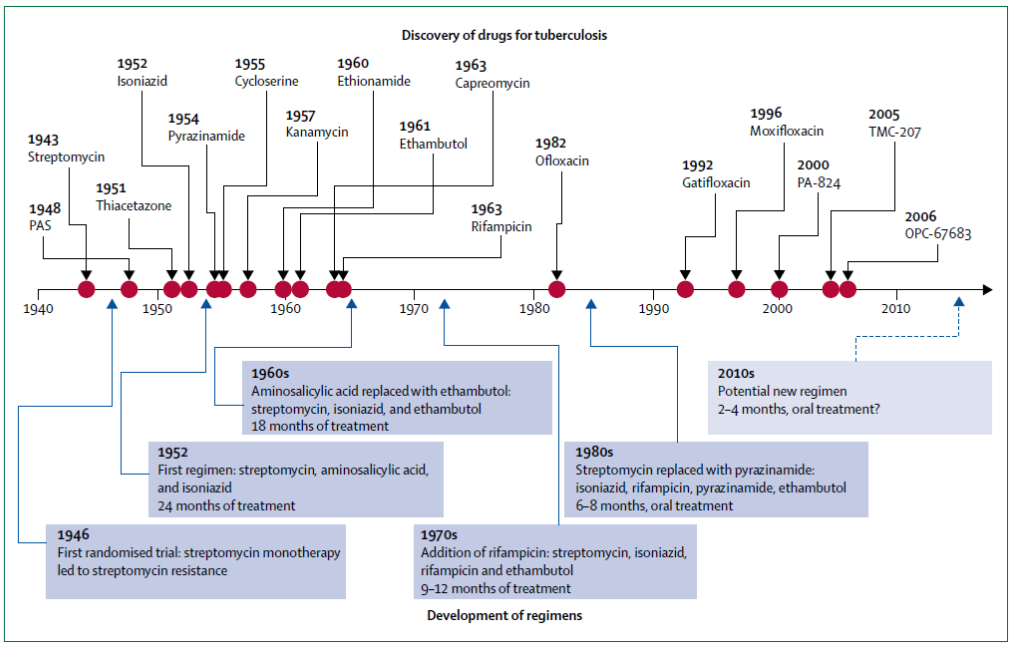

Figure 2. History of drug discovery and development of treatment regimens for TB. Reprinted from Ma et al. (2010), with permission from Elsevier.

1.2.2 Ideal drug candidates

An ideal drug combination should consist of at least three drugs that are active against drug susceptible and drug resistant (MDR and XDR) tuberculosis and produce stable cure in a shorter period compared to the standard treatment. Such combination(s) should have potent, synergistic, and complementary activities against various subpopulations of Mtb (Dartois and Barry, 2010). In addition, it should also be suitable to treat patients co-infected with Mtb and HIV; which could be achieved by replacing rifampicin (drug interactions with anti-retroviral drugs) in the combination therapy (Ma et al., 2010).

1.2.3 Drug development pipeline

There are several new classes of compounds in various phases of drug discovery, preclinical and clinical development (Figure 3) (Ginsberg, 2010; Lienhardt et al., 2012). Among others, the following candidates are presently

being evaluated as potential TB drugs: rifapentine (a semisynthetic rifamycin) having longer half-life than rifampicin; SQ-109, a highly modified derivative of ethambutol; oxazolidinones (linezolid, PNU-100480 and AZD5847); fluoroquinolones (ofloxacin, gatifloxacin and moxifloxacin); nitroimidazoles (PA-824 and OPC-67683) and TMC207. Interestingly, OPC-67683 (delamanid) and TMC207 (bedaquiline) demonstrated activity against drug-resistant strains of Mtb in patients (Cox and Laessig, 2014; Diacon et al., 2014; Gler et al., 2012). The mechanisms of action of the current drug candidates are summarized in Figure 4. Drugs with novel mechanisms of action are needed to create new combination regimens active against all drug-resistant strains of TB and compatible with HIV treatment.

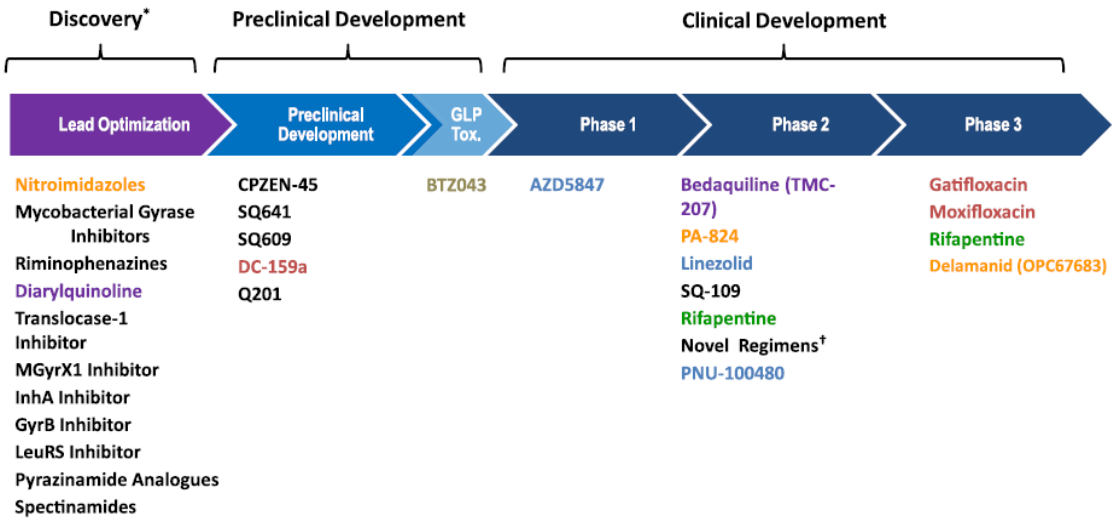

Figure 3. Global tuberculosis drug pipeline. With permission of Oxford University Press Lienhardt et al. (2012).

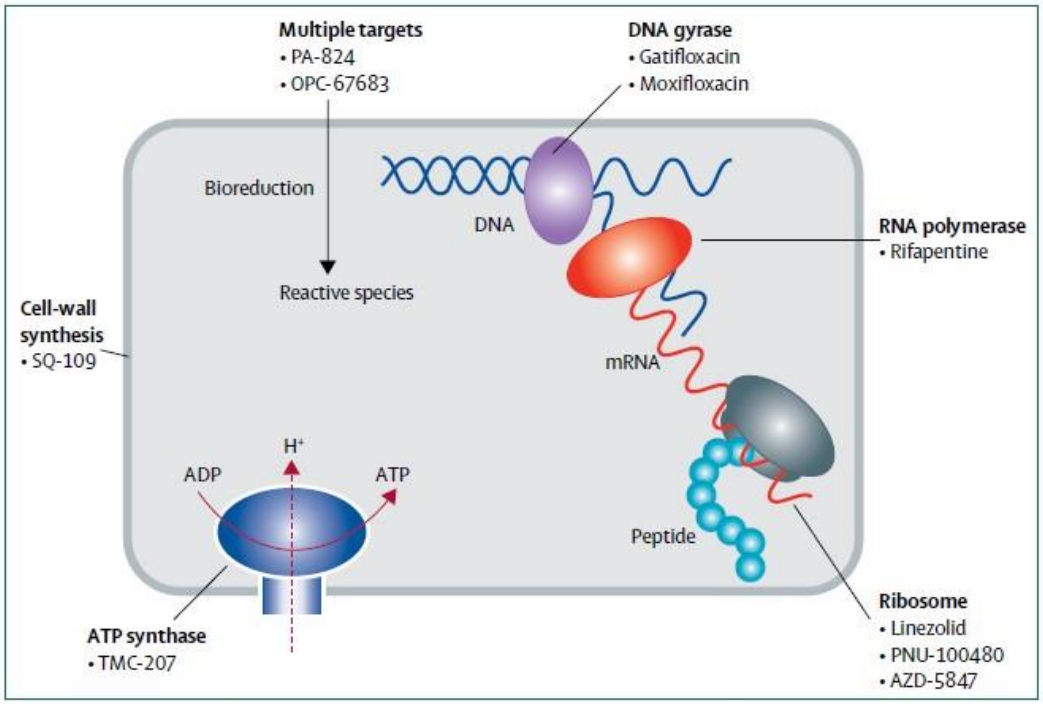

Figure 4. Mechanism of action of new compounds in clinical development for tuberculosis. Reprinted from Ma et al. (2010), with permission from Elsevier.

1.2.4 Combination therapy

Few phase III clinical trials were initiated to evaluate the possibility of shortening TB treatment by replacing one of the standard TB drugs (either isoniazid or ethambutol) by fluoroquinolones (either moxifloxacin or gatifloxacin). Surprisingly, recent reports demonstrated that none of the regimens was able to reduce TB treatment from 6 months to 4 months (Warner and Mizrahi, 2014). Although these new regimens displayed more rapid initial decline in bacterial load as compared to the control group, none of them showed superior activity compared to the standard regimen (Gillespie et al., 2014; Jindani et al., 2014; Merle et al., 2014). In addition, clinical trials with different combinations of moxifloxacin (fluoroquinolone), PA-824

(nitroimidazole), TMC-207 (bedaquiline) and other drugs (clofazimine) have been reported to be ongoing (TB Alliance, 2014) (Table 1).

Table 1. Tuberculosis clinical development pipeline. Data Source from TB Alliance (2014)

Phase 1	Phase 2	Phase 3	Phase 4
PK of first-line drugs in children < 5kg	NC-003	STAND	Optimized first-line drugs in children > 5 kg
Isoniazid / Rifampicin / Pyrazinamide / Ethambutol (Pediatric)	Bedaquiline / Clofazimine / PA-824	PA-824 / Moxifloxacin / Pyrazinamide	Ethambutol
	Bedaquiline / Pyrazinamide / PA-824		Rifampicin
	Bedaquiline / Clofazimine / Pyrazinamide / PA-824		Isoniazid
	Bedaquiline / Clofazimine / Pyrazinamide		Pyrazinamide

1.2.5 Challenges in TB drug discovery programs

Mtb is a slow growing pathogen that multiplies once in 22- 24 h and has a unique thick lipid cell wall which is a waxy coating primarily composed of mycolic acids. The *in vitro* potency of test compounds is determined in broth where their minimum inhibitory concentration (MIC) to the growth of Mtb is measured. MIC is determined in an extracellular environment, but Mtb resides inside the macrophages; hence an intracellular macrophage MIC (*ex vivo*) measurement is performed. In this case, compounds have to penetrate the cells to reach the bacterium and then exert their activity. The assay requires approximately 4 to 5 weeks and the final read out is the number of colony

forming units (CFU). The cell line of choice for this assay [such as human acute monocytic leukemia cell line (THP1) or bone marrow-derived macrophage (BMDM), activated or resting macrophages] is rather controversial and the sensitivity is generally not very good. Due to slow turn-around time, lack of sensitivity and controversy about the usage of different cells lines, this is considered a profiling assay and is run preferentially during the late drug discovery phase (Franzblau et al., 2012). In reality (*in vivo* situation), the site of infection is in the lungs and Mtb resides inside the macrophages. The compounds, dosed orally, need to overcome absorption and metabolism hurdles to reach systemic circulation and distribute into lungs to be available at the site of infection. In TB patients, the lungs also present granulomas, calcified granulomas, necrotic lesions, caseous lesions and this complexity has triggered a lot of discussion on which is the best representative animal model to mimic the human disease (Dartois and Barry, III, 2013).

The use of mice as animal model in drug discovery is widespread. They are relatively small, cost effective and well characterized as pharmacological models for screening purpose. They have been used as tool to assess the bactericidal and sterilizing potencies of individual drugs and drug combinations (Andries et al., 2010). Hall marks of pulmonary TB in humans are granulomas, caseous necrosis and/or cavitation and hypoxia (Barry, III et al., 2009; Rhoades et al., 1997) which are not reproduced in mice. Moreover, during the chronic phase of the disease, unlike humans, the lungs and spleen of mice contain high numbers of persisting bacteria (Boshoff and Barry, III, 2005). Alternative animals such as guinea pigs, rabbits (Kjellsson et al., 2012; Prideaux et al., 2011) and even cynomolgus monkeys have been used as

preclinical models as they mimic the pathogenesis of TB better than mice with features such as hypoxic lesions and solid necrotic granulomas (Via et al., 2008). Non-human primate models of TB that recapitulate the human disease are ideal for identifying the clinically relevant PK-PD predictors of sterilization efficacy of anti-TB agents. However, these models are very expensive and their accessibility limited due to ethical issues making them not suitable for screening purposes in the early stages of drug discovery.

In spite of the already mentioned limitations, most of the standard TB drugs have shown to be efficacious in the murine TB models, suggesting a certain translational relevance to the human situation. For this reason, the anti-TB activity of new drug candidates is generally tested in mice. There are two types of TB model in mouse: (a) acute and (b) established model. In the acute model the drug treatment starts one week post infection, which corresponds to rapidly growing Mtb (Pethe et al., 2010). In the chronic model the treatment starts 3-4 weeks post infection, when Mtb growth has reached a plateau (Rao et al., 2013). TB *in vivo* pharmacological studies are lengthy and resource intensive. Depending on the model, it takes 8 to 12 weeks to get one efficacy read out and high containment facilities are required to perform these experiments. In light of these, fast and simple assays, instead of the lengthy and resource intensive animal pharmacology studies would be much desirable for selecting the most promising molecules in early drug discovery for TB therapy.

1.3 Malaria

Malaria is the most prevalent infectious disease worldwide affecting about 3.3 billion people - half of the world's population is at risk of the infection (Greenwood and Mutabingwa, 2002). It is caused by parasites of the *Plasmodium* species. The disease is transmitted to people by the bite of an infected Anopheles mosquito. About 250 million people are infected each year resulting in approximately 1 million deaths annually. In 2012, there were approximately 207 million malaria cases and estimated 627 000 deaths (Murray et al., 2012; WHO, 2012c). It is common in parts of Africa, Asia and Latin America (Figure 5). Most deaths occur among children living in sub-Saharan Africa where a child dies every minute from malaria (WHO, 2014b).

There are five parasite species that cause malaria in humans. *Plasmodium falciparum*, *Plasmodium vivax*, *Plasmodium ovale*, *Plasmodium malariae* and *Plasmodium knowlesi*. *P. falciparum*, most prevalent in sub-Saharan Africa, is responsible for the majority of malaria deaths globally. *P. vivax* is the second most significant species prevalent in Southeast Asia and Latin America. *P. vivax* and *P. ovale* cause additional complication of dormant liver stage that can reactivate anytime leading to clinical symptoms. *P. ovale* and *P. malariae* represents only a small percentage of infections. The fifth species *P. knowlesi* generally infects primates but has also led to human malaria; however the exact mode of transmission is unclear.

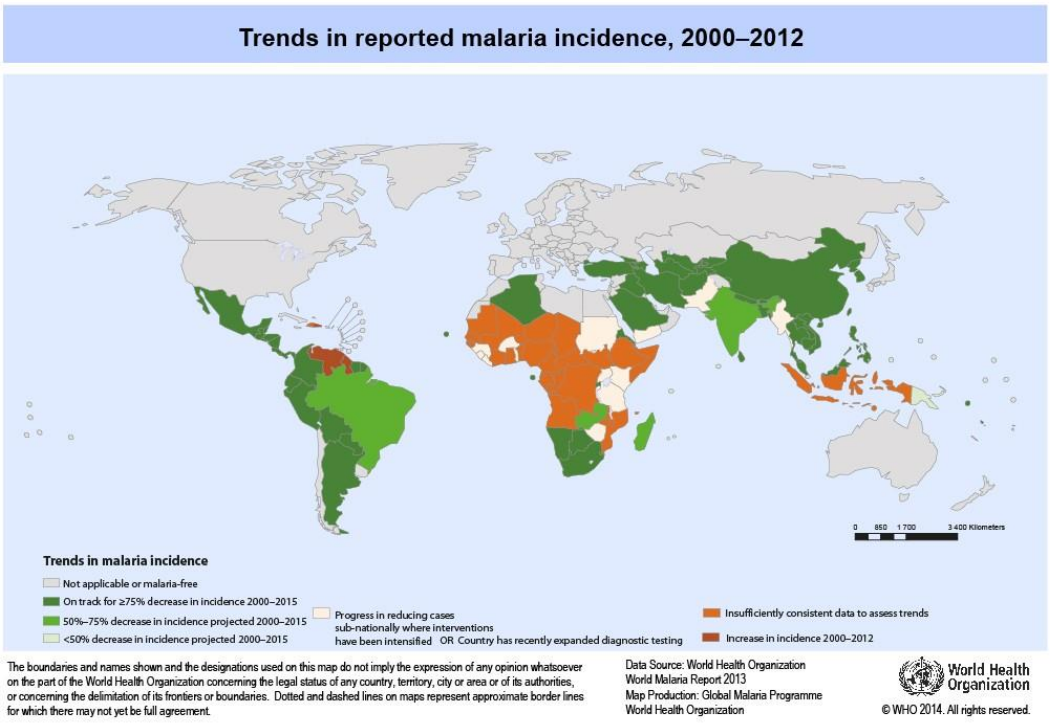

Figure 5. Estimated malaria incidence rates during 2000 – 2012. Data Source from WHO (2014b)

1.3.1 Discovery of antimalarial drugs

The standard antimalarial drugs are summarized in Table 2. They are classified by chemical class such as arylaminoalcohol, 4-aminoquinolines, 8-amionquinolines, sesquiterpene lactone (artemisinin), biguanides, diaminopyrimidines, sulfonamides, hydroxynaphthoquinone, and antibiotics. Quinine and quinidine are the first antimalarials extracted from cinchona alkaloids during the seventeenth century. Various other compounds active against *Plasmodia* were discovered later in the twentieth century. Artemisinin, isolated from the leaves of *Artemisia annua* by Chinese scientists in 1972, is one of the most important antimalarial principle (Warrell et al., 1993). The treatment for uncomplicated malaria requires 3 days of dosing.

Primaquine, is the only registered drug for the treatment of hypnozoites, a dormant form of the parasites (*P. vivax* and *P. ovale*) residing in the liver (latency) and responsible for recurring clinical symptoms (relapse). The drug needs to be dosed daily for 14 days and it is associated with gastro-intestinal side effects, risk of haemolytic anaemia for patients with low activity of glucose-6-phosphate dehydrogenase (G6PD) and is not safe in pregnant women. Tefenoquine, another 8-aminoquinoline derivative with better *in vitro* activity and wider therapeutic index compared to primaquine, is currently being evaluated for the treatment of *P. vivax* malaria (Burrows et al., 2014; Held et al., 2013).

It is noteworthy that emergence of resistance to traditional antimalarials has been reported within a few years of their introduction (Talisuna et al., 2004). This is mostly related to the extensive use of single drug based treatments. Additional contribution to drug resistance might be the sub-optimal doses administered to children or pregnant women (Barnes et al., 2008; Na-Bangchang and Karbwang, 2009; White et al., 2009). Widespread resistance against common antimalarials is responsible for the recent increase in malaria-related mortality (White, 2004). In order to reduce the risk of selecting drug resistance, WHO's recommendation is to combine artemisinin with other antimalarials. Currently the treatment of choice for uncomplicated falciparum malaria is a combination of two or more antimalarial drugs with different mechanism of action.

Table 2 and Figure 6 summarize the mode of action of antimalarial drugs together with the emergence of the corresponding drug resistance. Many of the antimalarials prevent haeme detoxification within the digestive vacuole.

Cell lysis and autodigestion are triggered by blocking the polymerization of the toxic byproduct of the haemoglobin degradation, the haem, into insoluble and non-toxic pigment granules (Olliaro and Yuthavong, 1999). Genetic changes in transporters chloroquine resistance transporter (PfCRT) and multidrug resistance protein-1 (PfMDR1) have led to the resistance of chloroquine and mefloquine. Likewise mutations in dihydropteroate synthetase (PfDHPS), dihydrofolate reductase (PfDHFR), and cytochrome bc1 complex (PfCYTB) have steered resistance to sulfadoxine (SDX), pyrimethamine (PYR) and atovaquone (ATO), respectively (Ding et al., 2012). Ideally new drug candidates should display different mechanisms of action to be considered as treatment against drug-resistant strains of malarial parasites.

The advantages of combination therapy should be balanced against the increased chance of drug interactions. Cytochrome P450's are frequently involved in the metabolism of antimalarial agents (Navaratnam et al., 2000) and due attention should be given when combinations are used (Giao and de Vries, 2001). Moreover, some artemisinin derivatives autoinduce their first-pass effect, resulting in a decline of bioavailability after repeated doses.

Table 2. Antimalarial drugs and their mode of action. Data Source from Warrell et al. (1993); Wongsrichanalai et al. (2002)

Class	Antimalarial drug	Mode of Action	Introduced	First reported resistance	Difference (years)
Arylaminoalcohol	Quinine (Cinchona alkaloids)	Interferes with parasite haem detoxification with in the digestive vacuole	1632	1910	278
	Quinidine				
	Mefloquine		1977	1982	5
	Halofantrine				
	Benflumetol (Lumefantrine)				
4-aminoquinolines	Chloroquine		1945	1957	12
	Amodiaquine				
	Pyronaridine				
8-aminoquinolines	Primaquine	Competitive inhibition of dihydro-orotate dehydrogenase involved in pyrimidine synthesis			
	Tafenoquine				
Artemisinin drugs (Sesquiterpene lactone)	Artemisinin (Artemisia annua)	Breakdown of peroxide bridge generates free radicals that undergo alkylating reaction. Inhibit calcium adenosine triphosphatase, PfATPase	1972	2008-2013	~36
	Dihyroartemisinin				
	Artetmether				
	Arteether				
	Artesunate				
Biguanides	Proguanil	Inhibits dihydrofolate reductase (block the synthesis of nucleic acids) (PfDHFR)	1948	1949	1
	Chlorproguanil				
Diaminopyrimidines	Pyrimethamine				
	Trimethoprim				

	Dapsone				
	Sulfonamides and sulphones	Competitive inhibitors of dihydropteroate synthase (PfDHPS)			
	Sulfadoxine - pyrimethamine		1967	1967	0
Hydroxynaphthoquinone	Atovaquone	Interferes with cytochrome electron transport (PfCYTB) causing inhibition of nucleic acid and adenosine triphosphate synthesis	1996	1996	0
Lincosamide antibiotic	Clindamycin	Inhibits early stages of protein synthesis similar to macrolides			
Antibiotics	Tetracyclines	Inhibitors of aminoacyl-tRNA binding during protein synthesis			
Tetracycline derivative	Doxycycline				

1.3.2 Ideal drug candidates

The ideal treatment for uncomplicated malaria should be highly efficacious (possibly as single oral dose to avoid compliance issues) and well tolerated with a very good safety profile. The requirements for drugs against severe malaria are slightly different, as parenteral administration is preferred to achieve rapid parasite clearance. If the goal is a malarial causal prophylactic agent, the drug should be active against the liver stage of the parasites (Wells et al., 2009) and be exquisitely safe. Furthermore, the new selected candidate should be reasonably cheap to produce and effective against drug resistant strains. Combination of two or more agents is a common and successful strategy in the field of antimalarial therapy. The combination partners should have synergistic action to minimize drug-related adverse effects and further reduce the risk of selecting resistant mutants of the parasites (Held et al., 2013).

1.3.3 Drug development pipeline

There are several new classes of compounds in various phases of preclinical and clinical development (Figure 7). Different approaches have been pursued to identify new drug candidates. Ferroquine (SR97193), a chloroquine derivative acting against chloroquine-resistant parasites *in vitro* and arterolane (OZ277), an endoperoxide, designed based on the active pharmacophore of artemisinins are two examples of traditional drug discovery (Held et al., 2013). OZ439, a second generation endoperoxide known to have improved PK, has demonstrated clinical efficacy in humans and is currently being tested in combination efficacy studies (Charman et al., 2011; Moehrle et al., 2013).

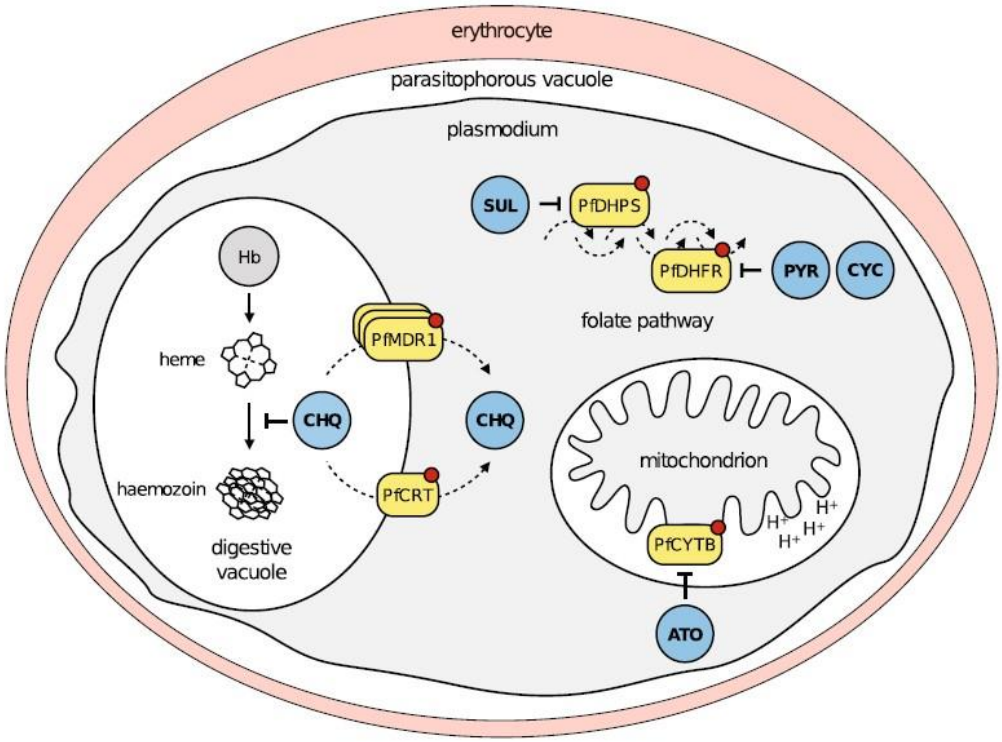

Figure 6. Known genetic determinants of naturally occurring resistant mechanisms; mutations (red dot). Ding et al. (2012), with permission of Biomed Central Ltd.

Rational drug design has successfully led to DSM265 and P218 that are currently evaluated in preclinical and clinical phase (Baldwin et al., 2005; Coteron et al., 2011; Yuthavong et al., 2012).

Finally, phenotypic high throughput screening successfully identified two clinical candidates (KAE609 and KAF156) (Smith et al., 2014). KAE609 (formerly called NITD609) represents a new chemotype. It belongs to the spiroindolone class and is not only active against blood stage but also against liver and transmission stages (Rottmann et al., 2010; Yeung et al., 2010). The compound inhibits the P-type sodium transporter ATPase 4 (PfATP4) resulting in an increased (toxic) sodium concentration in the parasite (Spillman et al., 2013). This compound has demonstrated safety and clinical efficacy in phase I and II trials (Leong et al., 2014a; White et al., 2014). The second

compound KAF156 from the imidazolopiperazine class showed good *in vitro* activity against all stages of parasites including liver and transmission stages. It is currently undergoing phase II clinical trials (Kuhen et al., 2014; Leong et al., 2014b; Nagle et al., 2012). This class of compounds acts via a novel mechanism, involving a previously unannotated gene now called *P. falciparum* cyclic amine resistance locus (Pfcarl) (Meister et al., 2011).

1.3.4 Combination therapy

The following are the artemisinin-based combination therapies (ACTs) recommended for the treatment of uncomplicated falciparum malaria: artemether plus lumefantrine, artesunate plus amodiaquine or mefloquine or sulfadoxine-pyrimethamine, dihydroartemisinin plus piperaquine. These combinations must be given for at least three days for an optimum effect. ACTs are currently the most effective treatment for malaria, with a 95% cure rate against falciparum malaria (German and Aweeka, 2008). There are reports of artemisinin resistance at the Cambodia–Thai border and recently ACTs exhibited delayed parasite clearance in patients emphasizing the need for new medicines with novel mechanisms of action (Dondorp et al., 2009; Ferreira et al., 2013; Miotto et al., 2013; Noedl et al., 2008). Second-line treatments (alternative ACT) against resistant malaria are also available and consist of, for example, artesunate plus tetracycline or doxycycline or clindamycin, quinine plus tetracycline or doxycycline or clindamycin. These combinations should be administered for 7 days.

Translational		Development			Access
Preclinical	Human volunteers	Patient exploratory	Patient confirmatory	Under review	Post approval*
P218 DHFR	DSM265	OZ439/PQP	Tafenoquine	Rectal Artesunate	Artemether-Lumefantrine Dispersible **1**
ELQ300	MMV048	OZ439/FQ	Pyronaridine-Artesunate Paediatric	Sulfadoxine pyrimethamine + amodiaquine	Artesunate for injection **2**
SJ733		KAE609	Dihydroartemisinin-Piperaquine Paediatric		Dihydroartemisinin-Piperaquine **3**
MMV121		KAF156			Pyronaridine-Artesunate **4**
					Artesunate-Amodiaquine **5**
					Artesunate-Mefloquine **6**

Figure 7. Global antimalarial drug pipeline. Data Source from MMV (2014)

1.3.5 Challenges in Malaria drug discovery programs

Plasmodium species has a complex lifecycle (Figure 8). Infected female Anopheles mosquitos transmit the parasites to humans. The mosquitos inject sporozoites into the bloodstream of the human host. These sporozoites reach to the liver and rapidly invade the liver cells. In all species of *Plasmodium*, sporozoites develop into schizonts, which in turn mature to form several thousand merozoites. In *P. vivax* and *P. ovale*, but not in *P. falciparum*, a proportion of the liver-stage parasites (known as hypnozoites) remain dormant in the hepatocytes. This stage of the parasite can remain dormant for months or several years and eventually can lead to relapsing malaria. When the liver cells rupture, the merozoites are released into the bloodstream where they rapidly invade the red blood cells. These blood-stage parasites replicate asexually - through ring, trophozoite and schizont - rapidly attaining a high

parasite burden and destroying the infected red blood cells, leading to the clinical symptoms of malaria (fever, chills, headache, muscle aches, tiredness, nausea, vomiting and diarrhea). The disease is considered uncomplicated when clinical or laboratory signs of vital organ dysfunction are absent. *P. falciparum* infections, if not promptly treated, can quickly progress to severe malaria (leading to coma, severe breathing difficulties, low blood sugar, and low blood haemoglobin) and lead to death. Children are particularly vulnerable since they have little or no immunity to the parasite. A small percentage of merozoites, differentiate into male and female gametocytes, which are taken up by the mosquito in her blood meal. Male and female gametocytes fuse within the mosquito forming diploid zygotes, which in turn become ookinetes, migrate to the midgut of the insect, pass through the gut wall and form the oocysts. Meiotic division of the oocysts occurs and sporozoites are formed, which then migrate to the salivary glands of the female Anopheles mosquitos ready to continue the cycle of transmission back to man.

Ideally, drugs should be active against all stages of the parasites. Antimalarial activity will be assessed on the basis of *in vitro* activity against *P. falciparum* and *in vivo* efficacy in animal models following oral dose administration of test compounds (Charman et al., 2011; Fidock et al., 2004). *Plasmodium* species that cause human disease (*P. falciparum* – blood stage, *P. vivax* – liver stage) are essentially unable to infect common laboratory animals. Humanized mice have been developed that sustain *P. falciparum* infection of human erythrocytes *in vivo* (Jimenez-Diaz et al., 2013; Moreno et al., 2001). This model is complex and expensive as it requires daily infusions

of human erythrocytes in severe immunodeficient mice. In addition, the relevance and the value of such model remain controversial (Held et al., 2013).

Plasmodium berghei is a species that infects rodents and is extensively used in preclinical drug testing. It has been validated through the identification of several antimalarials, such as mefloquine (Peters et al., 1977), halofantrine (Peters et al., 1987) and artemisinin derivatives (Posner et al., 2003; Vennerstrom et al., 2000). Screening test compounds in the *P. berghei* murine model is standard practice in malaria drug discovery and development (Fidock et al., 2004). Such studies can also generate robust PK-PD data that could be further used for dose optimization as reported for DHA (Gibbons et al., 2007), chloroquine (Moore et al., 2011) and piperaquine (Moore et al., 2008). Additionally, they are a useful tool for the comparison of single-dose and combination therapies not easily feasible in the clinical setting (Moore et al., 2008).

For decades, the efficacy of test compounds against the dormant liver stage (hypnozoites) has been studied in rhesus monkeys infected with *P. cynomolgi*, a simian parasite that unlike *P. berghei* develops hypnozoites (Deye et al., 2012). Primaquine has been the only available hypnozoitocidal drug for half a century.

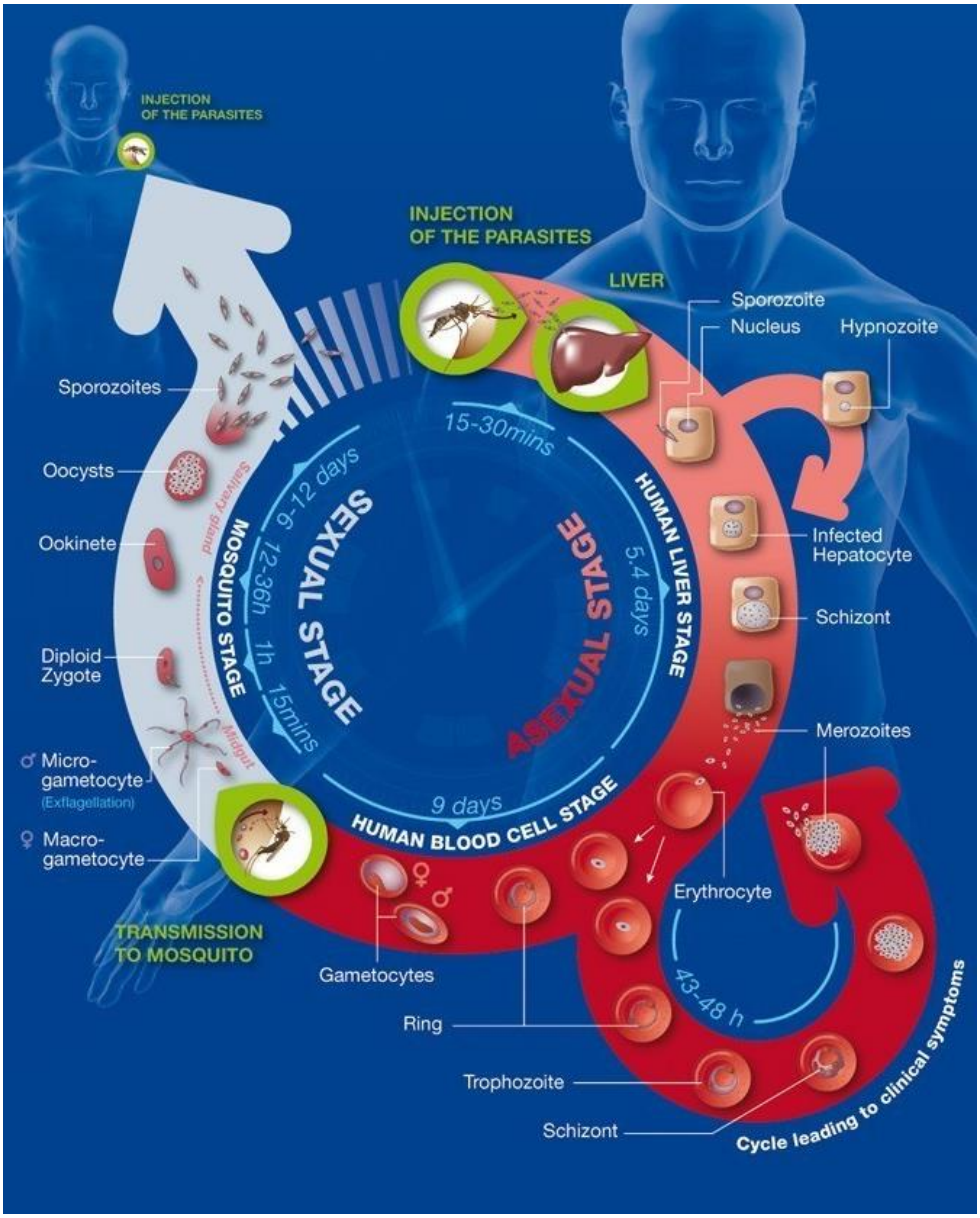

Figure 8. *Plasmodium* life cycle. Data Source from MMV (2014)

A recent report suggested that low dose primaquine regimens retain adequate efficacy in some areas, but not uniformly. The efficacy and safety of high dose primaquine regimens need to be assessed in a range of endemic and geographical locations (John et al., 2012). Tefanoquine, like primaquine, belongs to the class of 8-aminoquinolines and is being developed for radical cure (blood and liver stage elimination) of *P. vivax* malaria. Recent reports in *P. cynomolgi*-infected rhesus monkeys, demonstrated ten-fold lower doses

(1.8 mg/kg vs 18 mg/kg) may be effective against *P. vivax* hypnozoites if the drug is deployed in combination with a blood-schizonticidal drugs than as monotherapy (Dow et al., 2011).

Although murine and monkey malaria models are useful tools to screen and characterize drug candidates, they also present limitations. Firstly, the plasmodia species can differ significantly in their degree of infection, lethality and synchronicity which could affect the results compared to human plasmodia species (Fidock et al., 2004). Secondly, species differences might make the extrapolation from one to another *Plasmodium* not accurate (Langhorne et al., 2011). However, all the standard antimalarial drugs available have demonstrated efficacy in both mouse and monkey model for blood stage and liver stage malaria, respectively. Hence, it is reasonable to expect new chemical entities to do the same as a filter before entering into clinical trials. Ideally, since these animal models are resource and time intensive, it would be very valuable to identify assays and readouts to screen and prioritize promising candidates before moving into lengthy animal pharmacology studies.

1.4 Drug Discovery Strategies

Drug discovery and development is risky, expensive and lengthy (Dickson and Gagnon, 2004b). The high attrition rate for new chemical entities is largely responsible for the high cost of bringing drugs to market. Most drug candidates fail before they reach the clinic, and only one in nine compounds makes it through development and gets approval by the regulatory authorities and finally reaches the market (Nwaka and Ridley, 2003). In 2001, the average

cost of discovering and developing a new drug was in the order of US $800 million; current estimates are closer to approximately US $900 million (Alanine et al., 2003; Rawlins, 2004). Further, drug development is a lengthy process. As an example, it took in average 12 years and 10 months for the drugs approved in 2002 to be developed (Figure 9) (Dickson and Gagnon, 2004a). Rigorous "go/no-go" decision criteria are important early in drug discovery and development (Alanine et al., 2003) to select and progress the most promising candidates.

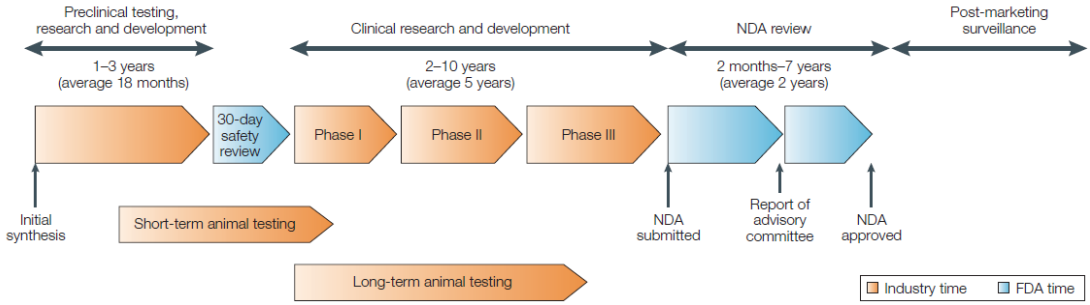

Figure 9. Drug development process and time involvement. Reprinted by permission from Macmillan Publishers Ltd: Dickson and Gagnon (2004a)

Drug discovery is an articulated process that consists of following phases: target selection, target validation, hit identification, lead identification, lead optimization and candidate selection (Figure 10). It is integrative in nature, based on close interactions, communication and collaboration between scientists with different core expertise (e.g. chemistry, biology, pharmacology and pharmacokinetics) and involves iterative cycles (Alanine et al., 2003; Bleicher et al., 2003). The challenge of any drug discovery effort is to identify and develop compounds that will be efficacious and safe in humans (Fidock et al., 2004). During the early drug discovery phase, it is important to define the ideal Target Product Profile (TPP) for a particular indication. The progression

criteria (i.e., potency, efficacy, physicochemical properties, pharmacokinetics and toxicological properties) are specified based on the standard of care (Gabrielsson et al., 2009).

Drug discovery starts conventionally with the screening of chemical libraries against a specific drug target (biochemical assay) or in whole cell (phenotypic assay). They result typically in a large number of compounds (hits) that need to be followed up on. As a consequence, the corresponding assays must be high throughput, conservative in sample use, inexpensive and rapid (Kerns and Di, 2003). Promising hits from a screening campaign can be developed into lead series following a comprehensive assessment of chemical integrity, synthetic robustness, structure-activity relationships (SAR), as well as bio-physicochemical properties (Fidock et al., 2004).

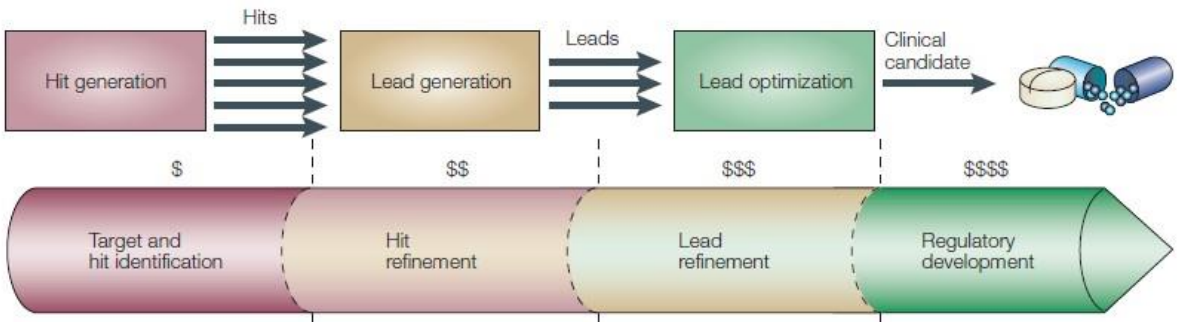

Figure 10. Drug discovery process. Reprinted by permission from Macmillan Publishers Ltd: Bleicher et al. (2003)

Lead identification can be driven through chemical modification of the hits to achieve improved potency, safety or ease of synthesis (Alanine et al., 2003). SAR is explored to derive the relationship between molecular properties of drugs and their activity. Structure-pharmacokinetic relationship (SPR) is investigated to identify which structural modifications lead to improved absorption, distribution, metabolism and elimination (ADME) properties (Figure 11). These relationships once established could be useful to

predict the properties of new compounds. Promising lead series are progressed to lead optimization (Kerns and Di, 2003).

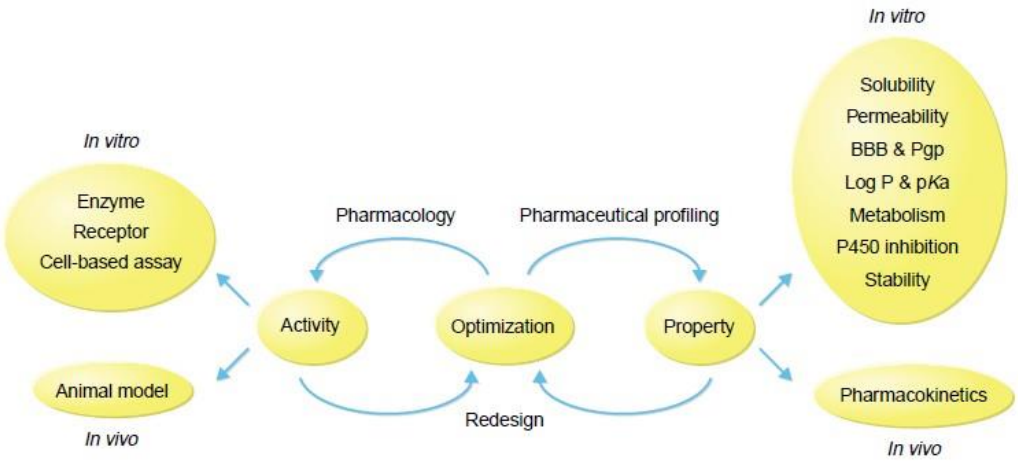

Figure 11. Parallel optimization of SAR and SPR. Reprinted from Di and Kerns (2003), with permission from Elsevier.

Lead optimization (LO) is labor intensive and perhaps the most important phase in drug discovery, as many compounds fail at this stage. It is imperative that each LO project has multiple leads or lead series, since the dropout rate is typically ~ 25-50% (Alanine et al., 2003). The overall properties of the lead compounds are optimized by structural modifications and the most promising drug candidates are selected for further evaluation. Applying ISIVIVC to predict PK properties at this stage is useful and reduces the turnaround time. Balancing all properties is challenging. The goal is to identify compounds that meet the proposed target product profile. Further PK and toxicological assessments in rodents and non-rodents follow not only because of regulatory requirements, but also more importantly to predict the clinical outcome. Pharmacokinetic-pharmacodynamic relationships established in relevant preclinical models can be a useful guide for human dose predictions (Gabrielsson and Weiner, 2006). Development candidates also need to be easy to manufacture, stable, readily formulated, bioavailable,

have an acceptable half-life and be well tolerated (Fidock et al., 2004). Early understanding of the liabilities of a compound class, *in silico - in vitro - in vivo* correlations, dose-response relationship and early integration of PK-PD analysis are important to reduce attrition and maximize success of drug discovery and development (Gabrielsson et al., 2009).

In summary, there is a need for new drugs with novel mechanism of actions against tuberculosis and malaria. Given the various challenges, it is imperative early on in the drug discovery programs to identify surrogate readouts and assays for screening and selecting the most promising candidates to progress into lengthy animal pharmacology studies and later into clinical studies. In this context, we have undertaken the effort to evaluate *in silico - in vitro - in vivo* correlations for standard TB drugs (chapter 3) and PK-PD relationships for a class of nitroimidazoles (chapter 4) and spiroindolones (chapter 5) for the treatment of tuberculosis and malaria, respectively.

1.4.1 *In silico – in vitro – in vivo* correlations

It is widely recognized that, apart from *in vitro* potency at the desired target, physicochemical as well as absorption, distribution, metabolism and elimination properties need to be considered for the selection of drug candidates. Studies in the late 1990s pointed out poor PK and toxicity as important causes of costly late-stage failures in drug development. Following such studies, a battery of tests to assess ADME properties as well as potential toxicity of test compounds were integrated in the early stages of drug discovery and resulted in a dramatic reduction of attrition associated with poor drug exposure (Figure 12) (Kola and Landis, 2004).

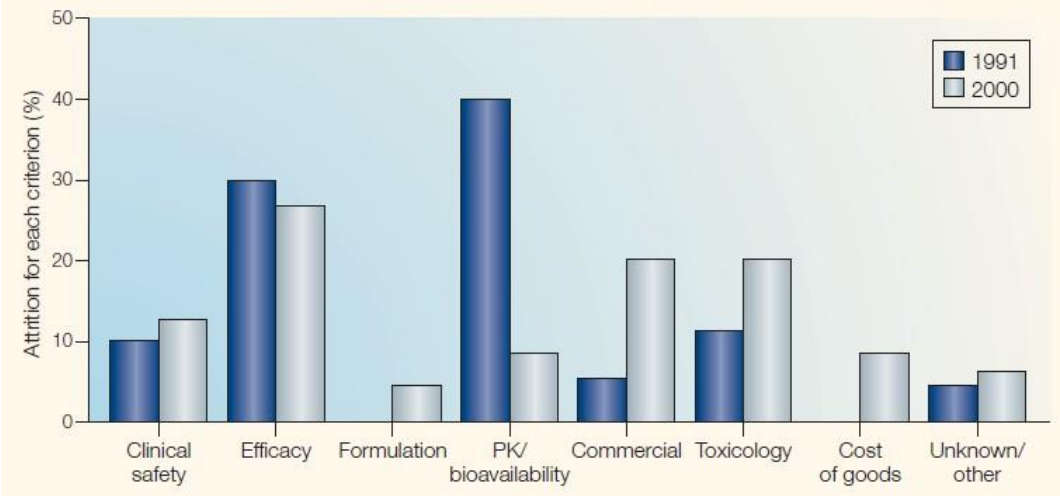

Figure 12. Reasons for attrition (1991 - 2000). Reprinted by permission from Macmillan Publishers Ltd: Kola and Landis (2004).

Although clinical trials are indispensable to ultimately demonstrate efficacy and safety of novel therapeutic agents, in the early phases of drug discovery when dealing with large numbers of compounds an efficient multi-dimensional approach is necessary. There are three categories of experiments: *in vitro* (Latin for within the glass), *in vivo* (Latin for within the living) and *in silico* (performed on computer) studies. Each of them has pros and cons. Understanding the limitation of each approach is the key to apply them effectively to accomplish the objective. Establishing ISIVIVC is particularly valuable when such correlations can be used to predict certain properties (e.g. clearance, half-life or bioavailability), thus decreasing cost and turnaround time (Figure 13). An additional advantage offered by the predictive approach is the decreased animal usage (Durairaj et al., 2009). The relationship between physicochemical properties and PK has been investigated for drugs in various indications: neuromuscular blocking agents (Proost et al., 1997), bisphosphonates (Hirabayashi et al., 2001), beta adrenergic antagonists and dihydropyridine calcium channel antagonists (van de Waterbeemd et al., 2001;

van De et al., 2001). The outcome suggests that PK can be optimized by modulating physicochemical properties.

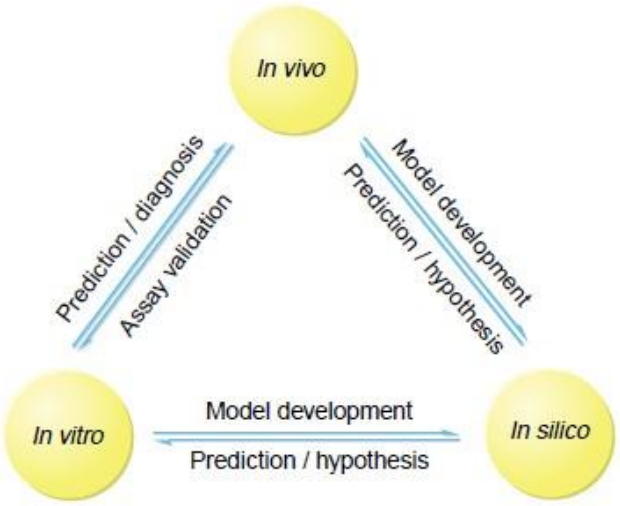

Figure 13. *In silico - in vitro - in vivo* relationship. Reprinted from Di and Kerns (2003), with permission from Elsevier.

Lipophilicity appears to be one of the key physicochemical parameters with an impact on various PK properties. It is often computed *in silico* or determined experimentally and has been widely used to build structure property relationships. The ability of molecules to partition into biological membranes is governed by molecular size and lipophilicity and hence they are the major factors in determining drug disposition. Increasing molecular weight often leads to higher lipophilicity resulting in higher potency, but also contributes to decreased dissolution/solubility limiting oral absorption (van de Waterbeemd et al., 2001). Increasing lipophilicity influences permeability, plasma protein binding (PPB) and volume of distribution (V_d). Further, highly lipophilic compounds also become more prone to P450 metabolism, resulting in increased clearance (Davis et al., 2000; Proost et al., 1997; Smith et al., 1996; van de Waterbeemd et al., 2001; van De et al., 2001). Activity, physicochemical parameters and developability of a compound need to be

balanced against each other. For this reason early understanding of the *in silico - in vitro - in vivo* relationship for a compound class is important and can lead to the identification of candidates with optimal properties in a more efficient and faster way.

In this context, we have undertaken the effort to evaluate and understand the *in silico - in vitro - in vivo* correlations for standard TB drugs (chapter 3).

1.4.2 Pharmacokinetic-Pharmacodynamic (PK-PD) relationships

In vitro potency, physicochemical and PK properties are the critical determinants of *in vivo* efficacy. Understanding PK-PD relationships in drug discovery is important to select the best compound among many, guide lead optimization, design optimal pharmacology experiments, minimize attrition rate and eventually guide human dose prediction and or support clinical trial preparation.

In modern antibiotic drug development, PK-PD principles are applied to select doses and dosing regimens. The PK profiles obtained in animal models and human volunteers are combined with values of drug potency *in vitro* and efficacy in animal models to calculate PK-PD indices that inform rational trial design (Craig, 1998; Craig, 2001; Scaglione and Paraboni, 2006). Based on this approach, antibiotics have been classified as exerting concentration-dependent or time-dependent killing. PK-PD parameters such as AUC/MIC (area under the curve/minimum inhibitory concentration) and C_{max}/MIC (maximum concentration/minimum inhibitory concentration) correlate to the efficacy of concentration dependent killing agents while time

during which serum levels remain above MIC ($T_{>MIC}$) correlate to the efficacy of time dependent killing agents (Figure 14) (Craig, 1998; Schuck and Derendorf, 2005). Regardless of the specific efficacy driver, this information has enabled the selection of dosing regimens that optimize clinical efficacy while suppressing the emergence of resistant organisms, and has supported the determination of clinically relevant susceptibility breakpoints (Drusano, 2007).

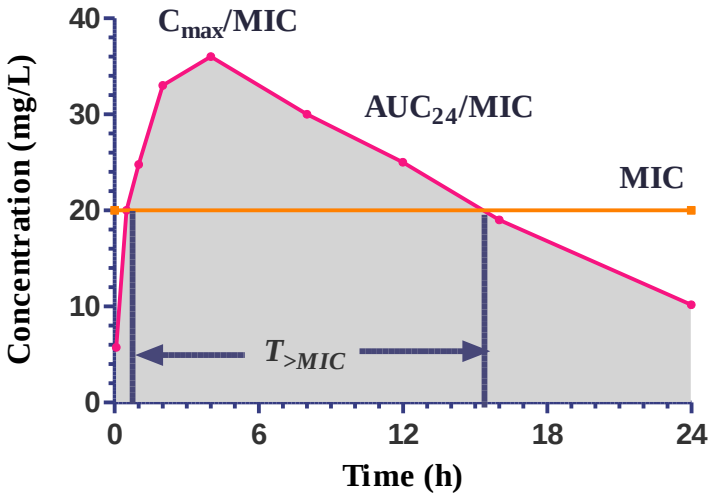

Figure 14. PK-PD indices used in anti-infectives. Redrawn from Schuck and Derendorf (2005)

1.4.2.1 PK-PD for antibacterials

PK-PD principles are well established for some antibacterial drugs but are not universally understood for all antibiotic classes. Fluoroquinolones, for example, display concentration dependent killing and bactericidal effect against gram-negative bacilli was observed at a C_{max}/MIC of >12 or AUC/MIC of $\geq$ 100-125. Maximum activity of fluoroquinolones is achieved when the AUC/MIC exceeds 250 (Figure 15) (Craig, 2001; Wright et al.,

2000). Penicillins and cephalosporins show time dependent killing. Bacteriostatic effect is observed with 30-40% of $T_{>MIC}$, maximum effect is observed with 60-70% of $T_{>MIC}$ (Figure 16).

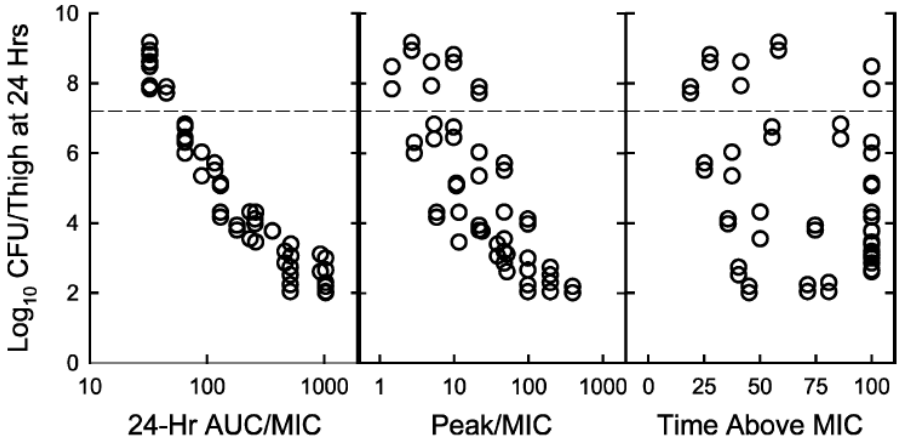

Figure 15. PK-PD relationship for levofloxacin in a thigh infection model of *S. pneumonia.* Reprinted from Andes and Craig (2002), with permission from Elsevier.

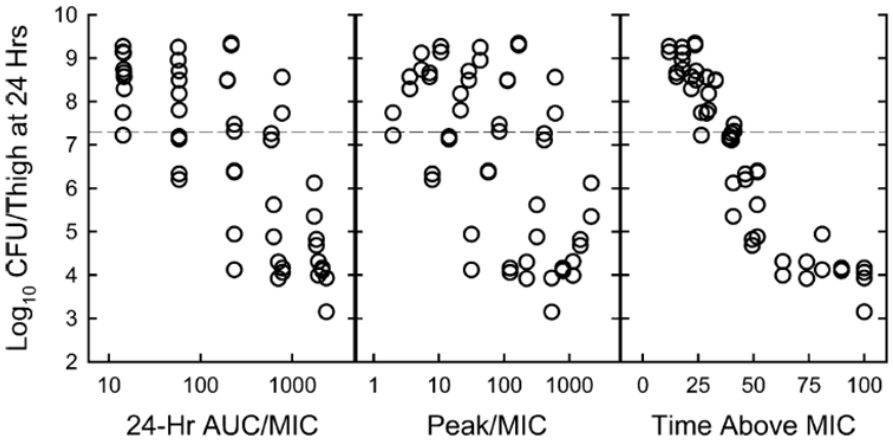

Figure 16. PK-PD relationship for ceftazidime in a lung infection model of *K. pneumonia.* Reprinted from Andes and Craig (2002), with permission from Elsevier.

Generally, the correlation between antibacterial effect and PK-PD indices is similar for compounds belonging to the same class. Examples are fluoroquinolones (Figure 17A), penicillins, cephalosporins and carbapenems against various pathogens in the lungs and thighs of neutropenic mice (Figure 17B). As a consequence, the magnitude of the effect shown by a compound

can be predicted using *in vitro* potency and *in vivo* PK (C_{max}/MIC, AUC/MIC and $T_{>MIC}$) (Andes and Craig, 2002).

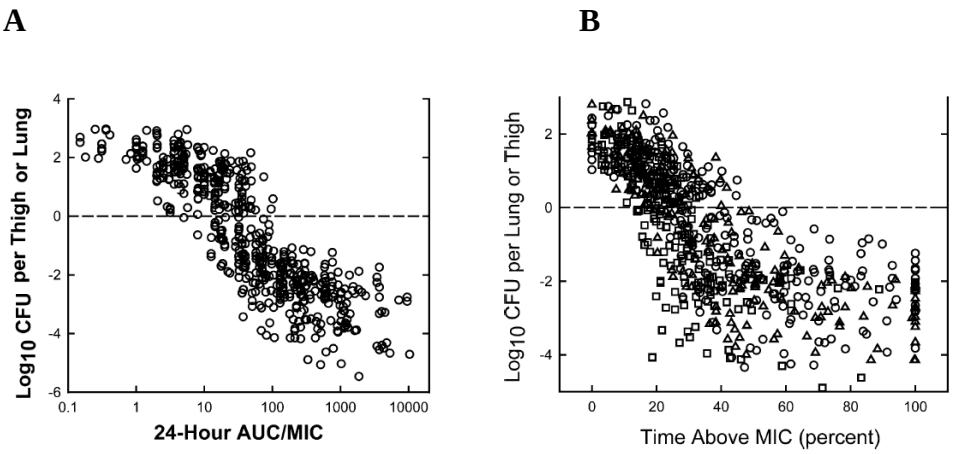

Figure 17. PK-PD relationship of various fluoroquinolones (A); penicillins, cephalosporins and carbapenems (B) in different models of infection. Reprinted from Andes and Craig (2002), with permission from Elsevier.

Which PK-PD index best correlates with efficacy depends on several factors, including mechanism of action and kill kinetics. As a general rule, antimicrobial agents that act via the inhibition of an enzyme or the bacterial growth display concentration dependent killing and their efficacy correlate well with the AUC/MIC or C_{max}/MIC. Conversely, antimicrobials that act on the cell wall display time-dependent killing and their efficacy correlate with $fT_{>MIC}$ (Barbour et al., 2010). Once the relationship is established for a compound class, it can be applied to new compounds of the same class to predict their efficacy and prioritize the most promising ones. Overall, understanding the PK-PD relationship of a class of compounds early on is important for lead optimization and for optimal study design and certainly contributes to a successful program.

1.4.2.2 PK-PD for Tuberculosis

In the last decade PK-PD relationships for standard TB drugs in preclinical murine models were established. AUC/MIC is the PK-PD parameter that best correlated with the *in vivo* efficacy for rifampicin (Jayaram et al., 2003), isoniazid (Jayaram et al., 2004), fluoroquinolones (moxifloxacin, ofloxacin and sparfloxacin) (Shandil et al., 2007) and TMC207 (Rouan et al., 2012). % $T_{>MIC}$ is the PK-PD parameter that best described the *in vivo* efficacy for PA-824 (Ahmad et al., 2011). Based on the results obtained for rifampicin, further clinical studies have been initiated to optimize the clinical dose (Burman et al., 2011; Rosenthal et al., 2012; Steingart et al., 2011; van et al., 2011). This illustrates the importance and the potential impact of a thorough understanding of the relationship between drug exposure and antibacterial effect for new and existing TB drugs.

In this context, we have undertaken the effort to evaluate the PK-PD relationship for a class of nitroimidazoles (chapter 4) currently under preclinical evaluation as potential treatment against TB.

1.4.2.3 PK-PD for Malaria

PK-PD relationships are not well understood for antimalarial drugs and therapeutic strategies are largely based on empirical clinical evidence. Many antimalarials in use today were developed and clinically tested before the modern era of rational dose selection. The doses and dose regimens in initial clinical trials, including those for the newer and most effective artemisinin

derivatives (Gautam et al., 2009), were derived empirically (Newton et al., 2006).

In recent years, numerous drug monitoring programs have been launched to assess the adequacy of doses and to model dose-response in uncomplicated and severe malaria (Hoshen et al., 2001; Svensson et al., 2002; White et al., 2008). Quantitative PD read-outs, such as parasitemia, parasite clearance rates, and parasite clearance time, have been used to assess parasitological response to treatment in relation to clinical outcome (Ashley et al., 2008; White, 2002). Based on these more precise definition of clinical and parasitological responses (Price et al., 2007), new drug combinations have been proposed (D'Alessandro, 2009; Hoshen et al., 2002), and doses have been revised when required (Newton et al., 2006). Although a standardized relationship between parasitological responses *in vitro* and clinical outcome remains to be fully established (White, 1997), progress has been made in understanding the PK-PD relationship for standard antimalarial drugs such as chloroquine and artimisinin (Bakshi et al., 2013). The field is clearly moving towards the rational selection of dose, dosing frequency and duration of antimalarial treatment (White, 2013).

In this context, we have undertaken the effort to evaluate the PK-PD relationship for a class of spiroindolones (chapter 5) currently in clinical development for the treatment of malaria.

Chapter 2. Hypotheses and Objectives

Hypotheses and Objectives

Two working hypotheses are proposed in this thesis. The first hypothesis addresses the relationship between the physicochemical properties and the pharmacokinetic parameters of the anti-mycobacterial compounds. The second hypothesis, addresses the complex nature of the PK-PD relationship with specific emphasis on two classes of anti-mycobacterial and anti-malarial compounds, respectively.

In recent years there has been an increase in the understanding of the relationship between several parameters during early drug discovery. The *in silico – in vitro – in vivo* relationship between various physicochemical and pharmacokinetic parameters of drug molecules have been established in other therapeutic areas (Section 1.4.1). However, this kind of analysis is lacking for the anti-mycobacterial compounds.

<u>Hypothesis 1</u>: The pharmacokinetic properties of anti-mycobacterial candidates are dependent on their physicochemical properties and once a relationship is established between these two parameters; it can be used to predict the PK parameters of a new compound from its physicochemical properties. This hypothesis will be tested in Part 1 with the standard anti-mycobacterial compounds.

The first part of the research project is to profile the standard anti-mycobacterial drugs currently available in the market or undergoing preclinical and clinical development. These drugs belong to different chemical class and display different mechanism of action. Nevertheless, the pharmacokinetic properties of all drugs are dependent on their physicochemical properties but not on their mechanism of action. Hence, the

objective of the part I study is to identify physicochemical properties of anti-mycobacterial candidates and their influence on the pharmacokinetic profiles. Specific objectives were:

- Systematic compilation of *in silico* physicochemical properties for a set of 36 anti-mycobacterial compounds.
- Evaluate *in vitro* PK parameters.
- Systematic compilation of the *in vivo* pharmacokinetic parameters.
- Establish the correlations between the *in silico, in vitro* and *in vivo* parameters.

Secondly, there is an increased awareness in understanding the relationship between pharmacokinetic and pharmacodynamics properties to facilitate the early drug discovery programs. These relationships have been established for several classes of anti-infective agents (Section 1.4.2). However, this kind of analysis is lacking for the anti-mycobacterial and anti-malarial compounds.

Hypothesis 2: The PK-PD correlation established from the lead compounds in the anti-mycobacterial and anti-malarial agents can be applied for analogs from the same classes of compounds, provided they share the same mechanism of action. This hypothesis will be tested in Part 2 (the nitroimidazole analogs of the anti-mycobacterial compounds) and Part 3 (the spiroindolone analogs of the anti-malarial compounds) of this thesis.

The second part of the research project is to evaluate the PK-PD relationships for compounds belonging to the chemical class of the nitroimidazoles. Dose fractionation PK-PD studies in mice indicate that the efficacy of PA-824 is driven by the time during which its free plasma

concentration is above its minimum inhibitory concentration. To test our hypothesis, we evaluated whether the same PK-PD relationship holds true for nitroimidazole analogs sharing the same mechanism of action. Specific objectives were:

- A panel of closely related bicyclic 4-nitroimidazoles was profiled in *in-vitro* potency and physicochemical assays.
- Evaluation of the *in vivo* pharmacokinetic parameters.
- Evaluation of the *in vivo* efficacy.
- Systematic PK-PD analysis was done to identify the efficacy driver.

The third part of the research project was to evaluate the PK-PD relationships for compounds belonging to the chemical class of the spiroindolones. KAE609, a spiroindolone analog, is currently in phase II clinical development and represents a promising potential treatment for malaria. The objective of this third part of the study was to assess dose-response relationship for a class of compounds and PK-PD relationship for the lead compound KAE609 in mice to determine whether the efficacy is concentration dependent or time dependent. Specific objectives were:

- A panel of closely related spiroindolones was profiled in both *in vitro* potency and *in vitro* pharmacokinetic assays.
- Evaluation of the *in vivo* pharmacokinetic parameters.
- Establish dose-response relationship for a class of spiroindolone analogs.
- Pharmacokinetic modeling for KAE609.
- Dose fractionation studies for KAE609.
- Derive PK-PD driver for current frontrunner KAE609.

Chapter 3. Comprehensive physicochemical, pharmacokinetic and activity profiling of anti-tuberculosis agents

3.1 Introduction

Studies in the late 1990s indicated that poor PK and toxicity were the common causes of many costly late-stage failures in drug development. In light of these situations, a battery of tests to assess ADME properties as well as potential toxicity of new drug candidates, were integrated in the early stages of drug discovery and resulted in a dramatic reduction of attrition associated with PK- and toxicity-related factors (Kola and Landis, 2004). Physicochemical parameters affect absorption, oral bioavailability and other ADME parameters. Experimental and computational analyses of very large sets of small molecule drugs resulted in various empirical rules such as, Lipinski's Rule of Five, whereby poor absorption or permeation is more likely if a compound exhibits one or more of the following properties: molecular weight (MW) >500, cLogP >5, hydrogen bond donors (HBD) >5 or acceptors (HBA) >10 (Lipinski et al., 2001). Veber's rule added that compounds with less than 10 rotatable bonds and a polar surface area (PSA) <140 $Å^2$ are more likely to have good oral bioavailability (Veber et al., 2002). Further Gleeson's analysis revealed that almost all ADME parameters (solubility, permeability, bioavailability, volume of distribution, plasma protein binding and clearance) are compromised with either increasing molecular weight, logP, or both. In general, as the MW and/or logP increases, the solubility, permeability and bioavailability decreases while the *in vivo* clearance increases, thus recommending MW <400, and cLogP <4 to improve ADME parameters (Gleeson, 2008). In addition, Egan showed that cLogP and PSA could be used as a tool (Egan Egg model) for predicting good passive gut absorption (Egan et al., 2000).

In the early drug discovery, emphasis is most often placed on the *in vitro* potency, while desirable physicochemical and PK parameters are considered as secondary attributes in the decision making process. To be efficacious, anti-infectives have to (i) effectively penetrate the microbe and inhibit an essential cellular process and (ii) reach the site of infection – lung tissue and lesions for pulmonary TB. Hence, the chemical space occupied by antibacterials (O'Shea and Moser, 2008) and anti-mycobacterials (Koul et al., 2011) is distinct from that of drugs targeting non-infectious diseases.

Recently, a comprehensive analysis (Franzblau et al., 2012) of various microbiological and animal study protocols used by different TB research groups was carried out. A guide for medicinal chemist to optimize compounds against TB has also been discussed (Cooper, 2013; Dartois and Barry, III, 2013). Further, physicochemical, biopharmaceutical and clinical PK-PD properties of selected anti-TB compounds and novel agents under development have been reviewed (Brennan and Young, 2008; Budha et al., 2008; Dartois and Barry, 2010; Davies and Nuermberger, 2008; Holdiness, 1984; Nuermberger and Grosset, 2004; Vaddady et al., 2010). These reviews do not include comparative analyses and correlation between *in silico* parameters, including the *in vitro* potency, *in vitro* PK and *in vivo* PK properties. Hence, in this chapter, we have collated the *in vitro* potency and *in vitro* PK parameters for a set of 36 compounds generated using the standardized procedures. *In silico* physicochemical and *in vivo* pharmacological parameters were also compiled. We have used computational approaches to seek relationships between *in silico* properties, *in vitro* potency, *in vitro* PK and human *in vivo* PK parameters, with the objective to develop a

correlation that will help guiding early drug discovery efforts against TB. Not surprisingly, lipophilicity emerged as a major factor driving *in vitro* and *in vivo* PK properties.

3.2 Materials and Methods

3.2.1 Chemicals

All the standard compounds were obtained from commercial sources (Sigma-Aldrich, Sequoia research products and Cayman chemicals) except bedaquiline (TMC-207), PA-824, delamanid (OPC-67683), valnemulin and PNU-100480 which were synthesized at Novartis (Table 3). Stock solutions of the compounds were prepared using 90% DMSO. The 36 compounds used in the study were isoniazid, rifampicin, pyrazinamide, ethambutol, streptomycin, kanamycin, amikacin, *p*-aminosalicylic acid, cycloserine, ethionamide, rifabutin, rifapentine, moxifloxacin, levofloxacin, gatifloxacin, ciprofloxacin, ofloxacin, sparfloxacin, capreomycin, thioacetazone, linezolid, prothionamide, clarithromycin, amoxicillin, clavulanate, meropenem, clofazimine, metronidazole, thioridazine, mefloquine, vancomycin, valnemulin, PNU-100480, PA-824, bedaquiline and delamanid.

3.2.2 Physicochemical parameters

Molecular weight, cLogP (calculated octanol:water partitioning coefficient), PSA (which measures the surface sum of overall polar atoms), rotatable bonds, HBD and HBA were generated using proprietary software based on standard algorithms (Medchem FOCUS).

3.2.3 *In vitro* potency and cytotoxicity

Minimum inhibitory concentration (MIC_{50}) was determined using the lab strain Mtb H37Rv by turbidimetric assay as described previously (Kurabachew et al., 2008; Pethe et al., 2010) (Appendix 1). Cytotoxicity was tested in hepatocyte cell line (HepG2) (ATCC, #HB-8065) for hepatotoxicity and baby hamster kidney cell line (BHK21) (ATCC, #CCL-10) for renal toxicity, in 96-well microplates as described elsewhere (Pethe et al., 2010). Briefly, the cells were seeded at a density of 10^5 cells per mL, incubated at 37 ° C for 24 h and exposed to twofold serial diluted compounds for 3 days. Cell viability was monitored using the Cell Proliferation Kit II (Invitrogen). Relative fluorescence units were measured at OD_{450}, using a Tecan Safire^2, and CC_{50} curves were plotted using Graph Pad Prism 5 software.

3.2.4 *In vitro* PK studies

In vitro PK parameters such as solubility, permeability [parallel artificial membrane permeability assay (PAMPA) and colon carcinoma cell line (Caco-2) assay], metabolic stability in mouse and human liver microsomes were measured at Cyprotex using standard protocols as described at www.cyprotex.com/admepk/ (Obach, 1999; Wohnsland and Faller, 2001). Thirty two compounds were profiled in various assays. Thermodynamic solubility was determined in phosphate buffer saline (PBS) buffer at pH 7.4 using high performance liquid chromatography (HPLC). For solubility (mg/mL) mean values from two independent replicates are given. Mean apparent permeability (P_{app} with units being 10^{-6} cm/sec) values from four

replicates are given for PAMPA permeability. Caco-2 permeability was provided as mean P_{app} (10^{-6} cm/sec) (1) from apical to basolateral (A-B), and (2) from basolateral to apical (B-A), as well as the ratio between the two values, from two independent replicates. *In vitro* metabolic stability in both mouse and human liver microsomes was determined and their intrinsic clearance (CL_{int}, µL/min/mg protein) values are given. PAMPA, Caco-2 permeability and metabolic stability sample analysis was carried out using optimized LC-MS/MS methods (Appendix 2). Plasma protein binding data were obtained either from published literature (section 3.2.6) or *in silico* methods using GastroplusTM 8.5, simulations Plus, Inc. (www.simulations-plus.com).

3.2.5 Mouse *in vivo* PK and efficacy studies

All procedures involving mice were reviewed and approved by the institutional animal care and use committee of the Novartis Institute for Tropical Diseases. Animal studies were carried out in accordance with the Guide for the Care and Use of Laboratory Animals. All animals were kept under specific pathogen-free conditions and fed water and chow *ad libitum*, and all efforts were made to minimize suffering or discomfort.

In vivo PK data for ethambutol, cycloserine, ethionamide, mefloquine, clofazimine, valnemulin and PA-824 were obtained in CD-1 female mice. For isoniazid, rifampicin, pyrazinamide, moxifloxacin, linezolid, and bedaquiline, PK parameters were compiled from the literature (Table 6). The compounds were formulated either in 0.5% carboxy methyl cellulose or 10% hydroxypropyl-beta-D-cyclodextrin; 10% lecithin (PA-824) (Stover et al.,

2000) suspension and administered orally at doses ranging from 10 to 200 mg/kg. Blood samples were collected by retro-orbital bleeding at various time points (0.08 to 24 h) post-dose. All procedures during pharmacokinetic experiments were performed under isoflurane anesthesia (Diehl et al., 2001). Groups of three mice were used for each time point. Blood was centrifuged at 13,000 rpm for 7 min at 4 ºC, and plasma was harvested and stored at –20 ºC until analysis. Plasma samples were analyzed using optimized LC-MS/MS conditions and PK parameters were calculated using WinNonLin software version 5.1.

In vivo acute mouse efficacy studies were carried out as described earlier (Pethe et al., 2010). Briefly, animals were infected intranasally with 10^3 Mtb H37Rv bacilli. One week post-infection animals were treated for one month with the appropriate dose. At 2 and 4 weeks post dosing, the lungs were aseptically removed, homogenized and the bacterial load were estimated by plating serial dilutions on 7H11 agar plates. Mean log cfu reductions (mean value ± SD) were calculated from five animals at each time point and compared to untreated controls.

3.2.6 Human *in vivo* PK properties

Human PK data were obtained from published literature: isoniazid (Brennan et al., 2008; Brunton et al., 2010; Nuermberger and Grosset, 2004; Vaddady et al., 2010), rifampicin (Brennan et al., 2008; Brunton et al., 2010; Nuermberger and Grosset, 2004; Vaddady et al., 2010), pyrazinamide (Brennan et al., 2008; Brunton et al., 2010; Nuermberger and Grosset, 2004), ethambutol (Brennan et al., 2008; Brunton et al., 2010; Vaddady et al., 2010), streptomycin (Brennan

et al., 2008; Dartois and Barry, 2010; Obach et al., 2008), kanamycin (Brennan et al., 2008; Dartois and Barry, 2010; Obach et al., 2008), amikacin (Brennan et al., 2008; Brunton et al., 2010; Dartois and Barry, 2010), p-aminosalicylic acid (Brennan et al., 2008; Dartois and Barry, 2010), cycloserine (Brennan et al., 2008; Dartois and Barry, 2010), ethionamide (Brennan et al., 2008; Dartois and Barry, 2010), rifabutin (Brennan et al., 2008; Dartois and Barry, 2010; Obach et al., 2008), rifapentine (Brennan et al., 2008; Nuermberger and Grosset, 2004), moxifloxacin (Brennan et al., 2008; Brunton et al., 2010; Dartois and Barry, 2010; Nuermberger and Grosset, 2004), levofloxacin (Brunton et al., 2010; Dartois and Barry, 2010; Nuermberger and Grosset, 2004), gatifloxacin (Brennan et al., 2008; Brunton et al., 2010; Dartois and Barry, 2010; Nuermberger and Grosset, 2004; Obach et al., 2008), ciprofloxacin (Brunton et al., 2010; Dartois and Barry, 2010; Nuermberger and Grosset, 2004), ofloxacin (Brunton et al., 2010; Dartois and Barry, 2010; Nuermberger and Grosset, 2004), sparfloxacin (Nuermberger and Grosset, 2004; Obach et al., 2008), capreomycin (Brennan et al., 2008; Dartois and Barry, 2010), thioacetazone (Vaddady et al., 2010), linezolid (Brennan et al., 2008; Dartois and Barry, 2010; Obach et al., 2008), prothionamide (Dartois and Barry, 2010), clarithromycin (Brennan et al., 2008; Obach et al., 2008), amoxicillin (Dartois and Barry, 2010; Obach et al., 2008), clavulanate (Dartois and Barry, 2010; Obach et al., 2008), meropenem (Obach et al., 2008), clofazimine (Dartois and Barry, 2010), metronidazole (Dartois and Barry, 2010; Obach et al., 2008), thioridazine (Brennan et al., 2008), mefloquine (Brunton et al., 2010; Karbwang et al., 1994), vancomycin (Healy et al., 1987; Obach et al., 2008), PNU-100480 (Wallis et al., 2010), PA-824

(Ginsberg et al., 2009), bedaquiline (Brennan et al., 2008; Dartois and Barry, 2010) and delamanid (Diacon et al., 2011). No human PK data was available in the published literature for valnemulin.

3.2.7 Statistical analysis

Correlations were tested using TIBCO Spotfire version 4.0.2 (http://spotfire.tibco.com). Statistical analysis was carried out using Prism software (GraphPad Prism, version 5.02, San Diego, California USA, www.graphpad.com). A Spearman's correlation analysis was performed to determine the relationship between various parameters.

3.3 Results and Discussion

To benchmark and compare physicochemical, potency and pharmacokinetic properties of available anti-TB agents, we experimentally determined and compiled these parameters for 36 anti-TB compounds, using standardized and centralized assays, thus ensuring direct comparability across drugs and drug classes. The compound set included first and second line anti-TB agents, clinical candidates as well as drugs that exhibited *in vitro* activity against Mtb (Table 3). Of the 36 compounds selected, 15 were natural products (compounds of natural origin and semi-synthetic derivatives) and the remaining 21 were fully synthetic molecules. The majority of these drugs are administered orally, with a few injectables. Half of the compounds were initially developed as either Gram-positive or Gram-negative antibacterials. These were introduced as part of combination regimens for the treatment of

MDR-TB, due to the emergence of resistance to first line anti-TB drugs (Table 3 and Figure 18).

Table 3. Anti-TB agents and their properties

No.	Compounds	SM / NP[#]	Route	Activity	Chemical class	Source
1	Isoniazid*	SM	Oral	TB	Pyridines	Sigma
2	Rifampicin	NP	Oral	TB/Gm+	Rifamycins	Sigma
3	Pyrazinamide*	SM	Oral	TB	Pyrazines	Sigma
4	Ethambutol	SM	Oral	TB	Ethylenediamine	Sigma
5	Streptomycin	NP	Injectable	TB/Gm+/Gm-	Aminoglycosides	Sigma
6	Kanamycin	NP	Injectable	Gm+/Gm-	Aminoglycosides	Sigma
7	Amikacin	NP	Injectable	Gm+/Gm-	Aminoglycosides	Sigma
8	*p*-aminosalicyclic acid*	SM	Oral	TB	Salicylates	Sigma
9	Cycloserine	NP	Oral	TB	-	Sigma
10	Ethionamide*	SM	Oral	TB	Pyridines (Thioamides)	Sigma
11	Rifabutin	NP	Oral	TB	Rifamycins	Sequoia
12	Rifapentine	NP	Oral	TB	Rifamycins	Sequoia
13	Moxifloxacin	SM	Oral	Gm+/Gm-	Fluoroquinolones	Sequoia
14	Levofloxacin	SM	Oral	Gm+/Gm-	Fluoroquinolones	Sigma
15	Gatifloxacin	SM	Oral	Gm+/Gm-	Fluoroquinolones	Sequoia
16	Ciprofloxacin	SM	Oral	Gm+/Gm-	Fluoroquinolones	Sigma
17	Ofloxacin	SM	Oral	Gm+/Gm-	Fluoroquinolones	Sigma
18	Sparfloxacin	SM	Oral	Gm+/Gm-	Fluoroquinolones	Sigma
19	Capreomycin	NP	Injectable	TB	Aminoglycosides	Sigma
20	Thioacetazone*	SM	Oral	TB	-	Sigma
21	Linezolid	SM	Oral	Gm+	Oxazolidinones	Sigma
22	Prothionamide*	SM	Oral	TB	Thiomides	Cayman
23	Clarithromycin	NP	Oral	Gm+	Macrolides	Sequoia
24	Amoxicillin	NP	Oral	Gm+/Gm-	Penicillins	Sigma
25	Clavulanate	NP	Oral	Gm+/Gm-	Beta Lactams	Sigma
26	Meropenem	NP	Injectable	Gm+/Gm-	Carbapenem	Sigma
27	Clofazimine	NP	Oral	Leprosy/TB	Riminophenazine	Sigma
28	Metronidazole*	SM	Oral	Anaerobic	Nitroimidazole	Sigma
29	Thioridazine	SM	Oral	Antipsychotic	Phenothiazine	Sigma
30	Mefloquine	SM	Oral	Antimalarial	Isoquinolines	Sigma
31	Vancomycin	NP	Injectable	Gm+	Polypeptides	Sigma
32	Valnemulin	NP	Oral	Gm-	Pleuromutilins	Novartis
33	PNU-100480*	SM	Oral	TB	Oxazolidinone	Novartis
34	PA-824*	SM	Oral	TB	Nitroimidazole	Novartis
35	Bedaquiline	SM	Oral	TB	Diarylquinoline	Novartis
36	Delamanid*	SM	Oral	TB	Nitroimidazole	Novartis

[#]SM, synthetic molecule; NP, natural product (including compounds of natural origin and semi-synthetic derivatives); Gm+, Gram-positive bacteria; Gm-, Gram-negative bacteria *: Pro-drug.

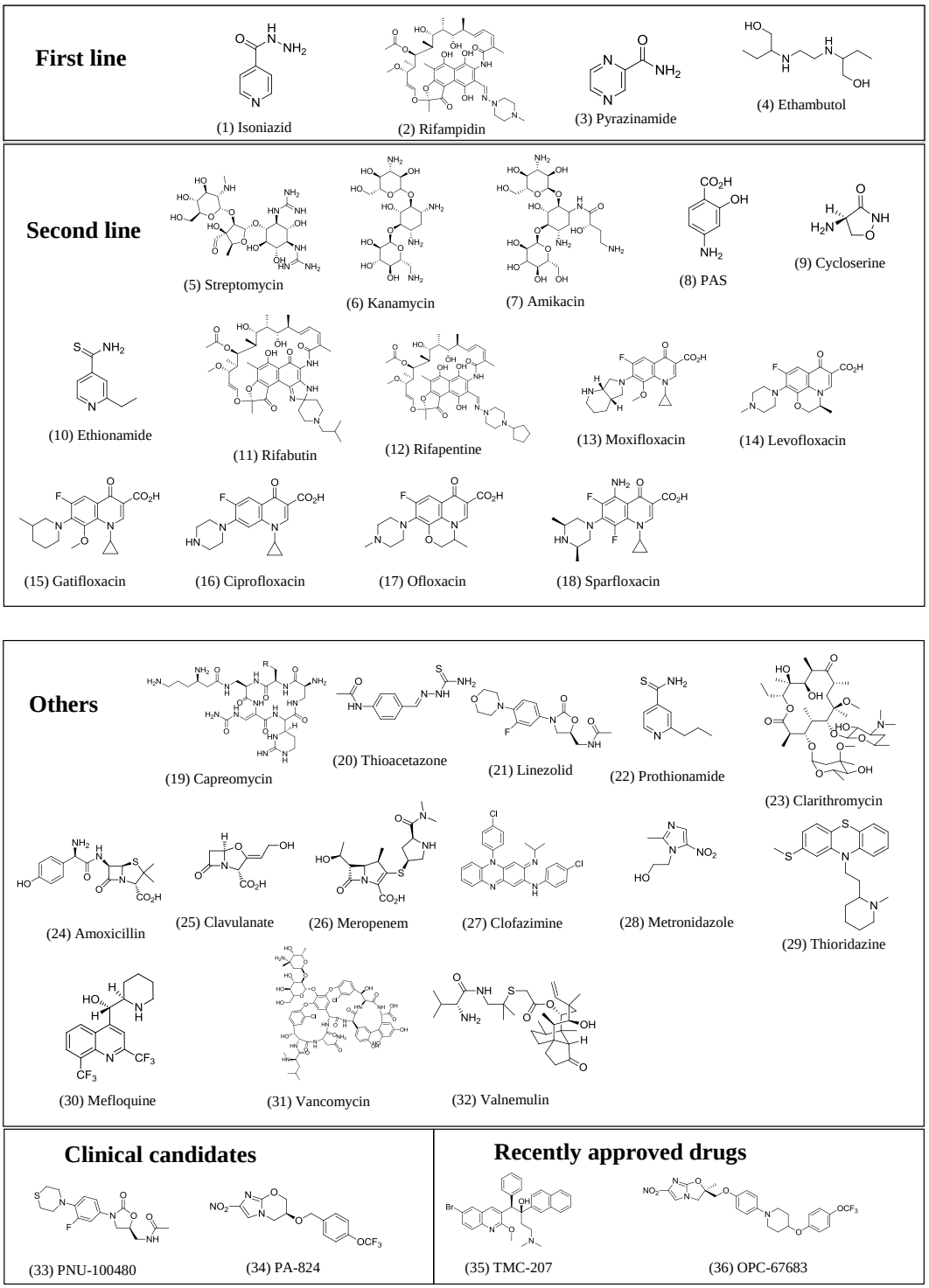

Figure 18. Chemical structures of 36 anti-TB compounds: the numbering matches Table 3

3.3.1 Physicochemical properties

Physicochemical parameters and Lipinski rule violations are presented in Table 4. Most compounds follow Lipinski's rule of five and Veber's rule with MW <500 (n=25), cLogP <5 (n=30), HBD <5 (n=29), HBA <10 (n=27), have PSA <140 $Å^2$ (n=27) and rotatable bonds <10 (n=34), which is predictive of good oral bioavailability (Table 4) (Lipinski et al., 2001; Veber et al., 2002). The majority of the compounds display acceptable drug-like properties with cLogP <5, the exception being natural product derivatives such as aminoglycosides and rifamycins (Figure 19A-E).

All compounds were subjected to the 'Egan egg' analysis (Figure 20) (Egan et al., 2000). Twenty-four compounds were within the inner ellipsoid and are therefore predicted to exhibit good passive absorption through the gastro-intestinal tract, in agreement with acceptable oral bioavailability (Table 9). Compounds falling outside the ellipsoid are natural products (Table 3). Interestingly, both rifampicin and rifapentine have good oral bioavailability in humans, suggesting that they may be actively transported (Egan et al., 2000). Amoxicillin, located on the borderline of the ellipsoid, is known to be absorbed by active transport processes (Tsuji et al., 1987).

Table 4. Physicochemical parameters

Compounds	MW	cLogP	HBD	HBA	Lipinski violations	PSA (Å^2)	RB
Isoniazid	137.14	-0.67	2	4	0	68.01	2
Rifampicin	822.96	3.71	6	16	3	220.15	5
Pyrazinamide	123.12	-0.68	1	4	0	68.87	1
Ethambutol	204.31	0.12	4	4	0	64.52	9
Streptomycin	581.58	-4.26	14	19	3	331.43	11
Kanamycin	484.51	-5.17	11	15	2	282.61	6
Amikacin	586.60	-6.36	13	18	3	326.15	10
p-aminosalicyclic acid	153.14	1.06	3	4	0	83.55	1
Cycloserine	102.09	-1.19	2	4	0	64.35	0
Ethionamide	166.25	1.73	1	2	0	38.91	2
Rifabutin	847.03	4.73	5	15	2	205.55	5
Rifapentine	877.05	5.09	6	16	4	220.15	6
Moxifloxacin	401.44	-0.08	2	7	0	86.27	4
Levofloxacin	361.38	-0.51	1	7	0	77.48	2
Gatifloxacin	374.42	3.40	1	6	0	74.24	4
Ciprofloxacin	331.35	-0.73	2	6	0	77.04	3
Ofloxacin	361.38	-0.51	1	7	0	77.48	2
Sparfloxacin	392.41	-0.61	3	7	0	103.06	3
Capreomycin	668.72	-7.06	15	22	4	375.92	10
Thioacetazone	236.30	0.88	3	5	0	79.51	4
Linezolid	337.35	0.17	1	7	0	71.11	4
Prothionamide	180.27	2.26	1	2	0	38.91	3
Clarithromycin	747.97	2.37	4	14	2	182.91	8
Amoxicillin	365.41	-1.87	4	8	0	132.96	4
Clavulanate	199.16	-1.07	2	6	0	87.07	2
Meropenem	383.47	-3.28	3	8	0	110.18	5
Clofazimine	473.41	7.70	1	4	1	44.68	4
Metronidazole	171.16	-0.46	1	6	0	86.34	3
Thioridazine	370.58	6.00	0	2	1	6.48	4
Mefloquine	378.32	3.67	2	3	0	45.15	4
Vancomycin	1449.29	-1.14	19	33		530.49	
Valnemulin	564.83	5.57	3	7	2	118.72	10
PNU-100480	353.42	1.00	1	6	0	61.88	4
PA-824	359.26	2.79	0	8	0	93.8	6
Bedaquiline	555.52	7.25	1	4	2	45.59	8
Delamanid	534.50	5.25	0	10	2	106.27	9
Anti-TB compounds n=36	428.31 (102 to 1449)	0.86 (-7.1 to 7.7)	3.78 (0 to 19)	8.59 (2 to 33)		127.71 (6.5 to 530.5)	0 to 11
Antibacterials (only gram + ve activity) n=33	813 (290 to 1880)	2.1 (-5.1 to 6.4)	7.1 (1 to 29)	16.3 (2 to 46)		243 (29 to 764)	
Antibacterials (only gram –ve activity) n=113	414 (138 to 1203)	-0.1 (-5.0 to 3.3)	5.1 (1 to 23)	9.4 (41 to 29)		165 (64 to 491)	

MW, molecular weight; cLogP, calculated logP or octanol:water partition coefficient; HBD: hydrogen bond donors; HBA: hydrogen bond acceptors; Lipinski violations, number of Lipinski rule violations (referring to Lipinski's rule of five), PSA: polar surface area; RB, rotatable bond. Mean values and ranges (in parentheses) are provided for the summary parameters. Gram-positive and Gram-negative antibacterial physicochemical parameters were obtained from O'Shea and Moser (O'Shea and Moser, 2008).

3.3.2 *In vitro* potency and cytotoxicity

Compounds displayed a wide range of MIC_{50} values from 0.01 to 11 mg/L (Table 5). Pyrazinamide, metronidazole, meropenem and amoxicillin were found to be inactive (MIC_{50} >30 mg/L). Pyrazinamide, known to be inactive in standard neutral pH medium, and require acidic pH to exert its growth inhibitory activity, showed an MIC_{50} of 25 mg/L at pH 5.5. Although metronidazole was inactive against growing Mtb, it was active against hypoxic non-growing Mtb (Wayne and Hayes, 1996). Meropenem in combination with clavulanate has shown good inhibitory activity both *in vitro* and *in vivo* (England et al., 2012; Hugonnet et al., 2009), but when tested individually neither drug showed any *in vitro* inhibitory activity. The MIC_{50} data presented in the current study are comparable to the data obtained by Franzblau and co-workers using similar media (Franzblau et al., 2012).

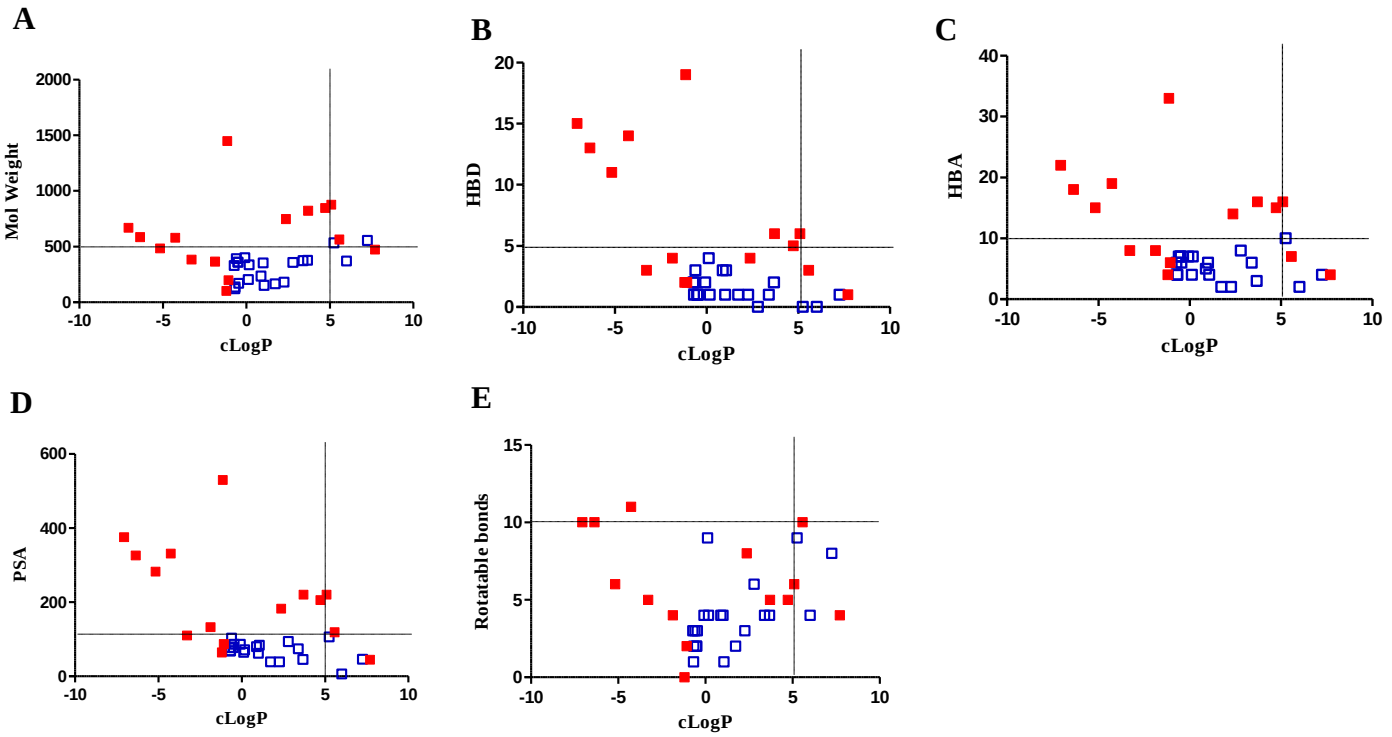

Figure 19. Physicochemical properties of anti-TB compounds and their relationship with cLogP
(A) molecular weight (B) hydrogen bond donors (HBD) (C) hydrogen bond acceptors (HBA) (D) polar surface area (PSA) and (E) rotatable bonds. The horizontal and vertical lines are the cut-offs from Lipinski's rule of five (A, B and C) and Veber's rule (D and E). The majority of the compounds lie within Lipinski's space (lower left quadrant). The compounds are categorized as synthetic molecules (blue open squares) and natural products (red filled squares) based on their origin (Table 3).

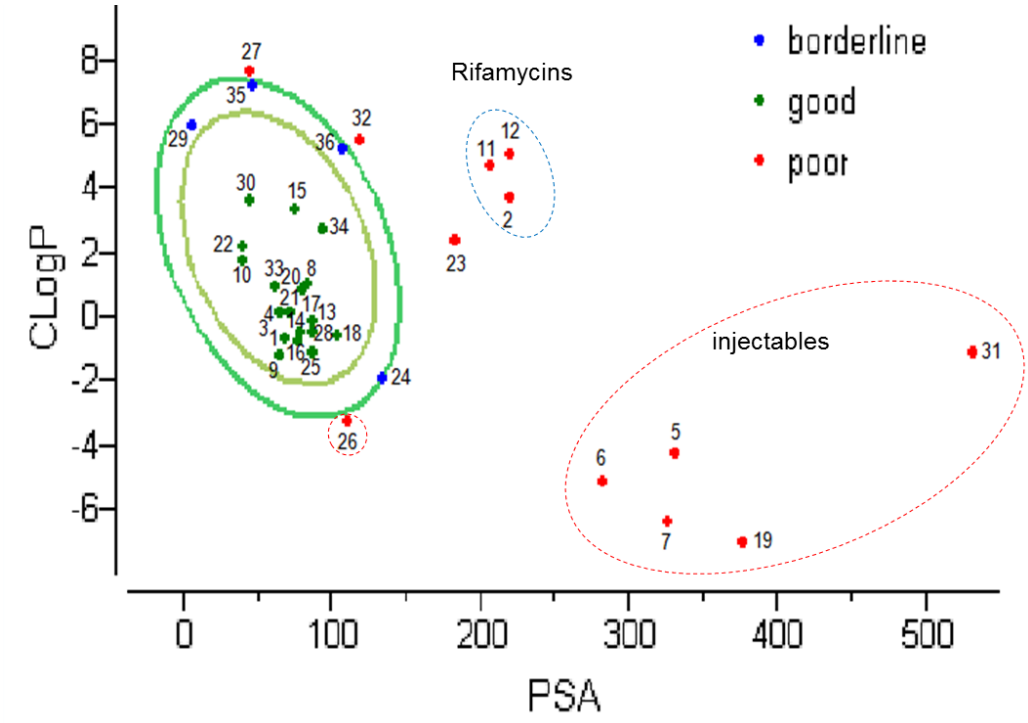

Figure 20. Egan egg analysis of 36 anti-TB compounds
The numbering of compounds is the same as in Table 3. Compounds within the ellipsoid are known to have good passive absorption and those outside have poor absorption. Compounds within the red and blue dotted circles are injectables and rifamycins, respectively.

A cytotoxicity (CC_{50}) measurement was carried out using two common cell lines, namely BHK21 (kidney cell line) and HepG2 (liver cell line). Most compounds tested were non-cytotoxic up to a maximum concentration tested (2.5 to 29 mg/L), with CC_{50} to MIC_{50} ratios of >7-800. Mefloquine was the only exception, with CC_{50} values of 4.2 and 2.8 mg/L and an MIC_{50} of 3.8 mg/L (Table 5). It is important to note here that many anti-TB agents are pro-drugs that are primarily activated inside Mtb. Cytotoxicity assays in human cell lines do not capture the potential toxicity of these active metabolites if bioconversion does not take place within host cells.

3.3.3 *In vitro* pharmacokinetics

In vitro solubility, permeability and liver microsomal metabolic stability are key predictors of oral bioavailability. These properties were determined using standardized assays and are summarized in Table 5. Ninety percent of the compounds showed moderate-to-high solubility, except clofazimine, PA-824 and bedaquiline which are poorly soluble. For predicting permeability, PAMPA is employed as a simple *in vitro* model of passive diffusion through an artificial membrane. The Caco-2 cell layer permeability assay is widely used as a more predictive *in vitro* model of absorption through the intestinal epithelium. While PAMPA only measures passive diffusion, the Caco-2 permeability assay integrates active uptake, efflux and permeation via the paracellular route. Most of the compounds (62%) exhibited low PAMPA permeability while 90% of the compounds showed moderate to high Caco-2 permeability and no or low active efflux except for rifampicin, thioacetazone and clarithromycin. Exceptions were streptomycin and clofazimine displaying low Caco-2 permeability. More than 90% of the compounds displayed low-to-medium intrinsic clearance in both mouse and human liver microsomes. There was a good correlation between the two species, except for ethionamide and prothionamide with high and medium clearance in mouse and human microsomes, respectively (Table 5). Anti-TB compounds displayed wide range of human plasma protein binding with majority of them having low to moderate binding.

Table 5. *In vitro* potency, cytotoxicity and *in vitro* PK properties for anti-mycobacterials

Compounds	**MIC_{50}**	***CC_{50} (HEPG2 / BHK21)**	**Solubility**	**PAMPA**	**Caco-2 permeability**		**Caco-2 efflux (B-A) / (A-B)**	**Mouse Cl_{int}**	**Human Cl_{int}**	**PPB**
					(A-B)	**(B-A)**				
	mg/L	mg/L	mg/L	(P_{app} 10^{-6} cm/s)				(µL/min/mg protein)		%
Isoniazid	0.04	>2.74	4.93	ND	ND	ND	-	21.7	13.9	1
Rifampicin	0.02	>16.46	1.79	1.6	1.52	18.4	12.1	3.04	2.84	90 (60-90)
Pyrazinamide	>9.85	>2.46	2.72	1.73	70.4	37.1	0.5	Low	Low	10
Ethambutol	0.60	>4.09	0.79	ND	ND	ND	-	Low	Low	30 (6-30)
Streptomycin	0.09	>11.63	2.04	ND	0.78	0.57	0.7	9.76	Low	35
Kanamycin	0.76	>9.69	ND	6.32	ND	ND	-	14.6	2.97	1
Amikacin	0.22	>11.73	2.94	ND	ND	ND	-	32.8	16.8	4 ± 8
p-aminosalicyclic acid	0.09	>3.06	0.97	ND	ND	ND	-	Low	41.9	75 (50-75)
Cycloserine	2.14	>2.04	2.94	ND	ND	ND	-	ND	ND	0
Ethionamide	0.34	>3.33	0.70	14.6	57.3	29.6	0.5	210	77.1	30
Rifabutin	0.01	>16.94	0.21	63.2	12.4	17.4	1.4	16.2	27.4	85
Rifapentine	0.02	>17.54	0.11	19.3	7.68	15	1.95	9.1	11.2	97[#]
Moxifloxacin	0.11	>8.03	2.76	0.22	17.2	29.1	1.7	Low	0.78	50
Levofloxacin	0.30	>7.23	3.1	0.02	8.23	17.3	2.1	Low	4.32	30 (24-38)
Gatifloxacin	0.07	>7.49	2.8	0.06	8.65	19.4	2.2	0.94	4.01	20
Ciprofloxacin	0.31	-	-	-	-	-	-	-	-	40
Ofloxacin	0.56	>7.23	2.11	0.02	9.25	20.1	2.2	2.77	5.8	25 ± 6
Sparfloxacin	0.08	>7.85	0.99	0.59	28.8	31.2	1.1	0.14	2.63	45
Capreomycin	0.67	>13.37	ND	0.09	ND	ND		8.24	0.80	-
Thioacetazone	0.05	-	0.16	ND	3.87	57.2	14.8	5.78	4.75	95
Linezolid	0.51	>6.75	1.97	0.05	18.1	31.2	1.7	2.98	0.89	30
Prothionamide	0.16	>3.61	0.26	52	58.5	27.8	0.5	264	56	60[#]

Clarithromycin	-	-	0.57	19.5	1.31	54.3	41.4	7.82	41.1	77 (70-80)
Amoxicillin	>29.23	>7.31	2.22	ND	ND	ND	-	Low	6.48	25
Clavulanate	>15.93	>3.98	>5	0.46	37.5	21.4	0.6	3.8	1.46	9
Meropenem	>30.68	>7.67	>5	ND	ND	ND	-	ND	ND	13
Clofazimine	0.12	>9.47	<0.005	2.58	0.17	0.18	1.0	Low	Low	70
Metronidazole	>136.93	>3.42	1.34	0.59	39.8	27.6	0.7	3.98	Low	4
Thioridazine	5.21	>7.41	2.57	91	3.8	5.0	1.3	107	44.6	96.6[#]
Mefloquine	3.78	4.20 / 2.80	-	-	-	-	-	-	-	98.2
Vancomycin	11.01	>28.99	-	-	-	-	-	-	-	30
Valnemulin	0.68	-	>5	ND	ND	ND	-	Low	0.62	94[#]
PNU-100480	0.18	-	0.45	92.8	5.54	5.9	1.1	0.91	1.41	78[#]
PA-824	0.3	>7.19	0.03	16.8	47.6	30.2	0.6	1.3	5.78	56[#]
Bedaquiline	0.18	>11.11	<0.005	ND	ND	ND	-	Low	2.33	99.9[#]
Delamanid	0.02	-	-	-	-	-	-	-	-	99.8[#]
Low[$]			10% (3)	62% (13)	10% (2)			90% (27)	93.3% (28)	66% (23)
Moderate[$]			33% (10)	-	19% (4)			3.3% (1)	6.7% (2)	20% (7)
High[$]			47% (14)	38% (8)	71% (15)			6.7% (2)	-	9% (3)
Very high[$]			10% (3)	-	-			-	-	6% (2)

$MIC_{50,}$ minimum inhibitory concentration; *CC_{50}, Cytotoxicity was measured in HepG2 (human hepatocellular carcinoma) and BHK21 (baby hamster kidney) cell lines. The highest concentration tested was equivalent to 20 µM, with all compounds having a CC_{50} >20 µM in both cell lines apart from mefloquine. For comparison purpose, CC_{50} values in the table are expressed in mg/L; -, Not tested; ND, not detected or data not available due to analytical/technical issues; [$]Compounds were grouped into various categories based on the following cut-offs. Solubility: low, <0.05 mg/mL; moderate, 0.05-1 mg/mL; high, 1-5 mg/mL and very high, >5 mg/mL. PAMPA (Parallel artificial membrane permeability assay): low, <10 P_{app} 10^{-6} cm/s; and high >10 P_{app} 10^{-6} cm/s. Caco-2 permeability: low, <1 P_{app} 10^{-6} cm/s; moderate, 1-5 P_{app} 10^{-6} cm/s; and high >5 P_{app} 10^{-6} cm/s. Cl_{int} (intrinsic clearance): low, <50 µL/min/mg of protein; moderate, 50-150 µL/min/mg of protein; and high >150 µL/min/mg of protein. PPB, human plasma protein binding obtained from published literature (Section 3.2.6); [#]human PPB predicted using Gastroplus™ 8.5, simulations Plus, Inc. (www.simulations-plus.com); PPB: low <70; moderate 70-95, high 95-99, very high >99%. Numbers in parentheses indicate the number of compounds in each group.

3.3.4 Mouse *in vivo* PK and *in vivo* efficacy

Mouse *in vivo* PK and efficacy data were either retrieved from the literature or generated as part of this study (Table 6). 14 compounds were chosen having good anti-mycobacterial activity (MIC < 10 mg/L) and that are administered orally. Doses were selected based on the efficacious exposure observed in humans. Based on the MIC_{50} and PK parameters, plasma PK-PD indices (fC_{max}/MIC, fAUC/MIC and $fT_{>MIC}$) were calculated and corrected for plasma protein binding to reflect the free drug fraction (indicated by "*f*"). Anti-TB compounds studied displayed wide range of fC_{max}/MIC, fAUC/MIC and $fT_{>MIC}$ (Table 6). Overall, unbound peak concentrations (C_{max}) were above the MIC at some point during the dosing interval, except for compounds with high plasma protein binding such as mefloquine, clofazimine and bedaquiline (Table 6 and 9).

The mean log CFU reduction at 2- and 4-weeks post dosing ranged between 0.5 and 6.7 (Table 6). Cycloserine displayed very poor efficacy in murine model of TB. The current clinical candidates, moxifloxacin, PA-824, bedaquiline and PNU-100480 showed good efficacy with 3.3 to 6.7 log CFU reductions. Among the four first line anti-TB compounds, isoniazid showed good efficacy (4.5 to 5 log reductions) compared to other three drugs i.e., rifampicin, ethambutol and pyrazinamide (0.5 to 2.5 log CFU reductions). Except for PA-824 – for which efficacy is driven by the fraction of the dosing interval during which free plasma concentration exceeds the MIC or $fT_{>MIC}$ (Ahmad et al., 2011) – the efficacy of all compounds tested (rifampicin, isoniazid, moxifloxacin, PA-824 and bedaquiline) was concentration-dependent, i.e. either fAUC/MIC and/or C_{max}/MIC best correlated with lung

cfu reduction (Jayaram et al., 2003; Jayaram et al., 2004; Rouan et al., 2012; Shandil et al., 2007).

However, no clear trend in correlations between PK-PD indices across compounds and mean log cfu reduction was observed. This is an important observation and clearly shows that simple PK-PD rules of thumb cannot be used to guide the discovery and development of novel TB drugs (Dartois and Barry, III, 2013). This feature is specific of TB drugs, which are in stark contrast with many other antibacterials for which plasma PK-PD indices usually fall within relatively narrow and reasonably predictive windows (Scaglione and Paraboni, 2006). The complexity of the TB pathology, where the pathogen resides in remote lesion compartments, likely contributes to the lack of correlation between plasma PK and efficacy (Dartois, 2014).

Table 6. Pharmacokinetic and pharmacodynamic parameters of selected anti-mycobacterials

Compounds	Dose (mg/kg)	C_{max} (µg/mL)	AUC (µg·h/mL)	T_{max} (h)	$t_{1/2}$ (h)	PPB (%)	MIC (mg/L)	fC_{max}/ MIC	fAUC/MIC	$fT_{>MIC}$	Mean Δlog cfu reduction ± SD	
											2 weeks	4 weeks
Isoniazid*	25	28.2	52.2	0.25	1.7	42	0.04	408.9	756.9	62	4.53 ± 0	5.2 ± 0
Rifampicin*	10	10.58	139.7	1.33	7.61	83	0.02	89.9	1187.5	100	0.98 ± 0.40	2.37 ± 0.37
Pyrazinamide*	150	146.1	303.8	0.42	1.05	42	9.85	8.6	17.9	15	0.46 ± 0.25	1.29 ± 0.2
Ethambutol[#]	100	6.44	19.79	1.5	1.49	25	0.6	8.1	24.7	25	1.4 ± 0.34	1.9 ± 0.31
Cycloserine[#@]	175	214.28	209.73	0.25	0.67	0	2.14	100.1	98.0	20	-0.19 ± 0.73	ND
Ethionamide[#]	12.5	0.57	0.21	0.08	0.28	30	0.34	1.2	0.4	0.6	1.58 ± 0.36	2.56 ± 0.52
Moxifloxacin*	200	4.53	23.58	0.5	4.03	60	0.11	16.5	85.7	70	3.28 ± 0.24	4.44 ± 0
Linezolid*[@]	100	65	73.4	0.33	0.65	31	0.51	87.9	99.3	19	1.35 ± 0.90	2.13 ± 0.70
PA-824[#]	100	16.25	276.11	4	3.28	89	0.3	6.0	101.2	52	5.94 ± 0	6.74 ± 0
Bedaquiline*[@]	12.5	0.55	9.7	2	58.6	99	0.18	0.03	0.5	0	4.33 ± 0	4.64 ± 0
Mefloquine[#]	25	1.8	30.84	4	23.18	80	3.78	0.1	1.6	0	0.64 ± 0.58	1.2 ± 0.35
PNU-100480	100	ND	ND	ND	ND	ND	ND	ND	ND	ND	5.32 ± 0.16	6.65 ± 0.40
Clofazimine[#]	25	0.94	37.6	8	32	99.8	0.12	0.02	0.6	0	2.05 ± 0.28	3.96 ± 0.32
Valnemulin[#]	25	0.92	5.0	1	5.3	80	0.68	0.3	1.5	0	0.47± 0.28	0.91 ± 0.34
Range	10-200							0.03 - 409	0.5 - 1188	0 - 100	0.46 – 5.94	0.91 – 6.74

C_{max}, maximum concentration reached in plasma; AUC, area under curve representing the exposure; T_{max}, time to reach maximum concentration; $t_{1/2}$, elimination half-life; PPB: plasma protein binding; MIC, minimum inhibitory concentration; fC_{max}/MIC, ratio of peak plasma concentration (C_{max}) to the minimum inhibitory concentration (MIC); fAUC/MIC, ratio of area under curve to MIC; $fT_{>MIC}$, 24 h period during which the compound concentration exceeded the MIC. "f" refers to free fraction. Mean Δlog cfu reduction: log10 of cfu reduction compared to untreated controls. Mean value ± SD from 5 animals are provided. *PK data from published literature (section 3.2.5). Isoniazid (Brennan and Young, 2008; Grosset and Ji, 1998), Rifampicin (Brennan and Young, 2008; Grosset and Ji, 1998), Pyrazinamide (Brennan and Young, 2008; Grosset and Ji, 1998), Moxifloxacin (Gaonkar et al., 2006), Linezolid (Brennan and Young, 2008; Slatter et al., 2002), Bedaquiline (Andries et al., 2005). [#] PK data obtained as part of this study; [@]PK estimated based on dose linearity; ND: Not determined

3.3.5 Correlations between *in silico* parameters and *in vitro* potency and *in vitro* PK parameters

Mycobacterium tuberculosis possesses a notoriously impermeable cell wall. Thus we tested the hypothesis that lipophilicity and permeability could be a determinant of *in vitro* potency. Across all drug classes included in this study, no apparent trend or significant correlation was observed between anti-mycobacterial activity and cLogP, PAMPA or Caco-2 permeability, indicating that permeability and/or lipophilicity is not a predictor of activity inside the mycobacterium, at least not across this large set of compound classes (Table 7). Examination of potential correlations within sub-groups of compounds (natural products, synthetic molecules, injectables and oral drugs) did not reveal any apparent association either (not shown). Within a given series however, a positive correlation is often detected between cLogP and potency, as recently published for indolcarboxamide and tetrahydropyrazolopyrimidine carboxamide series (Kondreddi et al., 2013; Yokokawa et al., 2013).

Table 7. Correlation between MIC and *in silico /in vitro* parameters

Parameters	**MIC (mg/L)**			
	Spearman r	P value	significance	Number of compounds
cLogP	-0.23	0.22	ns	30
PAMPA	-0.12	0.63	ns	17
Caco-2 permeability	0.21	0.41	ns	17

ns, not significant (P>0.05).

As expected, some level of correlation was observed between *in vitro* PK and *in silico* properties. Generally, compounds with MWs lower than 400

and cLogP of <4 showed better solubility, Caco-2 permeability and plasma protein binding (Figure 21A-F). This is in agreement with Gleeson's findings. Most of the outliers were natural products either belonging to the rifamycin class or aminoglycoside injectables. A significant negative correlation was observed between cLogP and solubility, MW and Caco-2 permeability. Furthermore, both MW and cLogP showed to be positively correlated with PPB . Interestingly, RB seemed to relate to Caco-2 permeability and PPB (Table 8). In addition, an apparent trend of correlations was observed between MW and solubility, as well as cLogP and Caco-2 permeability (Fig 21 A & D).

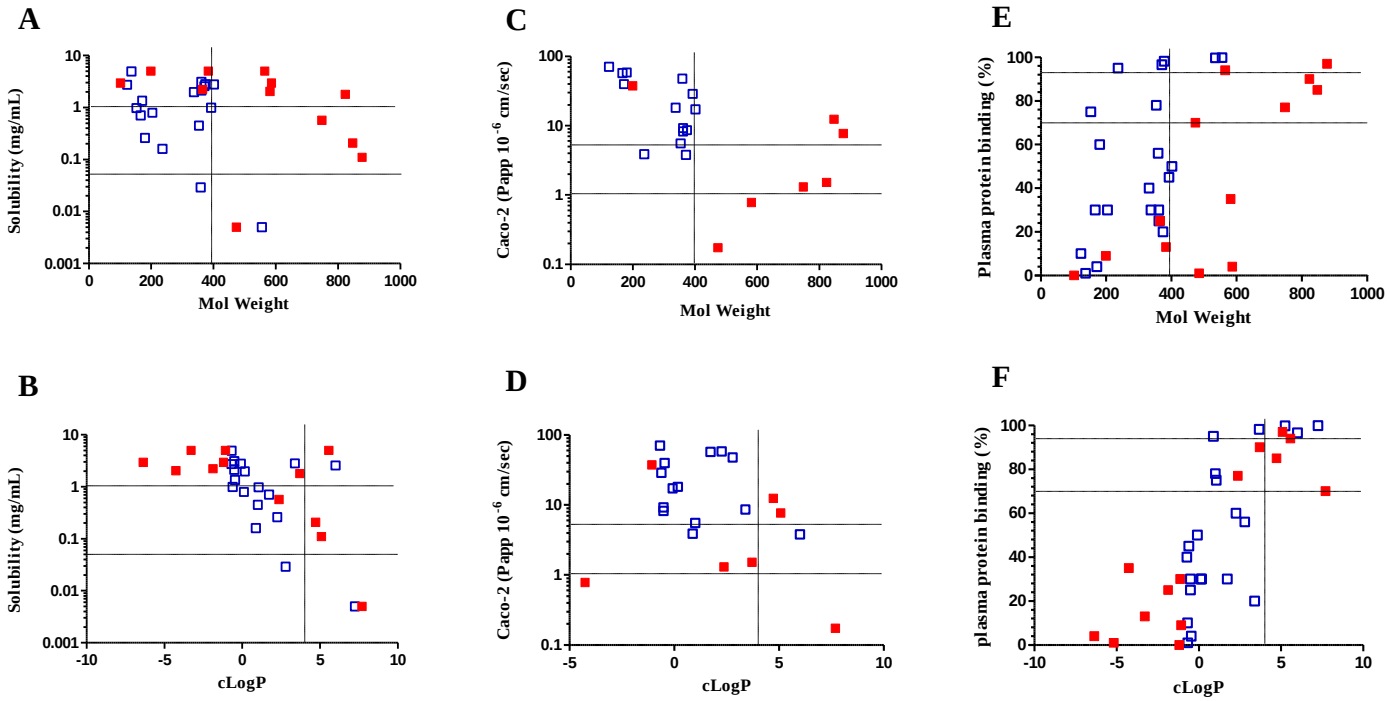

Figure 21. Correlation analysis between *in silico and in vitro* PK parameters
(A) Solubility versus molecular weight. (B) Solubility versus cLogP. (C) Caco-2 permeability versus molecular weight. (D) Caco-2 permeability versus cLogP. (E) Plasma protein binding versus molecular weight. (F) Plasma protein binding versus cLogP. The vertical lines indicate cut-off values as defined in Gleeson's analysis of molecular weight and cLogP. The horizontal lines delineate the boundaries between low, moderate and high categories for solubility (A and B), Caco-2 permeability (C and D) and plasma protein binding (E and F). The compounds are categorized as synthetic molecules (blue open squares) and natural products (red filled squares) based on their origin (Table 3).

Table 8. Correlation between *in silico* and *in vitro* parameters

Parameters	Solubility (mg/mL) (n=30)			Caco-2 permeability (10^{-6} cm/sec) (n=21)			PPB (%) (n=35)		
	r_s	p	sig[#]	r_s	p	sig[#]	r_s	p	sig[#]
MW	-0.17	0.364	ns	-0.68	0.0006	***	0.43	0.011	*
cLogP	-0.58	0.0007	***	-0.33	0.149	ns	0.83	<0.0001	***
HBD	0.08	0.667	ns	-0.38	0.086	ns	-0.11	0.542	ns
HBA	0.09	0.634	ns	-0.34	0.136	ns	-0.04	0.816	ns
PSA	0.15	0.429	ns	-0.24	0.292	ns	-0.09	0.611	ns
RB	-0.23	0.220	ns	-0.59	0.005	**	0.39	0.021	* (n=34)

r_s is the Spearman's rank correlations coefficient, p is the level of significance, [#]significance [***, represents extremely significant (P < 0.001); **, very significant (P = 0.001 to 0.01); *, significant (P = 0.01 to 0.05); ns, not significant (P > 0.05)], n = number of compounds

3.3.6 Human *in vivo* PK properties

Human PK parameters were collected from the literature (Section 3.2.6) and are summarized in Table 9. Anti-TB compounds displayed wide range of *in vivo* PK properties with majority of them having low to moderate volume of distribution, total systemic clearance and moderate to high oral bioavailability. There was a good correlation observed between *in vitro* and *in vivo* clearance (Table 5 and 9).

3.3.7 Correlations between *in silico, in vitro* and *in vivo* parameters

Further, examination of clinical PK parameters retrieved from the literature (Table 9) revealed a moderate-to-high oral bioavailability for compounds which follow Lipinski's rule of 5 and Veber's rule (Figure 22 A-E) (Lipinski

et al., 2001; Veber et al., 2002), as well as compounds with a solubility of >1 mg/mL and Caco-2 permeability of >5 X 10^{-6} cm/sec (Figure 22 F & G).

In addition, significant positive correlation was observed between (1) cLogP and volume of distribution, an indicator of drug distribution into tissues (Figure 23A), (2) cLogP and systemic clearance of the unbound fraction (Figure 23B), and (3) cLogP and plasma protein binding (Figure 23C). A significant negative correlation was observed for cLogP and oral bioavailability (Figure 23D). As expected, lipophilicity emerged as an important parameter influencing *in vitro* and *in vivo* PK parameters. Interestingly, except for cLogP, none of the other physicochemical parameters showed any apparent trend or good correlation with *in vivo* PK properties (Table 10).

3.4 Conclusion

Drug discovery aims to deliver a candidate that shows efficacy, exposure and tolerability in a relevant animal model and in man. *In silico* and *in vitro* assays are employed in lead finding and optimization, attempting to predict these *in vivo* properties. In the present study, we have comprehensively determined and compiled physicochemical parameters, *in vitro* pharmacokinetic properties and potency values of 36 anti-mycobacterials, most of which are in clinical use against TB.

TB drug discovery is challenging and complicated as Mtb is a slow growing pathogen, with thick lipid cell wall (Ma et al., 2010). Further, the biology of TB is intricate as organisms reside in multiple complex histopathological manifestations such as calcified granulomas, necrotic and caseous lesions in lungs (Barry, III et al., 2009).

Table 9. Clinical pharmacokinetic parameters

Drugs	**Dose (mg)**	**C_{max} (ug/mL)**	**F (%)**	**V_d (L/kg)**	**CL (mL/min/kg)**	***f*C_{max}/MIC**
Isoniazid	300	5.4 ± 2.0	100	0.67 ± 0.15	7.4 ± 2.0	139.0
Rifampicin	600	14.91	70	0.97 ± 0.36	3.5 ± 1.6	72.5
Pyrazinamide	1500	38.7 ± 5.9	70, 97	0.57 (0.13 – 1.04)	1.1 (0.2 – 2.3)	3.5
Ethambutol	1200	5	77 ± 8	1.6 ± 0.2	8.6 ± 0.8	5.8
Streptomycin	1000	25-50	-	0.34	0.78	262
Kanamycin	1000	22	-	0.26	1.4	28.8
Amikacin	1000	26 ± 4	-	0.27 ± 0.06	1.3 ± 0.6	115
p-aminosalicyclic acid	8000-12000	9-35 (20)	60	1.4	-	58.3
Cycloserine	500-1000	25-30	90	0.3 (0.25-0.5)	-	14.0
Ethionamide	500-1000	2.16	>90	2 (1.5-4)	-	4.5
Rifabutin	300	0.375 ± 0.267 (0.3-0.9)	20	9.3	2.4	6.6
Rifapentine	300	15.05 ± 4.62	70	-	0.56	19.1
Moxifloxacin	400	4.3	86 ± 1	2.05 ± 1.15	2.27 ± 0.24	19.8
Levofloxacin	500-750	6.2 (6-10)	99 ± 10	1.36 ± 0.21	2.52 ± 0.45	14.5
Gatifloxacin	400	3.8 ± 1.0	96	1.7 (1.5 – 2)	2.8 (2.7 – 3.0)	40.6
Ciprofloxacin	250-750	2.4	60 ± 12	2.2 ± 0.4	7.6 ± 0.8	4.6
Ofloxacin	1000	3	>95	1.8 ± 0.3	3.5 ± 0.7	4.0
Sparfloxacin	200	1.1	-	3.9	2.7	7.3
Capreomycin	1000	32 (20-47)	-	0.25-0.4	-	-
Thioacetazone	150	-	-	-	-	-
Linezolid	600-1200	12.9	100	0.58	1.8	17.6
Prothionamide	250-750	3-4	-	2-3	-	8.6
Clarithromycin	200-500	0.6 ± 0.43	55 ± 8	1.5	7.3	-
Amoxicillin	500	8-10	93 ± 10	0.21 ± 0.03	2.6 ± 0.4	0.2
Clavulanate	250	5-7	90	0.22	3.1	0.3
Meropenem	-	-	-	0.3	3.9	-
Clofazimine	200	0.5-2	45-62	20	-	3.0
Metronidazole	1500	8-22	99 ± 8	0.4	0.85	0.1
Thioridazine	100	0.025-0.150	-	21 ± 9	8.6 ± 2.9	0.6
Mefloquine	1250	2.21 ± 0.51	-	19 ± 6	0.43 ± 0.14	0.01
Vancomycin	1000	65.7 ± 7.9	-	0.54	1.3	4.2
Valnemulin	-	-	-	-	-	-
PNU-100480	1000	0.84	-	-	-	1.0
PA-824	200	1	-	-	2.14	2..8
Bedaquiline	400	3-8	-	-	-	0.03
Delamanid	200	0.23	-	-	-	0.03
Range			20 – 100	0.2 – 21	0.43 – 8.6	
Low[#]			5% (1)	48% (14)	80% (20)	

Moderate[#]	30% (6)	38% (11)	20% (5)
High[#]	65% (13)	14% (4)	

All clinical PK values were obtained from published literature as mentioned in material and methods section 3.2.6. C_{max}, maximum concentration reached in plasma; F, oral bioavailability; V_d, volume of distribution; CL, clearance; fC_{max}/MIC, ratio of free maximum plasma concentration to minimum inhibitory concentration. Dash (-): data not available; [#]compounds are grouped into various categories based on the following cut-offs. F: low <30, moderate 30-70, high >70%; V_d: low <1; moderate 1-5; high >5 L/Kg; CL: low <5, moderate 5-15 mL/min/Kg; Numbers in the parenthesis indicate the number of compounds in each group.

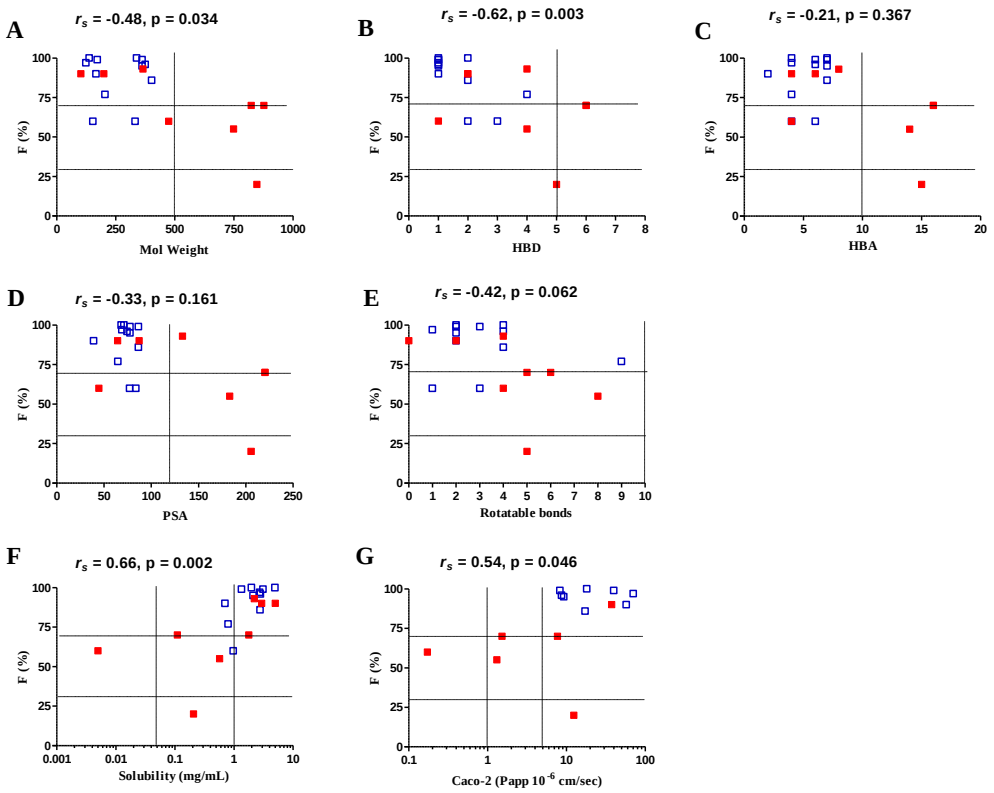

Figure 22. Correlation between *in silico* and *in vitro* properties and oral bioavailability in humans

(A) molecular weight; (B) hydrogen bond donors; (C) hydrogen bond acceptors; (D) polar surface area; (E) rotatable bonds; (F) solubility; (G) Caco-2 permeability. Vertical lines indicate the cut-off values as defined in Lipinski's rule of 5 (A-C) and Veber's rule (D and E). Horizontal lines delineate the boundaries between low, moderate and high categories for oral bioavailability. Double vertical lines delineate the boundaries between low, moderate and high categories for solubility (F), and Caco-2 permeability (G). Note the significant positive correlation observed between oral bioavailability and solubility, and oral bioavailability and Caco-2 permeability. The compounds are categorized as synthetic molecules (blue open squares) and natural products (red filled squares) based on their origin (Table 3). r_s is the Spearman's rank correlations coefficient, p is the level of significance.

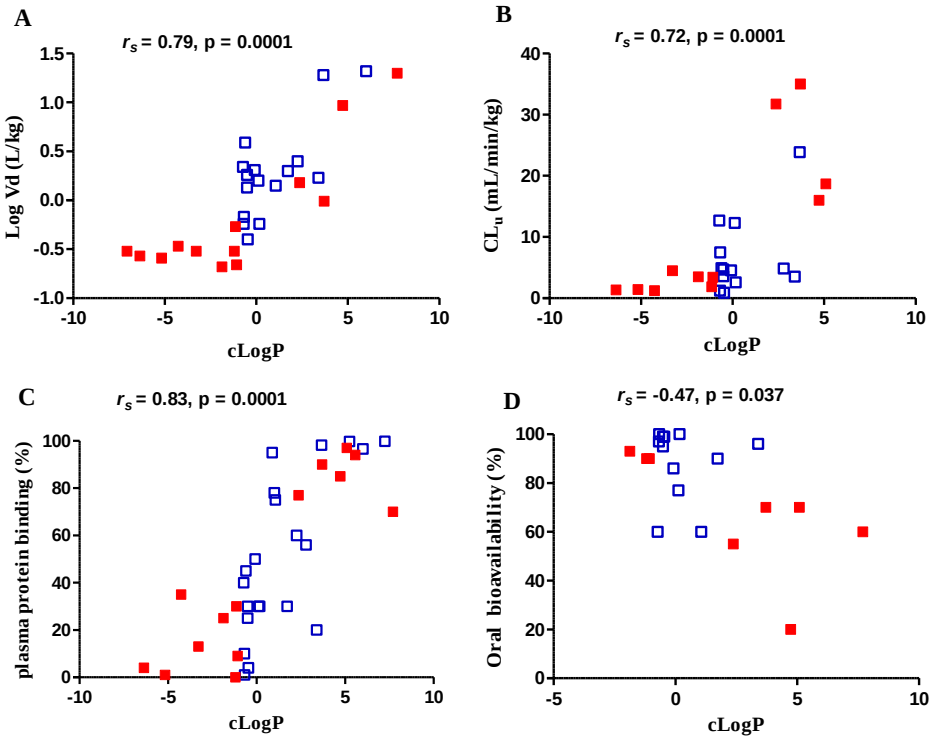

Figure 23. Correlation between cLogP and volume of distribution (A), unbound clearance (CL_u), (B) plasma protein binding (C) and oral bioavailability (D)
A significant positive correlation was observed between cLogP and volume of distribution, cLogP and unbound clearance (ratio of clearance and unbound fraction (Giuliano et al., 2005)), and cLogP and plasma protein binding. A significant negative correlation was observed between cLogP and oral bioavailability. The compounds are categorized as synthetic molecules (blue open squares) and natural products (red filled squares) based on their origin (Table 3). r_s is the Spearman's rank correlations coefficient and p is the level of significance.

Novel chemical entities have to be potent with favorable physicochemical properties to pass through these barriers and kill actively replicating and non-replicating Mtb in order to cure the disease. Anti-TB drugs studied displayed wide range of physicochemical properties. Acceptable solubility, permeability and plasma protein binding were displayed by

molecules with molecular weight <400 and cLogP <4. Good oral bioavailability observed with good solubility and permeability.

Table 10. Correlation between *in silico*, *in vitro* and *in vivo* parameters

Parameters	**V_d (L/kg) (n=29)**			**CL (mL/min/kg) (n=25)**			**F (%) (n=20)**		
	r_s	p	sig[#]	r_s	p	sig[#]	r_s	p	sig[#]
MW	0.03	0.87	ns	0.22	0.293	ns	-0.48	0.034	*
cLogP	0.79	<0.0001	***	0.72	<0.0001	***	-0.47	0.037	*
HBD	-0.45	0.014	*	-0.07	0.755	ns	-0.62	0.003	**
HBA	-0.49	0.006	**	-0.19	0.349	ns	-0.21	0.367	ns
PSA	-0.56	0.001	**	-0.27	0.197	ns	-0.33	0.161	ns
RB	-0.11	0.572	ns (n=28)	0.12	0.574	ns, (n=24)	-0.42	0.062	ns
Solubility	-	-	-	-	-	-	0.66	0.002	** (n=19)
Caco-2 permeability	-	-	-	-	-	-	0.54	0.046	* (n=14)

r_s is the Spearman's rank correlations coefficient, p is the level of significance, [#]significance [***, represents extremely significant (P < 0.001); **, very significant (P = 0.001 to 0.01); *, significant (P = 0.01 to 0.05); ns, not significant (P > 0.05)], n = number of compounds

Various *in vitro* and *in vivo* PK properties were influenced by lipophilicity. Positive correlation was observed with volume of distribution, clearance and plasma protein binding and negative correlation with solubility and oral bioavailability. Overall, lipophilicity is one of the important parameter that influences various PK properties. Co-incidentally, the majority of the NCE's identified and optimized recently, such as pyrazolocarboxamides, imidazo-pyrimidines (Pethe et al., 2013), indolecarboxamides (Kondreddi et al., 2013; Onajole et al., 2013; Rao et al., 2013), adamantyl urea (Grzegorzewicz et al., 2012), spiroindoles (Remuinan et al., 2013), bedaquiline (Andries et al., 2005) and delamanid (Matsumoto et

al., 2006) have cLogP >5. Although increasing lipophilicity may help in gaining potency, it could be detrimental to other properties and most often leading to poor solubility which limits oral absorption (van de Waterbeemd et al., 2001), thus lowering the exposure multiples. All the above compounds were identified by cell-based drug discovery approaches and it is possible that whole cell-screening against Mtb (with highly lipid rich cell wall) may preferentially identify lipophilic hits. Since, higher lipophilicity poses drug development challenges; it is appropriate to start with small and polar compounds during drug discovery. This provides enough space for medicinal chemistry based optimization of hit during the lead optimization phase. We hope that this standardized data set represents a useful reference for the TB drug discovery community.

Chapter 4. Pharmacokinetics-pharmacodynamics analysis of bicyclic 4-nitroimidazole analogs in a murine model of tuberculosis.

4.1 Introduction

PA-824 (Stover et al., 2000) and OPC-67683 (Matsumoto et al., 2006) are two bicyclic 4-nitroimidazoles currently in phase II clinical trials, representing a promising new class of therapeutics for TB (Kaneko et al., 2011). Preclinical testing of PA-824 showed bactericidal activity in various *in vitro* and *in vivo* models (Lenaerts et al., 2005; Tyagi et al., 2005). PA-824 was shown to be well tolerated in healthy subjects, following oral daily doses for 7 days (Ginsberg et al., 2009). These results, combined with the demonstrated activity of PA-824 against drug-sensitive and multidrug-resistant Mtb, supported the progression of this compound and its evaluation as a novel treatment against TB. An early bactericidal activity (EBA) study of PA-824 revealed a lack of dose-response between 200 and 1200 mg administered daily for 14 days (Diacon et al., 2010). Dose-fractionation PK-PD studies in mice showed the PK-PD driver of PA-824 to be the time during which the free drug concentrations in plasma were above the MIC ($fT_{>MIC}$) (Ahmad et al., 2011). In retrospect, clinical investigators established that $fT_{>MIC}$ was 100% at all doses between 200 and 1200 mg daily. An additional phase II trial between 50 and 200 mg was undertaken to establish the lowest efficacious dose (Diacon et al., 2012a). 200 mg of PA-824 was found to be efficacious and used in combination with other anti-TB drugs (Diacon et al., 2012b).

Physicochemical properties, *in vitro* potency, *in vitro* and *in vivo* pharmacokinetics (PK) are critical determinants for *in vivo* efficacy. PA-824 is highly lipophilic and exhibits poor aqueous solubility. To overcome the limitation of its low solubility and improve its oral bioavailability, a cyclodextrin formulation was developed and used for *in vivo* animal efficacy

studies (Lenaerts et al., 2005; Stover et al., 2000). Extensive lead optimization efforts were undertaken to improve aqueous solubility, metabolic stability, *in vitro* potency and *in vivo* efficacy of anti-tubercular nitroimidazoles and various analogs were synthesized (Barry et al., 2011; Blaser et al., 2012; Cherian et al., 2011; Denny and Palmer, 2010; Jiricek et al., 2007; Kim et al., 2009a; Kim et al., 2009b; Kmentova et al., 2010; Matsumoto et al., 2006; Palmer et al., 2010; Thompson et al., 2011). Comprehensive *in vivo* pharmacology studies are generally resource and time intensive. This is particularly true for TB because of the slow rate of *M. tuberculosis* growth, lengthy treatment duration and requirement of high containment facility. In this study, a panel of closely related potent bicyclic 4-nitroimidazoles (NI) was profiled both *in vitro* and *in vivo*. The data were retrospectively analyzed to identify the PK parameters that correlate with *in vivo* efficacy of a series of bicyclic 4-nitroimidazoles. The results of this investigation showed that PK properties such as volume of distribution and lung exposure predicts *in vivo* efficacy of bicyclic 4-nitroimidazoes better than other PK parameters. Thus, *in vitro* potency and lung PK could be used as surrogate to guide the prioritization of new pre-clinical candidates for lengthy efficacy studies, there by expediting drug discovery.

4.2 Materials and Methods

4.2.1 Chemicals

Synthesis of PA-824, Amino-824, AminoEthyl-824, NI-135, NI-147 and NI-136 have been previously reported (Cherian et al., 2011; Kim et al. 2009a). Other NI analogs NI-622, NI-644, NI-176, NI-269, NI-182, NI-145, NI-297 and NI-302 have been described in two patents (Barry et al., 2011; Jiricek et al., 2007) and synthesis of these compounds to be described elsewhere. All solutions were made as 20 mM stocks in DMSO. Hydroxypropyl-β-cyclodextrin, Lecithin, granular was purchased from Acros/Organics, New Jersey, and USA.

4.2.2 *In vitro* potency

M. tuberculosis (Mtb) (H37Rv, ATCC 27294) culture conditions have been described previously (Cherian et al., 2011). Minimum Inhibitory concentration (MIC_{99}) against wild type Mtb H37Rv and cofactor F_{420} deficient (*FbiC* mutant) (Manjunatha et al., 2006) was determined by the broth dilution method as described earlier (Cherian et al., 2011).

4.2.3 *In vitro* physicochemical properties

In vitro physicochemical and PK parameters like solubility, log P, PAMPA, Caco-2 permeability and mouse plasma protein binding were determined in-house in medium to high throughput format assays. Briefly, solubility was measured using a high throughput equilibrium-solubility assay using a novel miniaturized shake-flask approach and streamlined HPLC analysis (Zhou et

al., 2007); lipophilicity determination was carried out in 96-well micro titer plates and the diffusion of compounds between two aqueous compartments separated by a thin octanol liquid layer was measured (Wohnsland and Faller, 2001); PAMPA permeability experiments were carried out in 96-well micro titer filter plates at absorption wavelengths between 260 and 290 nm (Avdeef et al., 2007); Caco-2 permeability assay was carried out in a 96-well format, and compound concentrations in each chamber were measured by LC/MS as described previously (Marino et al., 2005) and plasma protein binding was determined in mouse plasma using an ultra-filtration method (Fung et al., 2003).

4.2.4 *In vivo* PK studies

All animal experimental protocols (protocol # 023/2009 and # 025/2009 for PK; protocol # 004/ 2010 for efficacy) involving mice were reviewed and approved by the Institutional Animal Care and Use Committee (IACUC) of Novartis Institute for Tropical Diseases. The animal research complied with Singapore Animal Veterinary Authority and global Novartis policy on the care and use of animals. Experimental and control animals infected with Mtb were euthanized at the end of the experiment. All procedures during pharmacokinetic experiments were performed under isoflurane anesthesia and all efforts were made to minimize suffering.

Female CD-1 mice obtained from Biological Resource Center in Singapore were used for *in vivo* PK studies. Mice were acclimatized before initiation of pharmacokinetic (PK) experiments. Feed and water were given *ad libitum*. The compounds were formulated at a concentration of 1, 2.5 or 5

mg/mL for a dose of 10 mg/kg (Amino-824, AminoEthyl-824) or 25 mg/kg (PA-824, NI-135, NI-147, NI-136, NI-176, NI-269, NI-182, NI-145, NI-297 and NI-302) or 50 mg/kg (NI-622 and NI-644) given orally and at 1 or 2 mg/mL concentration for a dose of 5 or 10 mg/kg given intravenously. For dose proportionality studies PA-824, NI-622 and NI-644 were administered at a dose of 10 and 250 mg/kg. The CM-2 formulations were prepared in 10% w/v hydroxypropyl-β-cyclodextrin and 10% v/v lecithin in water as described earlier (Lenaerts et al., 2005; Tyagi et al., 2005). The formulation was centrifuged and the supernatant was collected for intravenous administration. After oral dosing, blood and lung samples from mice were collected at various time points ranging from 0.08 h (but 0.02 h for i.v dosing) to 48 h. Groups of three mice were used for each time point. Blood was centrifuged at 13,000 rpm for 7 min at 4 ºC, plasma was harvested and stored at -20 ºC until analysis. Lung tissue samples were excised, dipped in PBS, gently blotted with absorbent paper, dried, weighed and stored at -20 ºC until further analysis.

For LC/MS/MS analysis, 50 µL of plasma samples were precipitated using 400 µL of acetonitrile:methanol:acetic acid (90:9.8:0.2) containing 500 ng/mL of either related compound or warfarin as internal standard. After vortexing and centrifuging the mixture, the supernatant was removed and 5 µL of sample analyzed. Whole lung tissue was homogenized in 2 mL of PBS. 50 µL of lung homogenate was taken and processed as described above for plasma samples. The standard calibration curve was prepared by spiking blank plasma and lung tissue with different concentrations of the compound. In addition, quality control samples with three different concentrations were prepared in respective blank matrix and analyzed together with the unknown

samples for validation purposes. Analyte quantitation was performed by LC/MS/MS using optimized conditions for each compound. Liquid chromatography was performed using an Agilent 1100 HPLC system (Santa Clara, CA), with the Agilent Zorbax XDB Phenyl (3.5µ, 4.6x75 mm) column at an oven temperature of 35 ºC and 45 ºC, coupled with a triple quadruple mass spectrometer (Applied Biosystems, Foster City, CA). Instrument control and data acquisition were performed using Applied Biosystems software Analyst 1.4.2. The mobile phases used were A: water-acetic acid (99.8:0.2, v/v) and B either as: acetonitrile-acetic acid (99.8:0.2, v/v) or methanol-acetic acid (99.8:0.2, v/v), using a gradient, with a flow rate of 1.0 mL/min, and a run time of 6 to 8 min. Under these conditions the retention times of various compounds ranged between 3.2 and 6.5 minutes. Multiple reaction monitoring (MRM) was combined with optimized mass spectrometry parameters to maximize detection specificity and sensitivity (Appendix 3). Most of the compounds were analyzed using electrospray ionization in the positive mode. The recovery of the compound from both plasma and lung tissue were good and consistent across the concentration range studied. The lower limit of quantification for different compounds ranged between 1 and 49 ng/mL in plasma and 1 and 132 ng/g in lungs. Calibration curve was prepared freshly and analyzed with every set of study samples. Intraday variability was established with triplicate quality control samples at three concentration levels. The results were accepted if relative standard deviation was less than 15%.

Mean values of compound concentrations in plasma and lungs were obtained from three animals at each time point and plotted against time to generate concentration-time profiles. PK parameters were determined using

Phoenix WinNonlin, version 6.3 (Pharsight, A Certara company, USA, www.pharsight.com), by non-compartmental modeling using built-in model (200 – 202) for extravascular and intravenous bolus dosing. The oral bioavailability (F) was calculated as the ratio between the area under the curve (AUC_{inf}) following oral administration and the AUC_{inf} following intravenous administration corrected for dose ($F = AUC_{p.o} * dose_{i.v.}/AUC_{i.v} * dose_{p.o}$).

4.2.5 *In vivo* mouse efficacy studies

In vivo mouse efficacy studies were determined after intranasal infection of Balb/c mice with 10^3 cfu Mtb H37Rv. Treatment was initiated 4 weeks after infection. Compounds were orally administered at 25 mg/kg and 100 mg/kg in CM-2 formulation for 4 weeks daily. Bacterial loads were determined at 2 and 4 weeks post treatment (Rao et al., 2013). Statistical analysis was done by a one-way analysis of variance, followed by a multiple comparison analysis of variance by a one-way Tukey test (GraphPad Prism, version 5.02, San Diago, California USA, www.graphpad.com). Differences were considered statistically significant at the 95% level of confidence (Lenaerts et al., 2005).

4.2.6 Calculation of PK-PD parameters

The MIC against Mtb was used to calculate PK-PD indices (C_{max}/MIC, AUC/MIC and $T_{>MIC}$). The C_{max}/MIC was defined as the ratio of peak plasma concentration (C_{max}) to the MIC, the AUC/MIC was defined as the ratio of the AUC_{0-24} to the MIC, and the time above MIC ($T_{>MIC}$) was defined as 24 h period during which the total compound concentration exceeded the MIC. C_{max}/MIC and AUC/MIC were calculated as ratios from PK parameter

obtained from non-compartmental analysis and MIC. $T_{>MIC}$ were derived from Phoenix WinNonlin software by specifying MIC as therapeutic response and time above therapeutic response was obtained. Using plasma protein binding, unbound concentrations in plasma were calculated, PK parameters were derived from Phoenix WinNonlin and PK-PD indices were defined as fC$_{max}$/MIC, fAUC/MIC and %$fT_{>MIC}$ where '*f*' refers to free concentration. For calculation and plotting of mean concentration-time curve, concentrations indicated as below the lower limit of quantification (LLOQ) were replaced by 0.5*LLOQ. Ignoring the values here would impact some of the PK-PD parameters. This approach has no impact on pharmacokinetic parameter calculations (Duijkers et al., 2002).

4.2.7 PK-PD analysis

PK-PD indices were estimated from the plasma and lung drug concentrations, *in vitro* potency and plasma protein binding. A Spearman's rank correlation (Djukic et al., 2012; Ferl et al., 2007) was run to determine the relationship between various PK parameters and mean log CFU reduction using Prism software (GraphPad Prism, version 5.02, San Diago, California USA, www.graphpad.com).

4.3 Results

4.3.1 *In vitro* potency and physicochemical properties

In an effort to improve the solubility and potency of PA-824, diverse structural analogs of PA-824 were synthesized and their *in vitro* activities reported

(Barry et al., 2011; Cherian et al., 2011; Jiricek et al., 2007; Kim et al., 2009a; Kim et al., 2009b). A few potent bicyclic 4-nitroimidazole analogs were selected and characterized in detail (Figure 24). *In vitro* Mtb potency and physicochemical properties of these nitroimidazole analogs are summarized in Table 11. All the NI analogs studied showed Mtb specific growth inhibitory activity and no cytotoxicity was observed in THP1 macrophage cell lines (Table 11). F_{420} deficient (*FbiC*) mutants were resistant to all these bicyclic 4-nitroimidazoles analogs (Table 11), suggesting a mechanism of action similar to PA-824, involving F_{420}-dependent bio-activation (Manjunatha et al., 2006). Modifications on the benzyl ring (NI-135, NI-147, NI-136 and NI-176), and oxazine ring (NI-269, NI-182, NI-145, NI-297, NI-302 and NI-176) showed significant improvement of *in vitro* potency compared to PA-824. The nitroimidazole (NI) analogs tested in this study displayed a wide range of solubility (<2 to 127 µg/mL). Amino-nitroimidazoles showed improved solubility compared to their respective benzyl ether analogs (Amino-824 versus PA-824 and NI-269 versus NI-145). NI-297, a biphenyl derivative of NI-182, had very poor aqueous solubility (<2 µg/mL) due to its high lipophilicity (logP 6). In general, the logP of all the other NI derivatives ranged between 2.4 and 3.8 and all showed high permeability except NI-644, which had moderate permeability in the Caco-2 assay. Overall the compounds exhibited moderate-to-high mouse plasma protein binding (80 to 98%), except for AminoEthyl-824, which showed the lowest binding (45%).

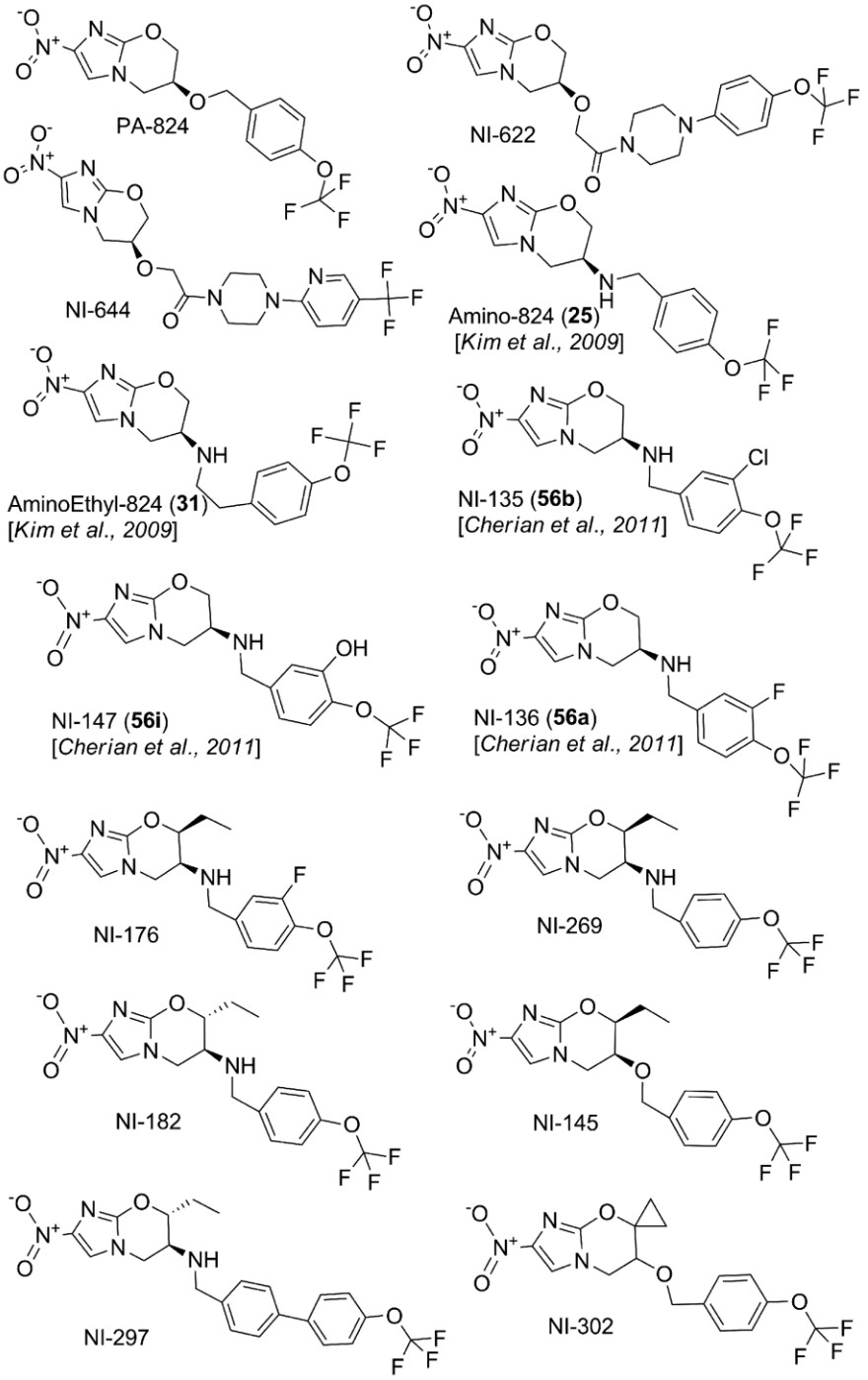

Figure 24. Chemical structures of bicyclic 4-nitroimidazole analogs used in this study

Table 11. *In vitro* potency and physicochemical properties for bicyclic 4-nitroimidazole analogs

Compound ID	H37Rv MIC_{99} (mg/L)	H37Rv::F_{420}-mutants MIC_{99} (mg/L)	Cytotoxicity CC_{50} (mg/L)	Solubility pH 6.8 (µg/mL)	Log P	PAMPA (Log Pe cm/sec, % FA)	Caco-2 permeability (P_{app}, 10^{-6} cm/sec)		Caco-2 efflux ratio	Mice PPB (%)
							A-B	B-A	B-A / A-B	
PA-824	0.30	> 10	> 10	13.0	2.75	-4.2, 99	27.6	20.4	0.8	90
NI-622	0.18	> 10	> 10	28.2	2.9	-5.3, 31	9.5	12.4	1.3	97
NI-644	0.09	> 10	> 10	14.0	2.6	-4.9, 83	2.8	13.7	4.8	90
Amino-824	0.14	> 10	> 10	127	2.5	-4.8, 91	35.4	21.0	0.6	80
AminoEthyl-824	0.06	> 10	> 10	104	3.6	-4.6, 85	18.6	20.7	1.1	45
NI-135	0.03	> 10	> 10	77.0	3	-4.5, 90	23.4	15.3	0.6	91.5
NI-147	0.03	> 10	nd	56.0	2.4	-5.2, 43		nd		nd
NI-136	0.03	> 10	> 10	43.0	2.6	-4.7, 83	15.4	12.6	0.8	82.7
NI-176	0.03	> 10	> 10	8.0	3.5	-3.7, 99		nd		nd
NI-269	0.03	> 10	> 10	12.0	3.15	-3.7, 99		nd		nd
NI-182	0.02	> 10	> 10	32.0	3.05	-3.8, 99	18.3	13.9	0.8	91.3
NI-145	0.06	> 10	> 10	<2.0	3.85	-3.85, 99		nd		nd
NI-297	0.02	> 10	> 10	<2.0	6	-4.1, 97		nd		98.2
NI-302	0.03	> 10	> 10	26.0	3.2	-3.6, 99	45.1	18.7	0.4	95.7

MIC_{99}=Minimum Inhibitory Concentration required to reduce the bacterial growth by 99%, MIC against both H37Rv (wild type) and F_{420} deficient (*FbiC*) mutants were tested. PAMPA = Parallel Artificial Membrane Permeability Assay, Caco-2 = Permeability using colon carcinoma cell lines, PPB= Plasma Protein Binding, Pe = effective permeability, FA = fraction absorbed, P_{app} = apparent permeability, A-B = Apical to Basolateral, B-A = Basolateral to Apical, nd = not determined, CC_{50} = Cytotoxicity against THP1 macrophage cell lines was determined as described previously (Pethe et al., 2010), with Puromycin as positive control (CC_{50} = 1.4 mg/L).

4.3.2 *In vivo* plasma PK properties

Each compound was subjected to intravenous and oral mouse PK in CM-2 formulation. The total compound concentration in mouse plasma was measured and free plasma concentrations were calculated using *in vitro* plasma protein binding (Table 11 and 12). NI-147 with a hydroxyl functional group on the benzyl ring, displayed markedly inferior PK properties (Table 12, Figure 25). The poor PK is likely due to glucuronidation of the hydroxyl group as suggested by the presence of an extra peak corresponding to + 176 Da in the mass spectrometry analysis. Hence NI-147 was not included in *in vivo* mouse efficacy studies. The NI analogs displayed a wide range of volume of distribution (V_{ss} = 0.7 to 4.2 L/kg) corresponding to 1.1 to 7 times total body water. NI-135 showed higher V_{ss} (4.2 L/kg), followed by NI-182, NI-297 and NI-269 (2.6 to 3 L/kg). All other analogs showed moderate V_{ss} similar to PA-824, except for NI-644, which showed a low volume of distribution (V_{ss} = 0.7 L/kg). The total systemic clearance was low to moderate (4 to 44 mL/min/kg) corresponding to 5 to 49% of hepatic blood flow. NI-135 and AminoEthyl-824 showed moderate clearance (41 and 44 mL/min/kg respectively). All other analogs showed clearance similar to PA-824 (10 to 25 mL/min/kg), except for NI-297 and NI-302, which showed very low clearance (5 mL/min/kg). The elimination half-life ranged between 0.7 h and 6.7 h for the NI analogs studied. NI-297, NI-135 and NI-302 showed long half-life (3.7 to 6.7 h). All other analogs showed half-life similar to PA-824 (1.3 to 2.8 h), except for NI-644 and AminoEthyl-824, which showed short half-life (<1 h). Generally, the NI analogs at comparable doses displayed rapid absorption (T_{max}, 0.3 to 4 h), except for NI-297, which showed delayed absorption with a T_{max} of 8 h,

possibly due to its higher lipophilicity and lower solubility. The peak plasma concentration (C_{max}) ranged between 1.2 µg/mL and 12.9 µg/mL and exposure (AUC) ranged between 4.8 µg·h/mL and 144 µg·h/mL (Table 12). NI-135 had significantly lower plasma C_{max}, exposure and oral bioavailability compared to PA-824, likely due to its three times higher *in vivo* clearance combined with higher volume of distribution. On the contrary, NI-302 and NI-297 had higher systemic plasma exposure mostly due to decreased *in vivo* clearance (Table 12, Figure 25). At comparable dose, NI-622 and NI-644 showed similar plasma C_{max}, exposure and oral bioavailability compared to PA-824. All other NI analogs showed moderate plasma exposure and oral bioavailability (64 to 88%) except for NI-135, NI-297 and NI-302. Despite, NI analogs displayed varied aqueous solubility (<2 to 127 ug/mL), in CM-2 formulation all the analogs showed moderate to high oral bioavailability (Table 12). Interestingly, NI-145 and NI-297 had least solubility (<2 µg/mL), in CM-2 formulation both compounds showed good oral bioavailability. The use of CM-2 (lipid coated cyclodextrin complexation) formulation is known to improve solubility and bioavailability (Stella and Rajewski, 1997). At 25 mg/kg, the free plasma C_{max} and AUC parameters ranged from 0.1 - 0.8 µg/mL and 0.4 – 5.1 µg·h/mL respectively. NI-644 showed similar free plasma concentration as PA-824, whereas all other NI analogs showed relatively lower free plasma C_{max} and exposure (Table 18).

Table 12. *In vivo* pharmacokinetic parameters in plasma for bicyclic 4-nitroimidazole analogs

Compound ID	Oral (p.o.) PK parameters						Intravenous (i.v.) PK parameters			
	Dose (mg/kg)	C_{max} (µg/mL)	AUC_{24} (µg·h/mL)	T_{max} (hr)	$t_{1/2}$ (p.o.)	F (%)	Dose (mg/kg)	V_{ss} (L/kg)	CL (mL/min/kg)	$t_{1/2}$ (i.v)
PA-824	25	6.0	50.9	2	2.7	100	10	1.6	12.1	1.6
NI-622	50	14.8	108.4	4	2.1	100	10	1.8	14.7	1.8
NI-644	50	16.2	89.5	1	3.6	100	10	0.7	9.5	0.9
Amino-824	10	1.7	6.0	0.3	2.0	74	10	2.3	20.5	2.0
AminoEthyl-824	10	1.0	2.9	1	1.7	76	10	2.0	44.0	0.7
NI-135	25	1.2	4.8	0.5	2.9	51	5	4.2	41.0	4.0
NI-147	25	0.04	0.02	0.1	0.2	0.3	5	0.4	70.8	0.3
NI-136	25	2.0	10.7	0.5	2.0	64	5	1.8	25.1	1.3
NI-176	25	2.2	13.7	1	4.3	86	5	1.8	22.2	1.0
NI-269	25	2.8	16.0	0.3	3.8	88	5	2.6	19.7	2.1
NI-182	25	3.5	22.5	0.5	2.0	82	5	3.0	15.2	2.8
NI-145	25	1.8	16.2	2	4.2	68	5	1.7	17.0	2.0
NI-297	25	6.0	99.1	8	4.9	100	5	2.6	5.0	6.7
NI-302	25	12.9	144.1	4	4.1	100	5	1.2	4.3	3.7

C_{max} = maximum concentration reached in plasma, AUC_{24} = exposure between 0 to 24 h, T_{max} = time to reach maximum concentration, $t_{1/2}$ = half-life, F = oral bioavailability, V_{ss} = volume of distribution at steady state, CL = total systemic clearance.

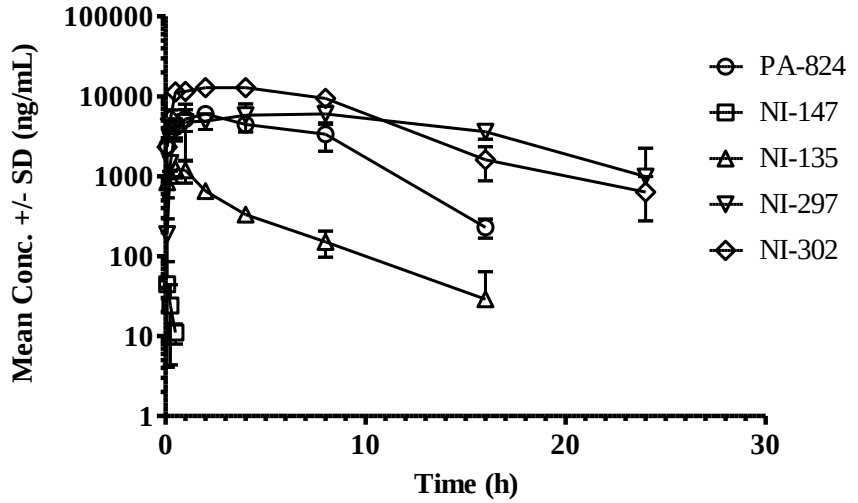

Figure 25. Plasma concentration time profiles of representative bicyclic 4-nitroimidazole analogs following an oral administration at a single 25 mg/kg dose in mice

4.3.3 *In vivo* lung PK properties

The primary and the most important site of Mtb infection in patients is lung tissue. To understand the effect of structural changes in the NI molecules on lung PK parameters, we measured total compound concentration in mouse lungs (Table 13). The NI analogs at 25 mg/kg dose showed a wide range of values for lung C_{max} (4.2 - 17.8 µg/g), T_{max} (0.08 – 2 h) and exposure (18.6 - 233 µg·h/g). All NI analogs displayed near parallel concentration-time profile in plasma and lung tissue, suggesting a rapid equilibrium between these two tissues. Interestingly, the lung-to-plasma partitioning varied from 0.5 to 4.6 for C_{max} and 0.4 to 3.9 for AUCs across the series in correlation with the observed volume of distribution (Table 13). NI-135, NI-136, NI-182 and NI-297 showed lung partitioning of 2.5 to 4.6 fold, and are comparable to PA-824. NI-622, NI-644, Amino-824 and NI-302 showed lower lung partitioning (<1) compared to PA-824. Although, NI-135 and NI-136 showed higher lung to plasma ratio (L/P) of 3.6 to 4.6, their absolute lung concentrations were 2.5 to

7.5 fold lower than PA-824. On the contrary, NI-302 showed lower lung partitioning, but its absolute concentrations were comparable to PA-824 (Table 13).

Table 13. *In vivo* pharmacokinetic parameters in lungs for bicyclic 4-nitroimidazole analogs

Compound	**Dose (mg/kg)**	**Lung PK parameters**				**Lung to Plasma ratio**	
		C_{max} (µg/g)	**AUC_{24} (µg·h/g)**	**T_{max} (hr)**	**$t_{1/2}$ (p.o.)**	**C_{max}**	**AUC_{24}**
PA-824	25	17.8	139.9	0.3	4.8	3.0	2.7
NI-622	50	10.2	71.1	0.5	1.8	0.7	0.7
NI-644	50	7.5	38.1	1	2.9	0.5	0.4
Amino-824	10	1.4	4.5	0.5	1.3	0.8	0.8
AminoEthyl-824	10	1.6	5.2	0.5	1.2	1.6	1.8
NI-135	25	5.5	18.6	0.5	3.3	4.6	3.9
NI-147	25	0.5	2.6	0.1	-	-	-
NI-136	25	7.2	39.8	0.5	2.5	3.6	3.7
NI-176	25	4.8	30.3	0.5	4.3	2.2	2.2
NI-269	25	5.4	27.5	0.3	2.7	1.9	1.7
NI-182	25	11.4	73.2	0.5	1.9	3.3	3.3
NI-145	25	4.2	34.6	2	4.1	2.3	2.1
NI-297	25	16.3	233.4	8	4.6	2.7	2.4
NI-302	25	9.7	100.3	2	4.1	0.8	0.7

C_{max} = maximum concentration reached in lungs, AUC_{24} = exposure between 0 to 24 h, T_{max} = time to reach maximum concentration, $t_{1/2}$ = half-life

4.3.4 Dose proportionality PK study

Dose range PK studies were done with three selected NI analogs (PA-824, NI-622 and NI-644). Pharmacokinetic parameters in plasma and lungs are summarized in Table 14 and 15 respectively. Despite, these NI analogs displayed low aqueous solubility (13 to 28.2 ug/mL) (Table 11), in CM-2 formulation, all of them showed moderate to high oral bioavailability across the dose range studied. Noteworthy, the calculated oral bioavailability was more than 100%. This might be due to nonlinear behavior of these three NI analogs in the dose range investigated. Interestingly, the lung-to-plasma partitioning was higher for PA-824 and ranged from 2.1 to 3.0 for both C_{max} and AUCs across the dose range studied indicating preferential lung distribution relative to plasma. However, both NI-622 and NI-644 showed lower lung partitioning (<1) at all the doses studied.

Plots of log-transformed C_{max}, AUC and the regression lines are shown in Figure 26 (plasma) and Figure 27 (lungs). Results from the regression analysis of the C_{max} and AUC in both plasma and lungs are summarized in Table 16. It was observed that the PK parameters, C_{max} and AUC increased with doses in plasma and lungs for both PA-824 and NI-622. However, the increases were not strictly proportional to the doses, in the dose range investigated, indicating possible saturation in some of the processes. Interestingly, there is dose related but over proportional increase in C_{max} (plasma only) and AUC was observed in both plasma and lungs for NI-644. Further, lung C_{max} seems to increase linearly with dose. These observations are supported by the slope of the regression line (Table 16), dose normalized C_{max} and AUC in both plasma (Table 14) and lungs (Table 15). Overall, all the NI

analogs showed an apparent dose related but nonlinear increase in C_{max} and exposure in both plasma and lungs. Due to the above nonlinear observation for three representative NI analogs and lack of dose proportionality, data analysis for other NI-analogs was done only with available experimental PK data.

Table 14. Pharmacokinetic parameters in plasma for bicyclic 4-nitroimidazoles after oral administration to mice

Compound ID	Dose (mg/kg)	Plasma PK parameters			Dose normalized parameters	
		C_{max} (µg/mL)	AUC_{24} (µg·h/mL)	F* (%)	C_{max}/Dose	AUC/Dose
PA-824	25	6.0	50.9	151	0.24	2.04
	50	10.3	119.9	185	0.21	2.10
	100	16.3	268.7	204	0.16	2.69
	250	22.8	336.1	156	0.09	1.34
NI-622	10	6.6	37.0	329	0.66	3.70
	50	14.8	108.5	192	0.30	2.17
	100	20.9	197.1	174	0.21	1.97
	250	50.7	627.4	222	0.20	2.51
NI-644	10	2.0	9.5	58	0.20	0.95
	50	16.2	89.5	96	0.32	1.79
	100	26.6	329.8	193	0.27	3.30
	250	79.9	986.4	231	0.32	3.95

*F was calculated using dose normalized exposures between p.o. and i.v. routes.

Table 15. Pharmacokinetic parameters in lungs for bicyclic 4-nitroimidazoles after oral administration to mice

Compound ID	Dose (mg/kg)	Lung PK parameters		Dose normalized parameters		Lung to Plasma ratio	
		C_{max} (µg/g)	AUC_{24} (µg·h/g)	C_{max}/Dose	AUC/Dose	C_{max}	AUC_{24}
PA-824	25	17.8	139.9	0.71	5.60	3.0	2.6
	50	22.9	262.6	0.46	5.25	2.2	2.1
	100	35.2	564.9	0.35	5.65	2.2	2.1
	250	55.5	778.9	0.22	3.12	2.4	2.2
NI-622	10	3.2	22.5	0.32	2.25	0.8	0.6
	50	10.2	71.1	0.20	1.42	0.7	0.7
	100	19.5	181.5	0.19	1.81	0.9	0.9
	250	35.5	472.0	0.14	1.89	0.7	0.8
NI-644	10	1.3	5.6	0.13	0.56	0.6	0.6
	50	7.5	38.1	0.15	0.76	0.5	0.4
	100	14.4	124.6	0.14	1.25	0.5	0.4
	250	37.5	481.6	0.15	1.93	0.5	0.5

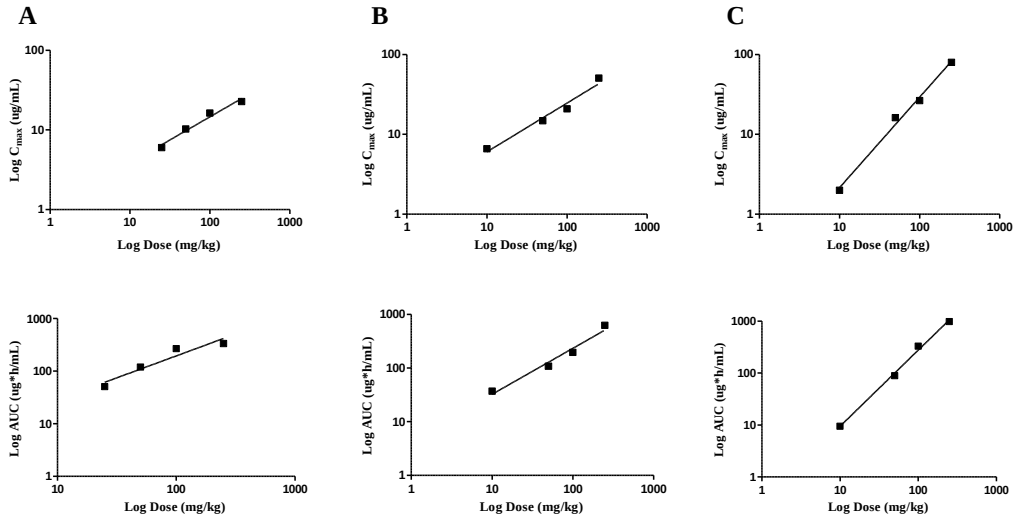

Figure 26. Dose linearity test by power regression analysis in plasma for C_{max} and AUC of PA-824 (A), NI-622 (B), and NI-644 (C)

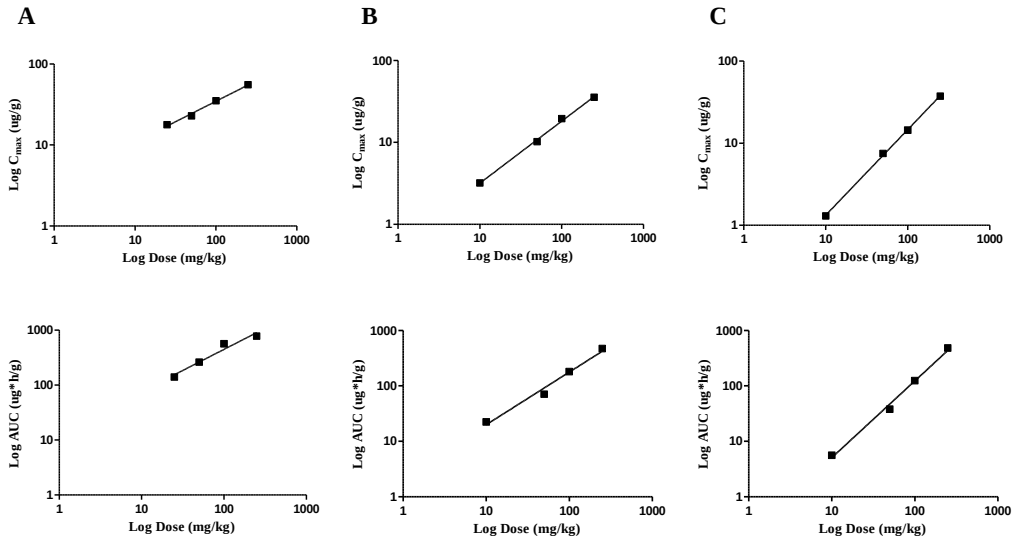

Figure 27. Dose linearity test by power regression analysis in lungs for C_{max} and AUC of PA-824 (A), NI-622 (B), and NI-644 (C)

Table 16. Dose proportionality test using power model

Compound	Dose Range (mg/kg)	Matrix	Parameter	R^2	Slope	95% Lower CI	95% Upper CI	Inference
PA-824	25 - 250	Plasma	C_{max}	0.97	0.58	0.28	0.88	Nonlinear
			AUC_{0-24}	0.92	0.83	0.05	1.62	Nonlinear
		Lungs	C_{max}	0.99	0.51	0.37	0.64	Nonlinear
			AUC_{0-24}	0.95	0.77	0.24	1.29	Nonlinear
NI-622	10 - 250	Plasma	C_{max}	0.97	0.61	0.27	0.95	Nonlinear
			AUC_{0-24}	0.97	0.86	0.42	1.30	Nonlinear
		Lungs	C_{max}	0.99	0.76	0.64	0.87	Nonlinear
			AUC_{0-24}	0.98	0.95	0.55	1.34	Nonlinear
NI-644	10 - 250	Plasma	C_{max}	0.99	1.13	0.83	1.43	Inconclusive
			AUC_{0-24}	0.99	1.47	1.18	1.75	Nonlinear
		Lungs	C_{max}	0.99	1.04	0.96	1.12	Linear
			AUC_{0-24}	0.99	1.39	1.06	1.71	Nonlinear

CI, confidence interval; The system was considered to be linear when $R^2 \sim 1$, Slope $CI_{lower} \geq 0.8$, and $CI_{upper} \leq 1.25$
Dose linearity tests on C_{max} and AUC_{0-24} were carried out by the regression of log-transformed data (power regression model) (Hummel et al., 2009; Smith et al., 2000). Doses and PK parameters were log-transformed, and correlation coefficient (R^2), slope, and 95% confidence intervals were calculated using the graphpad prism software. Inferences were made based on the $R^2 \sim 1$, theoretical slope of 1, and confidence limits of 0.8 and 1.25. If one of CI value is outside the range, it is inferred as inconclusive.

4.3.5 Established mouse efficacy

Based on the *in vitro* potency and the *in vitro* and *in vivo* PK results, ten compounds were selected for *in vivo* mouse efficacy studies with 4 weeks of daily oral treatment. The mean lung CFU reductions compared to untreated controls are summarized in Table 17. The efficacy ranged from 0.5 to 1.56 log at 25 mg/kg and 0.6 to 2.3 log at 100 mg/kg compared to vehicle treated animals. At 25 mg/kg, NI-622 and NI-644 were significantly ($P < 0.05$) less efficacious than PA-824, however other NI analogs (NI-135, NI-136, NI-182 and NI-297) showed comparable efficacy to PA-824. At 100 mg/kg, AminoEthyl-824, NI-135, NI-136 and NI-302 showed comparable efficacy to

PA-824, however NI-622, NI-644, Amino-824 and NI-182 were significantly ($P < 0.05$) less efficacious than PA-824. For PA-824, NI-135 and NI-136 a dose dependent increase in efficacy was observed, on the contrary, no dose-dependent increase in bactericidal activity was observed for NI-622, NI-644 and NI-182. However, none of the selected bicyclic 4-nitroimidazole analogs showed significantly better efficacy than PA-824 at respective 25 and 100 mg/kg doses.

Table 17. *In vivo* pharmacodynamics of bicyclic 4-nitroimidazole analogs studied in mice

	Mean log lung CFU ± SEM			**Δ Mean log lung CFU reduction ± SEM**	
Dose (mg/kg)	**Vehicle control**	**25**	**100**	**25**	**100**
PA-824	6.07 ± 0.12	4.67 ± 0.37	4.12 ± 0.13	1.40 ± 0.37	1.95 ± 0.13
	6.24 ± 0.02	4.67 ± 0.10	3.93 ± 0.09	1.57 ± 0.10	2.31 ± 0.09
	6.66 ± 0.14	5.20 ± 0.05	4.19 ± 0.11	1.46 ± 0.05	2.47 ± 0.11
				1.48 ± 0.09[$]	2.30 ± 0.08[$]
NI-622	6.66 ± 0.14	5.77 ± 0.08	5.85 ± 0.11	0.89 ± 0.08*	0.81 ± 0.11*
NI-644	6.66 ± 0.14	6.18 ± 0.03	6.09 ± 0.07	0.48 ± 0.03*	0.57 ± 0.07*
Amino-824	6.22 ± 0.08	nd	5.14 ± 0.08	nd	1.08 ± 0.08*
AminoEthyl-824	6.22 ± 0.08	nd	4.53 ± 0.07	nd	1.69 ± 0.07 [ns]
NI-135	6.24 ± 0.02	4.76 ± 0.07	4.36 ± 0.07	1.48 ± 0.07[ns]	1.88 ± 0.07 [ns]
NI-136	6.24 ± 0.02	4.93 ± 0.06	4.18 ± 0.17	1.31 ± 0.06[ns]	2.06 ± 0.17 [ns]
NI-182	6.07 ± 0.12	4.84 ± 0.14	4.81 ± 0.18	1.23 ± 0.14[ns]	1.26 ± 0.18*
NI-297	6.07 ± 0.12	4.51 ± 0.11	nd	1.56 ± 0.11[ns]	nd
NI-302	6.62 ± 0.11	nd	4.45 ± 0.22	nd	2.17 ± 0.22 [ns]

The mean log lung CFU's in five independent *in vivo* efficacy studies ranged between 6.07 and 6.66 in untreated infected mice. nd = not determined; Δ Mean log lung CFU reduction compared to untreated controls. Each data represents mean value ± SEM from 5 animals. [$]Mean value from three independent experiments (n=15). *Significant difference at $P < 0.05$ compared to respective PA-824 doses. [ns]No significant difference at $P < 0.05$ compared to respective PA-824 doses. Statistical analysis was done by a one-way analysis of variance, followed by a multiple comparison analysis of variance by a one-way Tukey test (GraphPad Prism, version 5.02, San Diego, California, USA, www.graphpad.com).

4.3.6 Correlation of PK parameters with efficacy

Further, mouse PK and efficacy data were used to understand the relationship of PK parameters with *in vivo* efficacy for a series of NI analogs. Both PK and efficacy data at 25 mg/kg were available for only 7 compounds. PK parameters were obtained after a single oral dose (Table 12), while efficacy studies were performed at oral daily doses of 25 and 100 mg/kg for 4 weeks (Table 17). The relationship between mean log CFU reduction and PK parameters (C_{max} and AUC) was analyzed in both plasma and lungs using the Spearman's rank correlation (Figure 28, Table 18). The free plasma concentrations were obtained by correcting for *in vitro* mouse plasma protein binding. As shown in Figure 28, with the limited set of compounds, the *in vivo* efficacy correlated well with lung PK parameters than plasma PK parameters. The Spearman's rank correlation coefficient for lung C_{max} and AUC were 0.76 and 0.52 respectively. Across the NI analogs studied, compounds with higher lung concentration (PA-824, NI-297 and NI-182) tended to achieve higher efficacy (Δlog CFUs ranging from 1.23 to 1.56), likewise compounds with lower lung concentration (NI-644 and NI-622) displayed only marginal efficacy (Δlog CFUs ranging from 0.48 to 0.89) (Table 13 and 17). In general, lung C_{max} and exposure showed positive correlation with *in vivo* efficacy for bicyclic 4-nitroimidazoles.

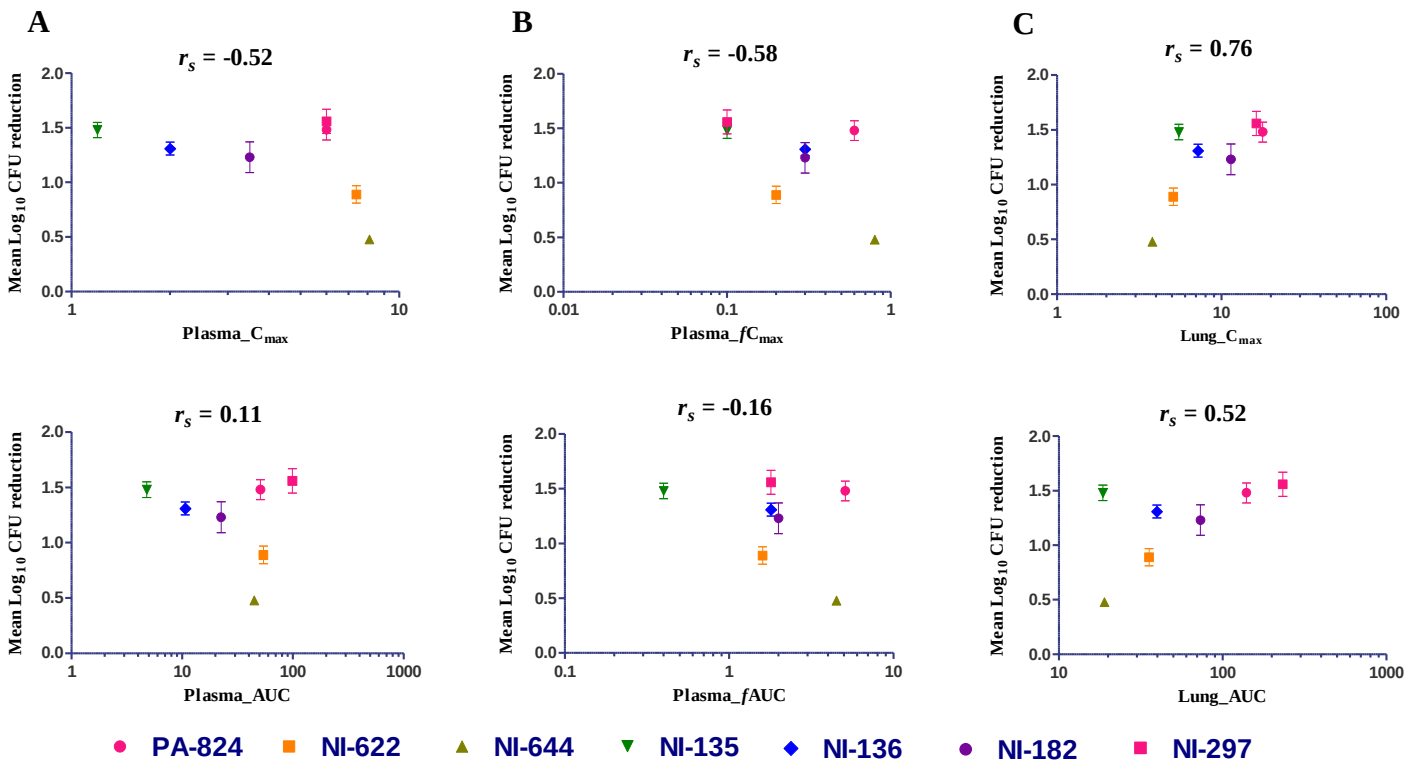

Figure 28. Correlation of PK parameters (C_{max}, AUC) with *in vivo* efficacy in mice for bicyclic 4-nitroimidazole analogs in total plasma (A), free plasma concentration (B) and total lung concentration (C)
Each data point represents Δ mean log lung CFU reduction compared to untreated controls (mean value ± SEM from 5 animals). r_s is the Spearman's rank correlations coefficient.

Table 18. Correlation of PK parameters with *in vivo* efficacy in mice for bicyclic 4-nitroimidazole analogs

Compound ID	Dose (mg/kg)	Plasma PK				Lung PK		Mean log lung CFU reduction ± SEM
		Total concentration		Free concentration		Total concentration		
		C_{max} (µg/mL)	AUC (µg·h/mL)	fC_{max} (µg/mL)	fAUC (µg·h/mL)	C_{max} (µg/g)	AUC (µg·h/g)	
PA-824	25	6	50.9	0.6	5.1	17.8	139.9	1.48 ± 0.09
NI-622	25[#]	7.4	54.2	0.2	1.6	5.1	35.6	0.89 ± 0.08
NI-644	25[#]	8.1	44.8	0.8	4.5	3.8	19	0.48 ± 0.03
NI-135	25	1.2	4.8	0.1	0.4	5.5	18.6	1.48 ± 0.07
NI-136	25	2	10.7	0.3	1.8	7.2	39.8	1.31 ± 0.06
NI-182	25	3.5	22.5	0.3	2.0	11.4	73.2	1.23 ± 0.14
NI-297	25	6	99.1	0.1	1.8	16.3	233.4	1.56 ± 0.11
Spearman correlation with efficacy		r_s = -0.52	r_s = 0.11	r_s = -0.58	r_s = -0.16	r_s = 0.76	r_s = 0.52	

PK parameters obtained from single dose PK data. Free concentrations in plasma were calculated using *in vitro* plasma protein binding. [#]PK parameters derived from 50 mg/kg. r_s = Spearman correlation coefficient. Δ Mean log lung CFU reduction compared to untreated controls. Each data represents mean value ± SEM from 5 animals.

4.3.7 Correlation of PK-PD indices with efficacy

In vitro activity against Mtb is one of the key determinants of *in vivo* efficacy, hence the relationship between mean log lung CFU reduction with three primary descriptive PK-PD indices (C_{max}/MIC, AUC/MIC and $T_{>MIC}$) was analyzed in both plasma and lungs (Figure 29, Table 19). As observed above, over all, the *in vivo* efficacy seems to have a stronger positive correlation with lung PK parameters than plasma. Among all the PK-PD indices, total lung $T_{>MIC}$ correlated best with *in vivo* efficacy (r_s = 0.88) than lung C_{max}/MIC (r_s = 0.63) and AUC/MIC (r_s = 0.63) (Figure 29C, Table 19). For all the compounds analyzed, the total lung $T_{>MIC}$ ranged between 64 and 100% resulting in 0.9 – 1.56 log lung CFU reduction. In this analysis, NI-644 was found to be an outlier, with $T_{>MIC}$ of 84% resulted in only 0.48 log CFU reduction. Overall, these results suggest that *in vivo* efficacy of bicyclic 4-nitroimidazole analogs correlates better with the time during which the total lung concentrations are above *in vitro* potency.

4.4 Discussion

PA-824, a bicyclic 4-nitroimidazole has demonstrated bactericidal activity in both preclinical and clinical settings (Diacon et al., 2010; Lenaerts et al., 2005; Tyagi et al., 2005). Extensive medicinal chemistry efforts to improve aqueous solubility, metabolic stability, *in vitro* potency and *in vivo* efficacy have independently generated several series of NI analogs (Barry et al., 2011; Blaser et al., 2012; Cherian et al., 2011; Denny and Palmer, 2010; Jiricek et al., 2007; Kim et al., 2009a; Kim et al., 2009b; Kmentova et al., 2010; Matsumoto et al., 2006; Palmer et al., 2010; Thompson et al., 2011). All the

bicyclic 4-nitroimidazole analogs analyzed in this study showed cofactor F_{420} dependent bio-activation (Table 11) suggesting the mechanism of action of these compounds similar to PA-824 (Manjunatha et al., 2006; Singh et al., 2008). Comprehensive *in vivo* efficacy studies are generally resource / time intensive and are particularly true for TB. Thus, prioritizing potential lead compounds for *in vivo* efficacy studies would be useful based on PK parameters.

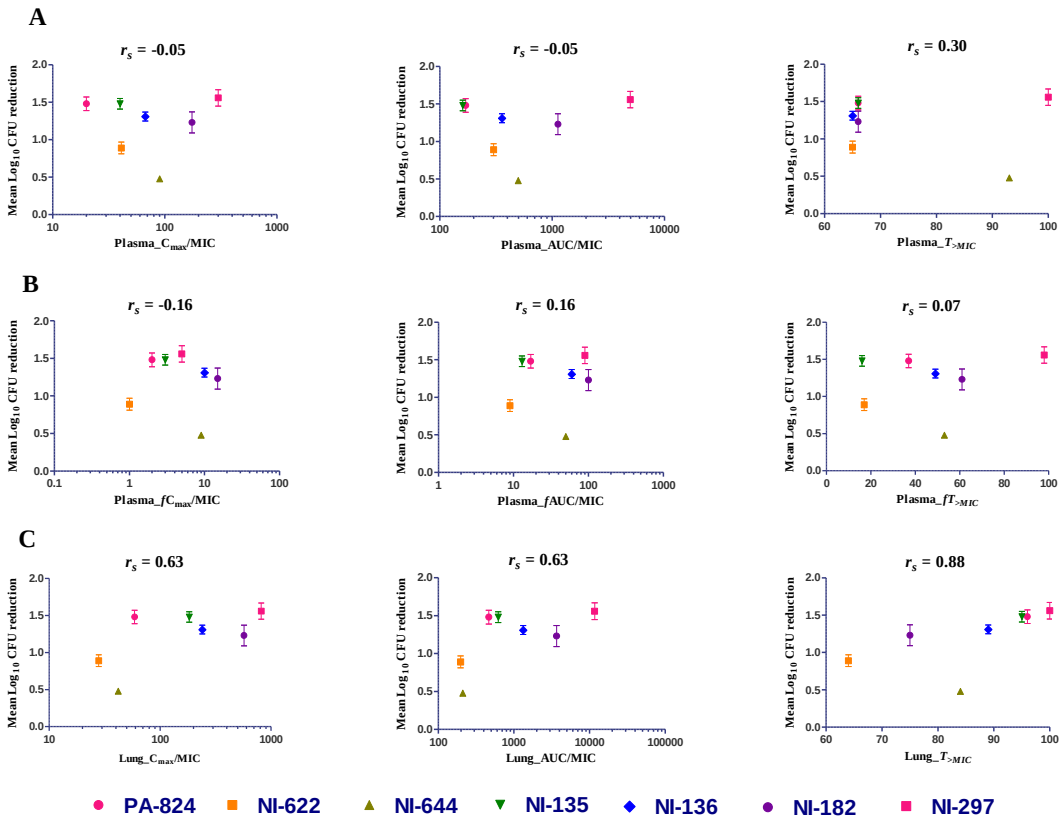

Figure 29. Correlation of PK-PD indices (C_{max}/MIC, AUC/MIC and $T_{>MIC}$) with *in vivo* efficacy in mice for bicyclic 4-nitroimidazole analogs in total plasma concentration (A), free plasma concentration (B) and total lung concentration (C)
Each data point represents Δ Mean log lung CFU reduction compared to untreated controls (mean value ± SEM from 5 animals). r_s is the Spearman's rank correlations coefficient.

Table 19. Correlation of PK-PD indices with *in vivo* efficacy in mice for bicyclic 4-nitroimidazole analogs

Compound ID	Dose (mg/kg)	Plasma PK-PD indices						Lung PK-PD indices			Mean log lung CFU reduction ± SEM
		Total concentration			Free concentration			Total concentration			
		C_{max}/MIC	AUC/MIC	$\%T_{>MIC}$	fC_{max}/MIC	fAUC/MIC	$fT_{>MIC}$	C_{max}/MIC	AUC/MIC	$\%T_{>MIC}$	
PA-824	25	20	170	66	2.0	17	37	59	466	96	1.48 ± 0.09
NI-622	25[#]	41	301	65	1.1	8.9	17	28	198	64	0.89 ± 0.08
NI-644	25[#]	90	498	93	8.9	50	53	42	211	84	0.48 ± 0.03
NI-135	25	40	160	66	3.3	13.3	16	183	620	95	1.48 ± 0.07
NI-136	25	67	357	65	10	60	49	240	1327	89	1.31 ± 0.06
NI-182	25	175	1125	66	15	100	61	570	3660	75	1.23 ± 0.14
NI-297	25	300	4955	100	5.0	90	98	815	11670	100	1.56 ± 0.11
Spearman correlation with efficacy		r_s = -0.05	r_s = -0.05	r_s = 0.30	r_s = -0.16	r_s = 0.16	r_s = 0.07	r_s = 0.63	r_s = 0.63	r_s = 0.88	

PK-PD indices were calculated using PK parameters obtained from single dose PK data and *in vitro* potency. Free concentrations in plasma were calculated using *in vitro* plasma protein binding. [#]PK parameters derived from 50 mg/kg. r_s = Spearman correlation coefficient. Δ Mean log lung CFU reduction compared to untreated controls. Each data represents mean value ± SEM from 5 animals.

This study is a retrospective analysis of *in vivo* efficacy with PK for bicyclic 4-nitroimidazole analogs to identify the PK parameters and PK-PD indices that correlate with the *in vivo* potency. The results of this analysis could potentially be exploited to prioritize new analogs for efficacy studies.

Mtb mainly resides in lung granulomatous structures and hence it is important for a drug to be available at the site of the infection for it to be active. The volume of distribution is a primary PK parameter defined by the physicochemical properties of the compound that indicates the extent of compound distribution in the body. Azithromycin, a macrolide antibiotic, with very high V_{ss} (33 L/kg) (Obach et al., 2008) is known to have higher lung concentration than serum (AUC lung/serum = 21) (Veber et al., 1993) and it correlates well with *in vivo* activity against respiratory pathogens. Likewise, moxifloxacin displays a high volume of distribution (V_{ss} = 2 to 5 L/kg) resulting in pronounced penetration into tissues (AUC L/P ratio of 3.3) (Siefert et al., 1999a; Siefert et al., 1999b) possibly leading to its potent *in vivo* efficacy against TB (Nuermberger et al., 2004). Recently, moxifloxacin has been shown to penetrate and accumulate in granulomatous lesions in TB infected rabbit lungs (Prideaux et al., 2011). TMC207, a diarylquinoline analog, extensively distributes to lungs (AUC L/P ratio of 22) and is efficacious against Mtb (Andries et al., 2005). In this study, NI analogs having moderate-to-high volume of distribution (V_{ss} = 1.6 to 4.2 L/kg) and L/P ratio of > 2 showed good efficacy in a murine TB model (Δlog CFUs ranging from 1.23 to 1.56) (Table 12, 13 and 17, Figure 30). Interestingly, NI-622 and NI-644 that showed lower lung to plasma ratio displayed only a marginal efficacy (Δlog CFUs ranging from 0.48 to 0.89). Although, NI-135 and NI-136 showed

higher lung to plasma ratio (3.6 to 4.6), their absolute lung concentrations were 2.5 to 7.5 fold lower than PA-824. However, both these compounds displayed 10 times better *in vitro* potency resulting in comparable *in vivo* efficacy to PA-824. Overall, the relationship between *in vivo* efficacy of bicyclic 4-nitroimidazoles displayed positive correlation with V_{ss} (r_s = 0.45) (Figure 30). Based on these observations, the V_{ss} and lung distribution could give an initial indication about a compound's potential for *in vivo* efficacy and thus these two parameters could be used for initial prioritization of compounds during early drug discovery.

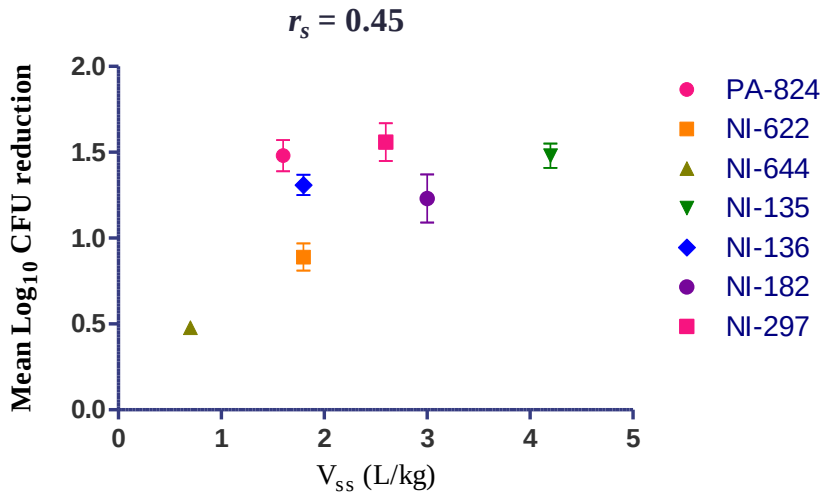

Figure 30. Correlation of volume of distribution with *in vivo* efficacy in mice for bicyclic 4-nitroimidazole analogs
Each data point represents Δ Mean log lung CFU reduction compared to untreated controls (mean value ± SEM from 5 animals). r_s is the Spearman's rank correlations coefficient.

A thorough dose fractionation study of PA-824 in a murine model showed that the primary PK-PD driver for *in vivo* efficacy is the duration during which the free concentration are above MIC ($fT_{>MIC}$) in plasma (Ahmad et al., 2011). In this study lung PK parameters have not been measured. Further, $fT_{>MIC}$ in plasma of 22%, 48% and 77% is required for it to show

bacteriostatic, 1-$\log_{10}$ and 1.59 $\log_{10}$ kill respectively (Ahmad et al., 2011). In general, the PK-PD parameter driving efficacy is conserved within a given class of compounds (Barbour et al., 2010), for example, the efficacy of all fluoroquinolone analogs are driven by AUC/MIC (Craig, 1998; Craig, 2001; Shandil et al., 2007), while the efficacy of β-lactams correlates with $T_{>MIC}$ (Andes and Craig, 2002; Craig, 2001; Scaglione and Paraboni, 2006). These studies are done with thorough dose fractionation of single compound with multiple doses and dosing regimen. During lead optimization program prioritization of promising compounds that show good *in vivo* efficacy is important to reduce the overall turnaround time. In this retrospective analysis with 7 different bicyclic 4-nitroimidazole analogs, we attempted to correlate *in vivo* efficacy at 25 mg/kg with PK parameters. On the contrary to what has been observed by Ahmad et al., in this study, with seven bicyclic 4-nitroimidazole analogs having varied lung distribution, *in vivo* efficacy showed weak correlation with free $T_{>MIC}$ in plasma. However, the total $T_{>MIC}$ in lungs showed positive correlation with *in vivo* efficacy (r_s = 0.88) likely due to their preferential distribution into lungs for some analogs. For all the compounds analyzed, the total lung $T_{>MIC}$ ranged between 64 - 100% resulting in 0.9 – 1.56 log lung CFU reduction, hence efficacy studies at lower doses (resulting in $T_{>MIC}$ less than 65%) might be necessary to see a better correlation. Overall, in this study a diverse set of bicyclic 4-nitroimidazoles with V_{ss} ranging from 0.7 L/kg to 4.2 L/kg, lung to plasma ratio ranging from 0.5 to 4.6 showed positive correlation with lung $T_{>MIC}$ than with any other parameters.

NI analogs (PA-824, NI-622 and NI-644) appear to exhibit dose related increase in pharmacokinetics (C_{max} and exposure) in mice in CM-2 formulation. Further, at comparable doses, NI-622 and NI-644 showed similar or higher C_{max} and exposure in plasma, but had lower lung partitioning (<1) compared to PA-824 (Section 4.3.4). Favorable lung distribution is a desirable attribute for compounds developed to treat pulmonary tuberculosis. In general, total lung concentration and partitioning from the preliminary pharmacokinetic study could be used in the initial drug discovery program to quickly prioritize the compounds for lengthy efficacy studies. The lack of dose related increase in efficacy for NI-622 and NI-644 cannot be explained in spite of increase in the lung concentrations with the dose. The underlying mechanism for this behavior is yet to be understood. Further investigation like free concentration at the site of infection, active species and transporter mechanisms are required to understand the thorough PK-PD relationship for a specific compound.

The results presented in this study must be interpreted with a couple of limitations in mind. First, single-dose PK parameters determined in healthy mice were assumed to be predictive of multiple-dose PK parameters in infected animals and were correlated with efficacy data. This assumption is supported by published preclinical data that has shown the absence of plasma accumulation of PA-824 in mice dosed for 2 months (Nuermberger et al., 2006). Further, in clinical studies with PA-824, the PK parameters from a single dose phase I study were similar to a multiple dose phase II study in patients (Diacon et al., 2010; Diacon et al., 2012a; Diacon et al., 2012b; Ginsberg et al., 2009). Another limitation of this study is that total concentrations in lungs rather than the free lung concentrations were used for

the PK-PD analysis. It is well accepted that for a given compound unbound drug concentrations in plasma are equivalent to unbound tissue concentrations when active transport is not involved in the drug distribution (Lin, 2006; Smith et al., 2010). Further, it is the unbound concentration of a compound at its target site driving the pharmacological effect (Gonzalez et al., 2013; Liu et al., 2002; Mouton et al., 2008; Muller et al., 2004; Smith et al., 2010; Theuretzbacher, 2007). Nevertheless, whole-tissue concentrations can be of some value in early drug discovery providing a first assessment of partition into the lungs (Mouton et al., 2008). Techniques like microdialysis in lungs can be applied to assess unbound tissue concentration (Brunner et al., 2005; Chaurasia et al., 2007). In TB patients, Mtb mainly resides in diverse and heterogeneous lesions in lungs. In general, interpretation of PD activity of anti-TB compounds is complicated by differential lung pathophysiology. PK in intrapulmonary compartments like the epithelial lining fluid and alveolar macrophages have also been studied in humans for standard TB drugs like rifampicin (Ziglam et al., 2002), isoniazid (Conte, Jr. et al., 2002b), ethambutol (Conte, Jr. et al., 2001), pyrazinamide (Conte, Jr. et al., 1999), rifapentine (Conte, Jr. et al., 2000), moxifloxacin (Soman et al., 1999), ofloxacin (Chierakul et al., 2001) and linezolid (Conte, Jr. et al., 2002a). The concentration in these sites could be the key factor governing the efficacy of anti-TB drugs. However, measurement of compound concentration in lungs by microdialysis, epithelial lining fluid and alveolar macrophages have limitations in sampling, methodology and interpretation of results (Kiem and Schentag, 2008; Mouton et al., 2008); and such studies have not been explored in preclinical settings for TB. The total lung concentration may not be equal to

the concentration in Mtb lesions, thus warranting lesion PK analysis to improve the predictive power for efficacy. Recently PK in lung lesions of mycobacterium-infected rabbits has been investigated for isoniazid, rifampicin, pyrazinamide and moxifloxacin (Kjellsson et al., 2012; Prideaux et al., 2011). Although lesion PK can offer better insights in understanding PK-PD relationships, it is not easily applicable to early drug discovery especially with mouse efficacy model as it doesn't display spectrum of lesions observed in TB patients or in higher animal models. In addition, similar studies with bicyclic 4-nitroimidazoles may be challenging as they undergo enzymatic transformation in Mtb to multiple stable and unstable metabolites (Singh et al., 2008).

Our findings show that the efficacy of all bicyclic 4-nitroimidazole analogs is most likely driven by PK parameters in lungs. A simple efficacy surrogate would be useful during the lead optimization to prioritize candidates for lengthy efficacy studies. For this class, efficacy correlated better with concentration in lungs rather than in plasma, consistent with V_{ss} and differential lung: plasma distributions. The results of this analysis potentially be exploited to prioritize new analogs for efficacy studies based on *in vitro* potency, volume of distribution and lung concentration.

Chapter 5. Pharmacokinetics-pharmacodynamics analysis of spiroindolone analogs and KAE609 in a murine malaria model

5.1 Introduction

During a whole cell screening campaign for *P. falciparum* proliferation inhibitors, a series of spiroindolones was identified. Lead optimization efforts were further undertaken to improve their pharmacokinetic properties and *in vitro* potencies against *P. falciparum* (Yeung et al., 2010). Spiroindolones act through a novel mechanism that disrupt intracellular Na^+ homeostasis through the inhibition of the parasite non-sarco(endo)plasmic reticulum Ca^{2+} (non-SERCA) P-type ATPase PfATP4 (Rottmann et al., 2010; Spillman et al., 2013). The same parasiticidal mechanism across the series is further supported by the conserved enantiomer specificity (Yeung et al., 2010). KAE609 is a spiroindolone product of the lead optimization efforts and is currently in clinical development for the treatment of *P. falciparum* and *P. vivax* malaria. We have previously shown that the compound exhibits pharmacokinetic properties in rodents compatible with once-daily oral dosing in human (Rottmann et al., 2010). In the murine *P. berghei* malaria model, a single oral dose of 100 mg/kg of body weight of KAE609 was sufficient to cure 100% of the animals. Three daily oral doses of 50 mg/kg also afforded complete cure, while a 50% cure rate was achieved with a single dose of 30 mg/kg. In light of these results, it was speculated that sustained reduction in parasitemia could be achieved at low doses in human (Rottmann et al., 2010).

Dose-response experiments were performed to investigate the relationship between dose and efficacy (i.e., reduction in parasitemia) across the spiroindolone series. In order to further characterize KAE609, the most promising of this new class of antimalarials, a classical dose fractionation approach was adopted to identify the PK-PD index that correlates best with a

reduction in parasitemia in the *P. berghei* malaria murine model. Once such a PK-PD relationship is established, we propose that it could be used to prioritize analogs within the same class of compounds and contribute to the efficacy study design, thereby facilitating early drug discovery and lead optimization programs.

5.2 Materials and Methods

5.2.1 Chemicals

All spiroindolone analogs studied (Figure 31) were synthesized at Novartis Institute for Tropical Diseases, as described elsewhere (Yeung et al., 2010). Organic solvents (acetonitrile and methanol) were purchased from Merck, Darmstadt, Germany; ethanol and hydrochloric acid (HCl) were obtained from Fisher Scientific, Leicestershire, United Kingdom; polyethylene glycol 400 (PEG400) was purchased from Acros Organics, New Jersey, USA; d-α-tocopheryl polyethylene glycol 1000 succinate (vitamin E TPGS) NF grade from Eastman, Anglesey, United Kingdom; Solutol HS15 was obtained from BASF, Ludwigshafen, Germany; and acetic acid, warfarin and citrate acid buffer (prepared from anhydrous citric acid) were obtained from Sigma Aldrich, St. Louis, MO, USA.

5.2.2 *In vitro* antimalarial activity of spiroindolone analogs

In vitro potency against *P. falciparum* and *P. berghei* were determined as described in Appendix 4. All assays were repeated at least three times. The results were recorded and expressed as a percentage of the untreated controls.

The 50% inhibitory concentrations (IC_{50}) were estimated by linear interpolation. In addition, for the PK-PD analysis of KAE609, a 99% inhibitory concentration (IC_{99}) value was determined by transforming the data from scintillation counter (Anscombe transformation) to account for Poissonian measurement error. The inhibitory concentrations conferring 50% (IC_{50}), 90% (IC_{90}) and 99% (IC_{99}) growth reduction were inferred from fitting a four parametric logistic function (equation 1) to the transformed data in dependence of the log-transformed concentrations. where *R* is the response measured at any given concentration, E_0 is the base line effect in the absence of the drug, E_{max} is the maximum possible effect in the presence of the drug, *C* is the concentration of the drug, IC_{50} is the concentration that cause 50% of the effect, *s* is the Hill slope describing the steepness of the curve. Each of the three replicates was performed on a distinct 96-well plate. This has been accounted for in the fitting procedure by means of a Bayesian hierarchical model. The software used for parameter inference was Stan (2014).

$$R = E_0 + E_{max} * C^s/(C^S + IC_{50}^S)$$ -------- Equation 1

5.2.3 *In vivo* PK studies for spiroindolone analogs in CD-1 mice

The Institutional Animal Care and Use Committee (IACUC) of the Novartis Institute for Tropical Diseases, registered with the Agri-Food and Veterinary authority (AVA), Government of Singapore, reviewed and approved all animal experimental protocols. For the *in vivo* PK studies, female CD-1 mice (25 to 30g) were obtained from the Biological Resource Center, Biopolis, Singapore, and were randomly assigned to cages. The mice were allowed to acclimate before the initiation of the experiments. Feed and water were given *ad libitum*. The compounds were formulated at concentrations of 2.5 mg/mL

for a dose of 25 mg/kg administered orally (p.o.) and at a concentration of 1 mg/mL for a dose of 5 mg/kg given intravenously (i.v.). The solution formulation for p.o. and i.v. dosing contained 10% ethanol, 30% PEG 400 and 60% of 10% vitamin E TPGS. The blood samples from the mice were collected at 0.02 (for i.v. only), 0.08, 0.25, 0.5, 1, 2, 4, 8, 16 and 24 h post dosing. The dose proportionality studies were conducted with KAE609. Formulations containing 0.1, 0.5 and 10 mg/mL were prepared to support oral dosages of 1, 5, and 100 mg/kg, respectively. Additional samples were collected at 32 h and 48 h post dose for the 1- and 5-mg/kg dose groups and up to 72 h post dose for the 100 mg/kg dose group. Groups of three mice were used for each time point. Blood was centrifuged at 13,000 rpm for 7 min at 4 °C, and plasma was harvested and stored at -20 °C until analysis.

Plasma samples were processed by protein precipitation using acetonitrile:methanol:acetic acid (90:9.8:0.2) to recover both analytes and internal standard (warfarin) using a 8 to 1 extractant to plasma ratio for all the analogs studied except (+)-1 (6 to 1 ratio) and (+)-6 (3.6 to 1 ratio) (Yeung et al., 2010). After vortexing and centrifuging the mixture, the supernatant was removed and 5 µL of sample analyzed. Analyte quantitation was performed by high-performance liquid chromatography coupled with tandem mass spectrometry (LC-MS/MS). Liquid chromatography was performed using an Agilent 1100 high-performance liquid chromatography (HPLC) system (Santa Clara, CA), with the Agilent Zorbax XDB Phenyl (3.5 µm, 4.6x75 mm) column at oven temperatures of 35 °C for all the analogs studied [except (+)-5, (+)-6 and (-)-6 at 45 °C], coupled with a API3200 triple quadruple mass spectrometry (Sciex Applied Biosystems, Foster City, CA) for all the analogs

studied except (+)-1, (+)-5, (+)-6 and (-)-6 that were analyzed using QTRAP 4000 triple quadruple mass spectrometer (Applied Biosystems, Foster City, CA). Instrument control and data acquisition were performed using Applied Biosystems software Analyst 1.4.2. The mobile phases used were A, water-acetic acid (99.8:0.2, vol/vol) and B, either acetonitrile-acetic acid (99.8:0.2, v/v) for (+)-1, (+)-5 and (-)-6 or methanol-acetic acid (99.8:0.2 v/v) for all the other analogs studied, using a gradient 0 to 0.2 min (10% B), 0.2 to 1.8 min (10 to 80% B), 1.8 to 2.5 min (80% B), 2.5 to 2.51 min (80 to 10% B) and 2.51 to 6 min (10% B), with flow rate of 1.0 mL/min, and run time of 6 min. Under these conditions, the retention time of various compounds ranged from 3.2 to 4.1 minutes. Multiple reaction monitoring (MRM) was combined with optimized MS parameters to maximize detection specificity and sensitivity. The most intense MRM transitions [338.3/295.1 for (+)-1, 370.1/327.0 for (+)-2, 370.0/326.9 for (+)-3, 354.1/310.8 for (+)-4, 354.1/311.2 for (+)-5, 372.1/329.1 for (+)-6, 388.0/331.8 for (+)-7, 372.1/316.1 for (-)-6 and 388/332 for (-)-7] were used for quantitation. Most compounds were analyzed using electrospray ionization in the negative mode, except (+)-1 which was analyzed using positive mode. The recovery of the compounds from plasma was good and consistent across the concentration range studied. The lower limits of quantification for different compounds ranged between 1.3 and 70 ng/mL in plasma. A calibration curve was prepared freshly and analyzed with every set of study samples. Intraday variability was established with triplicate quality control samples at three concentration levels. The results were accepted if relative standard deviation was less than 15%.

The mean values of the compound concentrations in plasma were obtained from three animals at each time point and plotted against time to generate concentration-time profiles. The pharmacokinetic parameters were determined using WinNonlin Professional, version 5.0.1 (Pharsight, California, USA), by noncompartmental modeling using software model 200 for oral dosing and model 201 for intravenous dosing. The oral bioavailability (F) was calculated as the ratio between the area under the curve from 0 to infinity (AUC_{inf}) following oral administration and the AUC_{inf} following intravenous administration corrected for dose ($F = AUC_{p.o.} \cdot dose_{i.v.} / AUC_{i.v.} \cdot dose_{p.o.}$).

5.2.4 *In vivo* antimalarial efficacy of spiroindolone analogs in NMRI mice

All *in vivo* studies conducted at the Swiss Tropical and Public Health Institute (TPH) were adhered to local and national regulations of laboratory animal welfare in Switzerland (permission number 1731). For *in vivo* efficacy, female (specific pathogen free) National Medical Research Institute (NMRI) mice were obtained from Janvier, Le Genest-Saint-Isle, France. Only mice without visible signs of disease were used for the study. Standard laboratory conditions were adopted for husbandry. *In vivo* antimalarial activity was assessed using groups of five female NMRI mice (20 to 22 g) intravenously infected on day zero with $2x10^7$ erythrocytes parasitized with *P. berghei* GFP ANKA malaria strain $PbGFP_{CON}$ (a donation from A. P. Waters and C. J. Janse, Leiden University) (Franke-Fayard et al., 2004). Upon inoculation of *P. berghei* parasites, the infection of untreated mice with *P. berghei* (ANKA strain) invariably takes a lethal course within 6 to 7 days (Rottmann et al., 2010).

Hence, both survival and a reduction in parasitemia can be monitored to evaluate (i) the ability of a drug candidate to clear all viable parasites, as measured by the absence of recrudescence up to 30 days post-infection (i.e., 'cure'), and (ii) drug-mediated reduction in parasitemia at the end of treatment. Untreated control mice typically died between day six and day seven post infection. Experimental compounds were formulated in 10% ethanol, 30% PEG400 and 60% of 10% vitamin E TPGS and were administered orally in a volume of 10 mL/kg. Dose-response efficacy studies were conducted for each spiroindolone analog. Doses of 2.5, 5, 10, 30 and 100 mg/kg were administered to groups of 5 mice as a single dose 24 h post infection. Parasitemia, expressed as parasitized red blood cells (pRBCs) over 100 RBC's, was determined 72 h post infection using standard flow cytometry techniques (Franke-Fayard et al., 2004).

5.2.5 Dose-response relationship analysis for spiroindolone analogs

Data analysis was done using nonlinear mixed effect modeling (NONMEM version VI 2.0), which analyzed the PD data from multiple dose groups obtained from different experiments simultaneously. Within NONMEM, first order conditional estimation (FOCE) was the method used (Silber et al., 2010) (Appendix 5). The log-transformed dose and level of parasitemia were used for analysis. For each compound a dose-response model was built and effective dose lowering 90% of parasitemia (ED_{90}) was determined using the equation 2 (Knudsen et al., 2000), where P is the parasitemia measured at any given dose, P_{max} is the maximum level of parasitemia, P_{min} is the minimum level of parasitemia, EZ_{50} is the dose required to produce 50% of the maximal

effect, s is the Hill slope describing the steepness of the curve and x is the dose (mg/kg).

$$P = P_{min} + \left[(P_{max} - P_{min}) / (1 + 10^{(logEZ_{50} - logx) \times s}) \right]$$ --------Equation 2

5.2.6 *In vivo* PK and dose fractionation studies for KAE609 in NMRI mice

For the *in vivo* PK studies, female NMRI mice (specific pathogen free) were obtained from Janvier, Le Genest-Saint-Isle, France. To investigate the influence of the disease status on the pharmacokinetics, a single oral dose (5.3 mg/kg) of KAE609 was given to both the infected and uninfected NMRI mice, and the PK parameters determined. The infected mice were dosed 24 h postinfection. The formulation, sampling times (0.25, 0.5, 1, 2, 4, 8, 24 and 48 h post dose), extraction and analysis were similar to the method described above.

The dose fractionation studies were conducted at daily oral doses of 0.5, 1, 2, 4, and 8 mg/kg. The total daily doses were either administered as a single dose (24 h postinfection) or divided into two (bid) or three oral doses (tid) per day. Four mice were used for each regimen, with control mice receiving vehicle only. Parasitemia, expressed as parasitized red blood cells (pRBCs) over 100 RBC's, was determined 72 h postinfection (48 h after initiation of treatment with KAE609) using standard flow cytometry techniques (Franke-Fayard et al., 2004).

5.2.7 PK modeling and simulation for KAE609

Population PK modeling of concentration-time data of KAE609 in mice was performed using naive pooling without intersubject variability using NONMEM version VI 2.0 (Appendix 6). A two-compartment

pharmacokinetic model with first-order absorption and nonlinear elimination was built to fit the time concentration-time data of KAE609 generated in (infected and healthy) NMRI mice at 5.3 mg/kg. In the model, clearance (CL) was described by the equation 3, where C_p is compound plasma concentration, V_{max}/K_m is the maximal clearance achievable when $C_p << K_m$, and K_m corresponds to the compound concentration at which the clearance reached 50% of the V_{max}. The primary model parameters derived were plasma clearance (CL, in liter/h/kg), inter compartmental clearance (Q, in liter/h/kg), central and peripheral volume of distribution (V_c and V_p, respectively in liter/kg) and the absorption rate constant (K_a, in h^{-1}). The diagnostic plots were analyzed for closeness to and randomness along the line of identity on the observed versus predicted concentration plot, as well as randomness along the weighted residual zero line on the predicted concentration or time. The estimates were accepted when plots showed no systematic pattern (Sinou et al., 2008). Based on the estimated primary model parameters (V_{max}, K_m, V_c, V_p, Q, and K_a), plasma concentration-time profiles and secondary pharmacokinetic parameters, such as C_{max}, AUC at different doses and dosing regimens, were simulated using Berkeley Madonna software (version 8.0.1) (Berkeley Madonna™, University of California, Berkeley, CA).

$$CL = V_{max} / (K_m + C_p)$$ -------Equation 3

5.2.8 PK-PD relationship analysis of KAE609 (dose fractionation study)

Preliminary analysis was done using IC_{50} values against *P. falciparum* and *P. berghei* parasite as threshold (not shown). However, IC_{50} refers to the concentration of compound inhibiting only 50% of the parasites. In order to

completely eliminate the parasites, 2*IC_{99} values are required. Further, mouse was infected with *P. berghei* parasite, hence 2*IC_{99} value against *P. berghei* was used for final PK-PD analysis. Initially, % activity (compared to vehicle treated animals) was used as efficacy read out. However, parasitemia was obtained for different compounds from different experiments. In order to evaluate dose-response relationship for a single compound from multiple experiments, the data points were pooled from different experiments; hence parasitemia was used as efficacy readout for final analysis.

The concentration of compounds which inhibited 99% of *P. berghei* growth (IC_{99}) was used to calculate the threshold (TRE = 2*IC_{99}) and the PK-PD indices. The C_{max}/TRE was defined as the ratio of peak plasma concentration (C_{max}) to the threshold (2*IC_{99}), the AUC_{0-48}/TRE was defined as the ratio of area under the concentration-time curve from 0 to 48 h (AUC_{0-48}) to the threshold (ratio without dimensions), and the percent time over threshold (%$T_{>TRE}$) was defined as the percentage of the 48 h period during which the compound concentration exceeded the threshold (Mouton et al., 2005). The C_{max}/TRE, AUC_{0-48}/TRE and %$T_{>TRE}$ at different doses and dosing regimen were calculated using Berkeley Madonna Software (version 8.0.1) (Berkeley Madonna™, University of California, Berkeley, CA).

The relationship between PK-PD indices (log transformed C_{max}/TRE, log transformed AUC_{0-48}/TRE, %$T_{>TRE}$) and log transformed parasitemia were analyzed by nonlinear regression analysis. An exploratory analysis of PK-PD data was done using various models such as maximum effect (E_{max}), sigmoid E_{max}, and with and without slope. A sigmoidal dose-response (variable slope) model without constants was fitted to the data. GraphPad Prism version 5.02

for windows (GraphPad software, San Diego, California, USA) was the software used for this analysis. The model choice was guided initially by a visual inspection of the y-by-x plots and then by correlation analysis and by evaluating the standard error of the estimate. The parasitemia (P) measures at any value of each different PK-PD index is expressed in equation 2, where P_{max} is the maximum parasitemia, P_{min} is the minimum parasitemia, EZ_{50} (otherwise referred to as EC_{50}) is the value of the specific PK-PD index (C_{max}/TRE, $AUC_{0\text{-}48}$/TRE and $\%T_{>TRE,}$ respectively) required to produce 50% of the maximal effect, s is the Hill slope describing the steepness of the curve and x is any of the PK-PD indices. The values of 'x' corresponding to the maximum reduction in parasitemia were derived by interpolation based on equation 2.

5.3 Results

5.3.1 *In vitro* potency of the spiroindolone analogs

A series of chiral spiroindolone analogs were synthesized as part of a lead optimization campaign against *P. falciparum* (Yeung et al., 2010) (Figure 31). These compounds were profiled *in vitro* against the human parasite *P. falciparum* and the rodent parasite *P. berghei* (Table 20). *In vitro* biological activity was mainly associated with the (+)-enantiomer across the class suggesting the inhibition of or interaction with a discrete molecular target. Interestingly, the compounds were consistently more potent against *P. falciparum* than *P. berghei*, with a 13- to 27-fold shift in the IC_{50}. This finding may be explained by some species selectivity against the ATP4 target

and/or differences in life cycle stage susceptibilities between the two parasites. It is important to mention that although the inactive enantiomers of our most potent analogs [(-)-**6** and (-)-**7**] displayed submicromolar *in vitro* activities against *P. falciparum*, both compounds showed no efficacy in the *P. berghei* mouse model. This apparent discrepancy could be explained by the enantiopurity of (-)-**6** and (-)-**7**, which despite having an enantiomer excess (e.e.) of >98%, still contained low amounts of the active (more potent) enantiomer as contaminant.

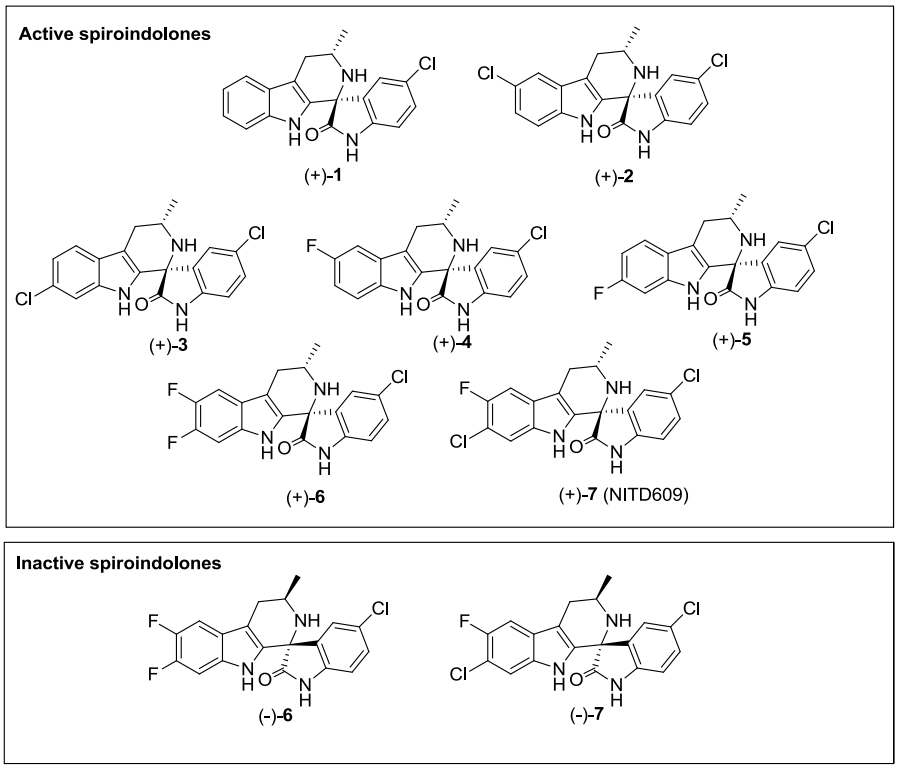

Figure 31. Structure of spiroindolone analogs
Active spiroindolones have the 1R, 3S configuration while inactive spiroindolones have the 1S, 3R configuration (Yeung et al., 2010).

Table 20. *In vitro* potency and *in vitro* PK properties of spiroindolone analogs

Compound	*P. falciparum NF54*[*] IC_{50} (nM)	*P. berghei* [§]IC_{50} (nM)	Solubility (pH 6.8, µM) [(a)]	PAMPA[(b)] %FA	Caco-2 permeability[(c)] P_{app}(A-B) 10^{-6} cm/sec	Hepatic CL_{int} in mouse liver microsomes[(d)] (µL/min/mg)	Mouse PPB[(e)] (%)	*RBC to Plasma Ratio*[(f)]
(+)-**1**	13 ± 2.2	242 ± 124	194	97	7.19	770	98.4	1.04
(+)-**2**	5.6 ± 0.9	75 ± 32	22	98	n.t	92	99.8	0.77
(+)-**3**	5.6 ± 0.7	140 ± 54	8	98	41.7	35	99.7	0.93
(+)-**4**	5.9 ± 0.9	104 ± 53	137	97	7.66	330	98.8	0.62
(+)-**5**	4.3 ± 0.4	88 ± 26	131	98	4.33	26	98.5	1.18
(+)-**6**	0.33 ± 0.06	7.5 ± 2.5	169	99	5.55	41	99.5	1.12
(+)-**7** (KAE609)	1.2 ± 0.2	26 ± 14	39	98	1.69	28	99.8	0.85
(-)-**6**	105 ± 20	2851 ± 897	112	97	4.8	36	99.6	0.81
(-)-**7**	210 ± 19	4908 ± 1445	35	98	1.73	21	99.4	0.52

[*]IC_{50}s were determined at least three times in independent assays (16 h + 8 h incubation periods, as indicated Appendix 4. [§]*P. berghei* GFP ANKA malaria strain $PbGFP_{CON}$ (n=3, Mean ± SD). The data in parentheses indicates whether the compound is the (+) or (-) optical isomer. *In vitro* PK parameters like solubility, PAMPA, Caco-2 permeability, hepatic clearance, mouse plasma protein binding and RBC to plasma partitioning were determined in a medium to high through put format using in-house standard assay protocols that are described in the literature. [(a)]HT-Equilibrium solubility at pH 6.8 (Zhou et al., 2007); [(b)]Parallel Artificial Membrane Permeability Assay expressed in % fraction absorbed (FA) (Avdeef, 2005; Avdeef et al., 2007); [(c)]Apparent permeability from apical to basolateral in Caco-2 cells expressed as P_{app} (A-B) 10^{-6} cm/sec (Balimane and Chong, 2005; Marino et al., 2005), n.t, not tested; [(d)]intrinsic clearance in mouse liver microsomes expressed as µL/min/mg protein, in the presence of liver enzymes (Obach, 1999); [(e)]Mouse plasma protein binding using rapid equilibrium dialysis method (Banker et al., 2003; Kariv et al., 2001), [(f)]RBC to plasma ratio, mean from 1 µM & 10 µM (Yu et al., 2005).

5.3.2 *In vivo* pharmacokinetics of the spiroindolone analogs

A complete set of *in vitro* PK parameters of all spiorindolone analogs can be found in Table 20. The *in vivo* PK parameters obtained following intravenous and oral administration of each compound in CD-1 mice are presented in Table 21. The results reflected a wide range of exposure, with C_{max} values from 0.7 µg/mL to 8.3 µg/mL and AUC_{0-24} (area under the concentration- time curve from 0 to 24 h) from 1.3 µg·h/mL to 107.3 µg·h/mL. The volume of distribution at steady state (V_{ss}) was moderate to high (0.9 to 13.7 liters/kg). The elimination half-life and systemic clearance varied widely and were consistent with the intrinsic clearance measured *in vitro* in liver microsomes. Most analogs showed moderate to high oral bioavailability (26 to 100%), in agreement with good solubility and permeability observed *in vitro* (Table 20 and 21).

5.3.3 Dose-response relationship of the spiroindolone analogs in the murine malaria model:

Dose-response experiments were conducted with spiroindolone analogs in the *P. berghei* mouse model at single oral doses of 2.5, 5, 10, 30 and 100 mg/kg, monitoring parasitemia as primary efficacy readout. Consistent with its poor *ex vivo* potency against *P. berghei*, (-)-**6** and (-)-**7** showed poor efficacy regardless of dose; hence, these two compounds were not included in the current evaluation. Additionally, for several compounds, parasitemia seemed not to change between 30 mg/kg and 100 mg/kg, approaching detection limit and indicating that the maximum effective concentration had been reached.

Table 21. Summary of *in vivo* pharmacokinetic parameters of spiroindolone analogs following single oral dosing at 25 mg/kg and intravenous (i.v.) dosing at 5 mg/kg to female CD-1 mice

Compound	Oral PK parameters					IV PK parameters		
	C_{max} (µg/mL)	T_{max} (h)	AUC_{0-24} (µg·h/mL)	$t_{1/2}$ (h)	F (%)	V_{ss} (L/kg)	CL (mL/min/kg)	$t_{1/2}$ (h)
(+)-**1**	1.2	0.25	1.3	0.7	13	0.9	49.7	0.4
(+)-**2**	0.6	1	2.9	4.3	62	9.9	92.6	4.6
(+)-**3**	0.7	2	5.8	6.2	91	13.7	60.1	4.3
(+)-**4**	1.0	0.25	3.9	5.6	26	1.9	24.0	4.7
(+)-**5**	3.1	0.25	17.7	4.0	47	1.6	11.8	3.8
(+)-**6**	3.1	2	26.8	3.2	53	1.6	8.5	2.9
(+)-**7** (KAE609)	0.1[a]	1	1.0	8.7	44	2.1	9.7	3.4
	0.25[b]	2	2.6	7.5	32			
	3.6	1	43.3	10.0	100			
	10.8[c]	24	186.9	9.4	100			
(-)-**6**	5	2	68.2	7.9	78	2.8	4.2	13.2
(-)-**7**	8.3	1	107.3	9.1	92	1.3	2.6	5.6

[a, b, c] Dose proportionality PK for KAE609 at 1.5, 5.6 and 105 mg/kg, respectively using the formulation, 1.1 equimolar 1N HCl, 5% Solutol HS15 in 50mM pH3 citrate acid buffer. C_{max}, maximum concentration of drug in plasma; T_{max}, time to C_{max}; AUC_{0-24}, area under the concentration-time curve from 0 to 24 h; $t_{1/2}$, elimination half-life; F, oral bioavailability; V_{ss}, volume of distribution at steady state; CL, total systemic clearance.

The relationship between parasitemia and doses was described by a sigmoid dose-response model (Figure 32). The model parameters such as P_{max}, P_{min}, ED_{90} and Hill slope were derived and are reported in Table 22. A goodness-of-fit profile for a representative compound [(+)-6] is shown in Figure 33. All the compounds studied displayed a maximum reduction in parasitemia, with ED_{90} ranging between 5.6 (KAE609) and 38.1 [(+)-5] mg/kg. KAE609 was identified as the most potent spiroindolone in the series. Interestingly, treatments with none of the spiroindolones except KAE609 resulted in complete cure (>30 days survival, data not shown).

5.3.4 KAE609 displays higher exposure in NMRI mice as compared to CD-1 mice

The oral PK properties of KAE609 were determined in infected and uninfected NMRI mice at 5.3 mg/kg (Table 23). No significant difference was observed in the PK profiles between the two groups, indicating that the disease status does not affect the PK properties of KAE609. However, at comparable dose (5 mg/kg), the C_{max} and exposure were significantly higher (4-fold) in the NMRI mice than those in the CD-1 mice (Table 21 and 23). Based on this finding, the concentration-time data in NMRI mice were used for modeling purposes and further PK-PD analysis.

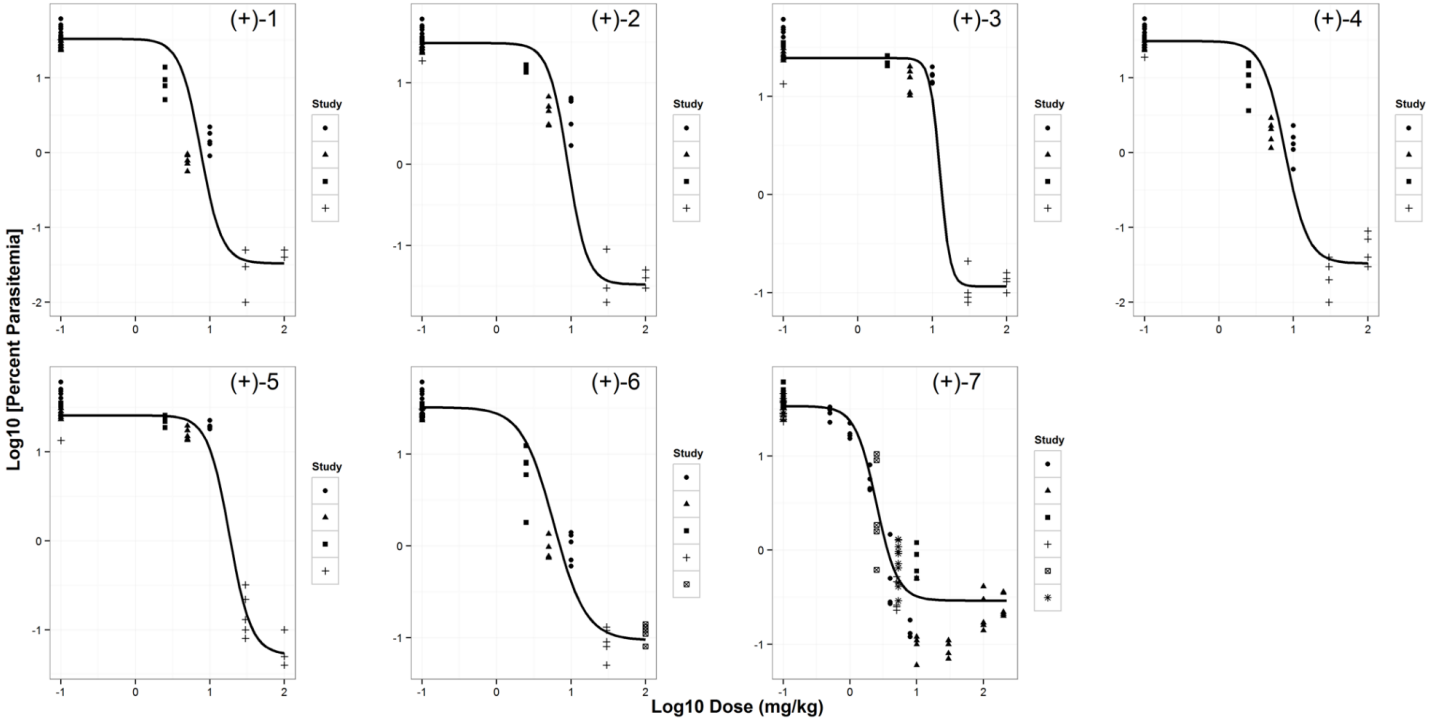

Figure 32. Relationship between dose and parasitemia for spiroindolone analogs

The plot shows the $\log_{10}$ parasitemia at day 4 versus $\log_{10}$ dose administered in mg/kg for a set of spiroindolone analogs in a *P. berghei* murine malaria model. A minimum of five dose levels for each compound were used for dose-response relationship (total doses of 2.5, 5, 10, 30 and 100 mg/kg were administered as single oral dose at 24 h postinfection). For (+)-7 (KAE609), additional doses ranging between 0.5 and 200 mg/kg

were studied. Each data point is from individual animal, and various symbols correspond to different studies. The solid line represents the predicted profile from the model.

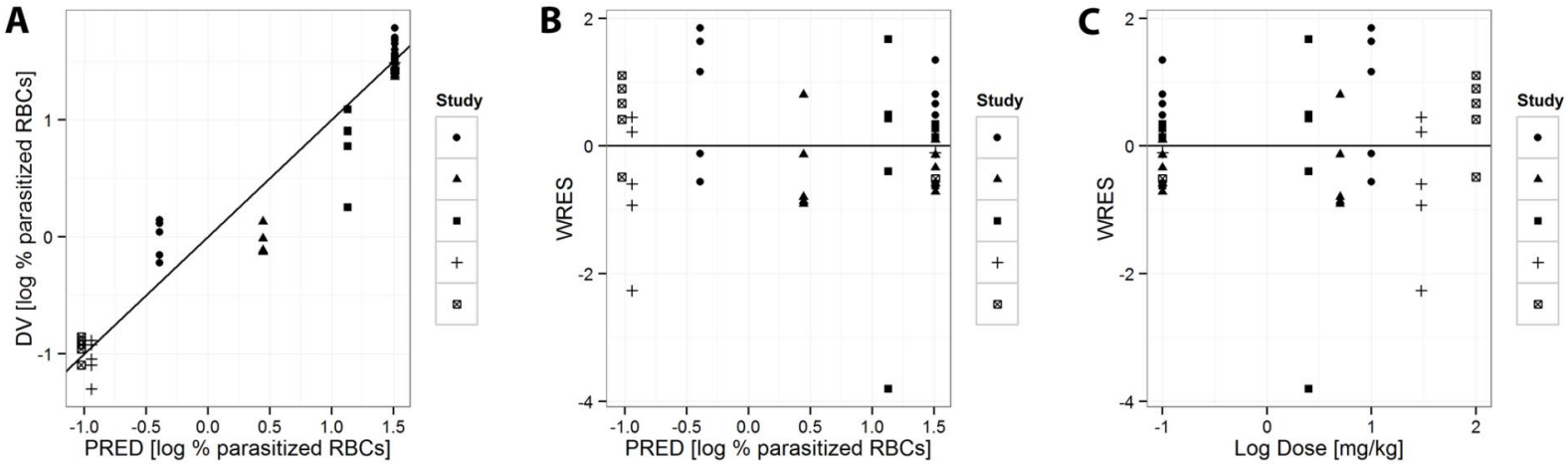

Figure 33. Goodness-of-fit plots for dose-response relationship

Goodness-of-fit plots for a representative compound [(+)-6] (A) observed data (DV) versus populations predictions (PRED) (B) weighted residuals (WRES) versus PRED (C) WRES versus Dose

Table 22. Dose-response relationship of spiroindolone analogs in the *P. berghei* malaria mouse model

Compound	P_{max} [a]	P_{min} [b]	ED_{90} (mg/kg) [c]	Hill Slope
(+)-**1**	33.11	0.03	15.3	-3.1
(+)-**2**	30.90	0.03	17.4	-3.36
(+)-**3**	24.55	0.12	17.9	-6.4
(+)-**4**	30.90	0.03	16.7	-2.87
(+)-**5**	25.70	0.05	38.1	-2.99
(+)-**6**	32.36	0.09	17.3	-2.03
(+)-**7** (KAE609)	33.88	0.29	5.6	-2.73

[a] P_{max}, maximum parasitemia; [b] P_{min}, minimum parasitemia ; [c] ED_{90}, effective dose causing a 90% in parasitemia.

5.3.5 Pharmacokinetic modeling

Nonlinear mixed-effect modeling of the oral PK data led to the estimation of model parameters that might describe the PK behavior of KAE609 in NMRI mice. For the purpose of modeling, a two-compartment PK model with first-order absorption and nonlinear elimination was built in NONMEM. The estimated PK parameters, such as V_{max}, K_m, V_c, V_p, Q and K_a, are summarized in Table 23. The linear and semi-logarithmic plots of the observed and modeled KAE609 plasma concentrations versus time are shown in Figure 34 (A & B, respectively). The goodness-of-fit was assessed and is depicted in Figure 35.

Table 23. Pharmacokinetic parameters following oral administration of KAE609 to NMRI (uninfected and infected) mice

Pharmacokinetic parameter[a]	Mouse infection status	
	Uninfected	Infected
C_{max} (µg/mL)	1.01	0.96
AUC_{inf} (µg·h/mL)	13.21	12.64
V_{max} (µg/hr/kg)	143	
K_m (µg/liter)	34.1	
V_c (liters/kg)	4.4	
V_p (liters/kg)	5.1	
Q (liters/h/kg)	0.61	
K_a (1/h)	1.78	

[a] C_{max}, maximum concentration of drug reached in plasma; AUC_{inf}, area under the curve from 0 to infinity; $CL = V_{max} / (K_m+C_p)$, where C_p is compound plasma concentration, K_m is the compound concentration to have 50% of clearance saturation, and V_{max}/K_m is the maximal clearance which can be approximated when $C_p << K_m$. The primary model parameters were, CL, plasma clearance; $V_{c,}$ central volume of distribution; V_p, peripheral volume of distribution Q, inter compartmental clearance; K_a absorption rate constant.

5.3.6 KAE609 exhibiting time dependent killing in the *P. berghei* malaria mouse model

In the *P. berghei* malaria mouse model, KAE609 showed 50%, 90% and 99% reductions in parasitemia after single oral dose of 1.2, 2.7 and 5.3 mg/kg, respectively (Rottmann et al., 2010). In order to expand the dynamic range of the pharmacological response, doses ranging from 0.5 to 8 mg/kg were selected for a dose fractionation study. The PK model parameters derived as described above were used to simulate oral plasma concentration time profiles at different doses and dosing regimens, and the corresponding PK parameters (C_{max} and AUC) were calculated using the Berkley Madonna software.

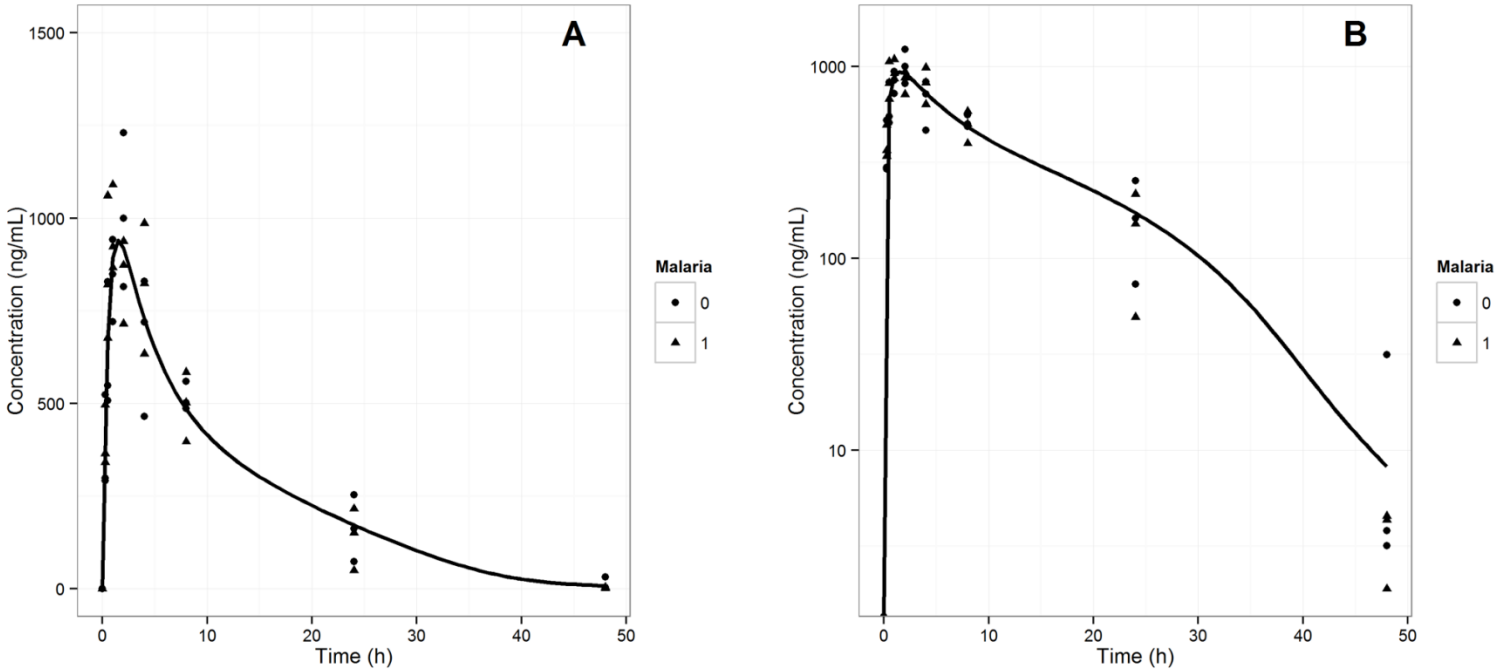

Figure 34. Pharmacokinetics of KAE609 in NMRI mice
Plot of linear (A) and semilog (B) concentration-time data for KAE609 in infected (0) and uninfected (1) NMRI mice following a single oral dose of 5.3 mg/kg. The line represents the predicted profile from the model.

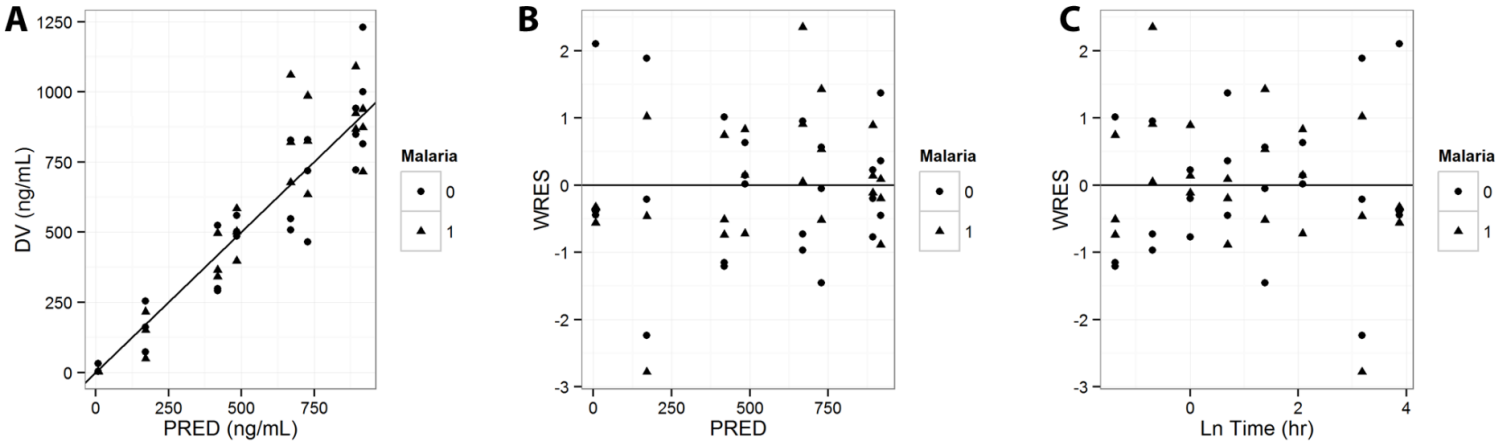

Figure 35. Goodness-of-fit plots for pharmacokinetic modeling of KAE609. (A) observed data (DV) versus populations predictions (PRED), (B) weighted residuals (WRES) versus PRED, (C) WRES versus Time.
PRED aligns well with the observations (DV) and did not show either any substantial or systematic deviations from the line of identity. Additionally, weighted residual plots are evenly distributed around zero when plotted against PRED or TIME, indicating the model did not show any pattern and is not biased either against concentration or time.

The IC_{99} obtained in the *ex vivo P. berghei* maturation assay was estimated (Section 5.2.2) to be 61.6 nM. The 2*IC_{99} values (123 nM or 48 ng/mL) was used as threshold (TRE). The PK-PD indices (C_{max}/TRE, AUC_{0-48}/TRE and $\%T_{>TRE}$) at different doses and dosing regimens, were calculated (Section 5.2.8) and are summarized in Table 24. The results showed that C_{max}/TRE ranged between 0.4 and 30, AUC_{0-48}/TRE ranged between 3 and 514, and finally, the $T_{>TRE}$ was approximately 0 to 100% (Table 24).

A sigmoid dose-response model was chosen to describe the data. The relationship between parasitemia and various PK-PD indices is described by equation 2. The derived model parameters such as P_{max}, P_{min}, EC_{50} and Hill slope, for various PK-PD indices (C_{max}/TRE, AUC_{0-48}/TRE and $\%T_{>TRE}$) are summarized in Table 25. These results suggest a strong correlation of the efficacy of KAE609 with all three PK-PD indices over a wide range of exposures as a consequence of parameter interdependency. Among the three indices, the percentage of the time that the KAE609 plasma concentration remained above 2*IC_{99} ($\%T_{>TRE}$) and the AUC_{0-48}/TRE correlated best (R^2 = 0.97 and 0.95, respectively) with a reduction in parasitemia, followed by the C_{max}/TRE (R^2 = 0.88) (Figure 36). Further, $\%T_{>TRE}$ displayed the lowest magnitude for the standard error of the estimate (standard deviation of the regression (Sy.x), 0.17) followed by AUC_{0-48}/TRE (0.22) and C_{max}/TRE (0.34). Residual plots of the three nonlinear regressions are shown in Figure 37. Collectively, our data indicate a trend favoring time over threshold and exposure over threshold as most important determinant of efficacy for KAE609 rather than the concentration over threshold.

Table 24. Dose fractionation and corresponding PK-PD indices and level of parasitemia for KAE609

Total Dose[a] (mg/kg)	Individual dose (mg/kg)	No. of doses	PK-PD indices			Parasitemia[b] (%)
			C_{max}/TRE	AUC_{0-48}/TRE	$\%T_{>TRE}$	Mean ± SD
8	8	1	29.95	513.68	99.9	0.15 ± 0.03
	4	2	19.4	414.93	99.8	0.18 ± 0.04
	2.67	3	16.44	383.23	99.8	0.16 ± 0.02
4	4	1	14.56	148.45	54.5	0.63 ± 0.57
	2	2	7.92	106.02	56.1	0.43 ± 0.38
	1.33	3	6.00	92.12	57.3	0.55 ± 0.28
2	2	1	6.93	45.07	23.0	5.64 ± 1.69
	1	2	3.37	30.66	22.7	6.48 ± 3.94
	0.67	3	2.24	25.18	22.3	10.83 ± 4.67
1	1	1	3.21	14.57	10.7	17.82 ± 3.05
	0.5	2	1.49	10.16	8.8	18.19 ± 6.81
	0.33	3	0.96	8.55	0	20.31 ± 5.71
0.5	0.5	1	1.45	4.98	4.3	28.82 ± 4.49
	0.25	2	0.67	3.75	0	38.28 ± 2.95
	0.17	3	0.43	3.34	0	35.37 ± 5.32
Vehicle	-	-	-	-	-	35.51 ± 3.86

[a]The total daily dose was given as one, two (once every 12 h), or three (once every 8 h) equally divided doses over 24 h. [b]Parasitemia expressed as parasitized red blood cells (pRBCs) over 100 RBC's (determined 48 h post treatment). C_{max}/TRE, ratio of peak plasma concentration (C_{max}) to the threshold (TRE = $2*IC_{99}$); AUC_{0-48}/TRE, ratio of area under the curve from 0 to 48 h (AUC_{0-48}) to the threshold and $\%T_{>TRE}$, percentage of the 48-h period during which the total compound concentration exceeded the threshold.

Table 25. PK-PD model parameters for KAE609

Parameter[a]	C_{max}/TRE	AUC_{0-48}/TRE	$\%T_{>TRE}$
P_{min}	0.12 (0.05 – 0.29)	0.13 (0.09 – 0.20)	0.15 (0.12 – 0.20)
P_{max}	34.51 (21.78 – 54.58)	32.66 (25.06 – 42.56)	53.09 (32.28 – 87.50)
EC_{50}	5.43 (4.2 – 7.0)	52.72 (44.16 – 62.95)	32.06 (28.04 – 36.07)
Hill Slope	-1.87 (-2.69 – -1.05)	-1.63 (-2.04 – -1.22)	-0.031 (-0.037 – -0.024)
R^2	0.88	0.95	0.97

[a] P_{max}, maximum parasitemia; P_{min}, minimum parasitemia, EC_{50}, value required to produce 50% of the maximal effect. C_{max}/TRE, ratio of peak plasma concentration (C_{max}) to the threshold (TRE = 2*IC_{99}); AUC_{0-48}/TRE, ratio of area under the curve from 0 to 48 h (AUC_{0-48}) to the threshold and $\%T_{>TRE}$, percentage of the 48- h period during which the total compound concentration exceeded the threshold. The numbers in the parenthesis are 95% confidence interval.

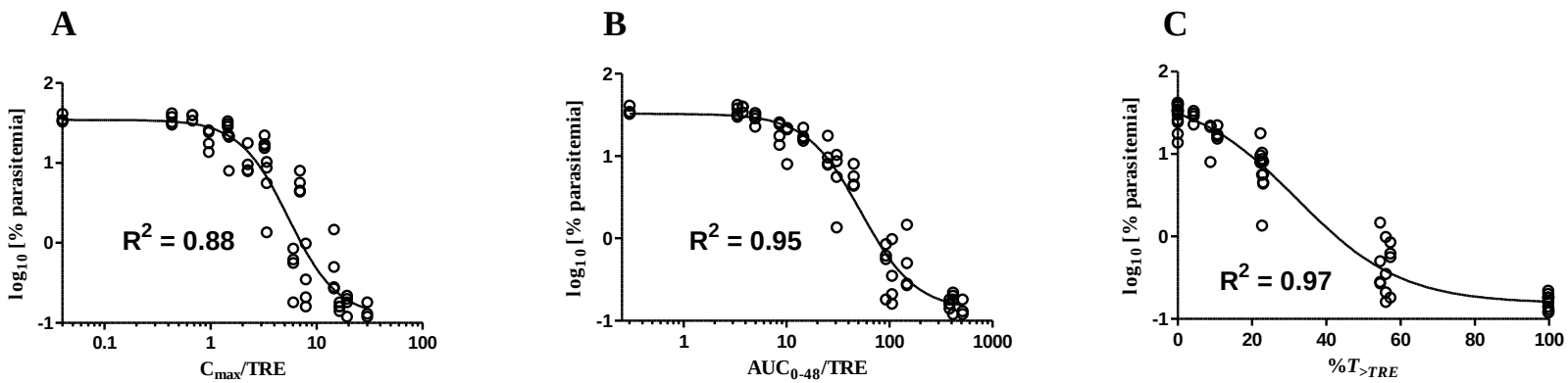

Figure 36. PK-PD relationship for KAE609

The relationships between C_{max}/TRE (A), $AUC_{0\text{-}48}$/TRE (B) and $\%T_{>TRE}$ (C) of KAE609 and parasitemia, when the total daily dose was administered as a single dose or fractionated in two or three equally divided doses over 24 h, are shown. The line represents the predicted profile from the model.

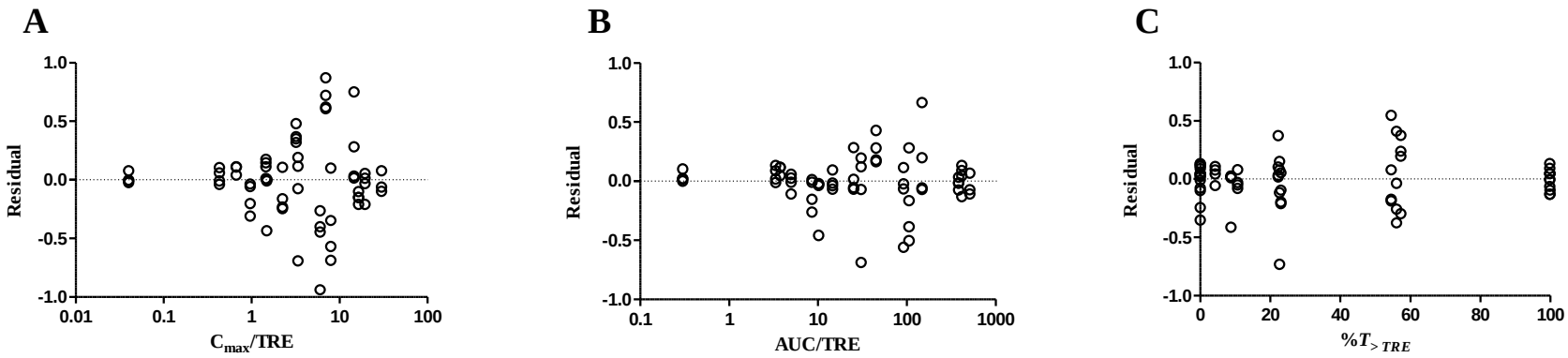

Figure 37. Residual plots (A) Residual versus C_{max}/TRE (B) Residual versus AUC/TRE and (C) Residual versus $\%T_{>TRE}$

Scatterplot of residuals against independent variables – residuals were randomly distributed around zero and spread of the residuals is same throughout the plot (no systematic pattern).

5.4 Discussion

In the field of anti-infectives, doses and regimens selected in clinical trials are increasingly informed by dose fractionation studies in animals (Craig, 1998; Craig, 2001). This approach was not traditionally adopted for antimalarial drugs, as most agents were developed when therapeutic strategies were largely based on empirical clinical evidence. Recently, PK-PD relationships have been established for chloroquine (time-dependent killing) and artesunate (concentration-dependent killing) (Bakshi et al., 2013). This study is an attempt to understand the dose- response relationship for a class of spiroindolone analogs and to identify the PK-PD driver of the reduction in parasitemia resulting from treatment with KAE609. The results presented in this study must be interpreted with a few limitations in mind. First, the single-dose PK parameters determined in NMRI mice were assumed to be similar to multiple-dose PK parameters and were correlated with the efficacy data for KAE609. Second, the PK data used for PK-PD analysis at different doses and regimens were simulated based on model parameters from single-dose PK under the assumption of nonlinearity observed in both NMRI and CD-1 mice. The third limitation of this study is that in the absence of supporting intravenous PK data in NMRI mice, oral bioavailability was assumed to be 100%.

A class of spiroindolones was identified in a whole-cell screening against the human malaria parasite *P. falciparum*. In order to support the selection of compounds to progress in the murine malaria model, the *in vitro* potency was also assessed against *P. berghei* (rodent parasite). A systematic 13- to 27-fold shift in IC_{50} was observed between *P. falciparum* and *P.*

berghei for all study compounds (Table 20). The likely explanations for the differential sensitivity to the spiroindolones could be either species susceptibility differences (*P. falciparum* versus *P. berghei*) or stage selectivity. It should indeed be noted that the *P. falciparum* assay covers intracellular parasite growth and reinfection of new blood cells, with growth inhibition measured after 24 h. In contrast, the *P. berghei in vitro (ex vivo)* assay is a schizont maturation assay over a single life cycle without reinvasion of new red blood cells over a 24-h period.

The dose-response experiments were performed in mice with a series of potent spiroindolones. Parasitemia was used as primary pharmacodynamic (PD) readout for multiple reasons. It provides a wide dynamic range and is a fast, easy, and reproducible measurement. Unfortunately, in this *P. berghei* model, a real-time measurement of parasitemia over time that could be used to determine the more clinically relevant parasitemia reduction ratio (PRR) was not feasible. For each compound, the data derived from all experiments (i.e., doses) were fitted simultaneously using nonlinear mixed-effect modeling (using NONMEM VI). A good correlation was observed between the doses and a reduction in parasitemia across the spiroindolone class (Figure 32, Table 22) with ED_{90}s ranging from 6 to 38 mg/kg. These results are in line with those available for the currently used antimalarials in the *P. berghei* ED_{90}-normalized assay (Jimenez-Diaz et al., 2013). Generally, the investigated compounds displayed a rather steep Hill slope (≥2). Specifically, for compounds (+)-3 and (+)-5, due the limited data points covering the middle portion of the dose-response curves, our confidence in the derived Hill slopes is rather moderate. Interestingly, all the spiroindolone analogs tested achieved

complete reduction in parasitemia (below the detection limit, < 0.1%), but only KAE609 showed complete cure (i.e., survival > 30 days). The reason underlying this observation is yet to be elucidated.

The most promising spiroindolone, KAE609, which is currently in clinical development, was selected for more extensive dose fractionation studies in the *P. berghei* murine model. The objective of such an investigation was to identify the PK-PD driver of efficacy and determine whether this compound exhibits time or concentration dependent killing. The results suggested that the time during which plasma concentrations remained above the $2*IC_{99}$ ($\%T_{>TRE}$) and the $AUC_{0\text{-}48}$/TRE correlated slightly better (although not statistically significantly) with reduction in parasitemia than did C_{max}/TRE. In our study, all three PK-PD indices (C_{max}/TRE, $AUC_{0\text{-}48}$/TRE and $\%T_{>TRE}$) correlated well with a reduction in parasitemia as a consequence of their significant interdependency (Spearman correlation coefficient of > 0.97; P value <0.0001). The PK properties of KAE609 (i.e., long half-life) and the almost complete reduction in parasitemia reached in a narrow dose range do not allow us at this stage to clearly distinguish between concentration and time dependent killing for KAE609 in the investigated model. A definitive conclusion could be achieved by a more extensive dose fractionation study up to 48 h with several different dosing regimens to break the colinearity (Ambrose et al., 2007; Drusano, 2004; Scaglione et al., 2003). Based on the correlation analysis and the standard error of the estimate, collectively, our data indicate a trend favoring time over threshold and exposure over threshold as most important determinant of efficacy. This would suggest time-dependent

rather than concentration-dependent killing for KAE609. In addition, a conservative interpretation of the results is the prediction that a dosing regimen covering a C_{max}/TRE of 30, AUC_{0-48}/TRE of 587 and $T_{>TRE}$ of 100% for an observation period of 48 h is likely to yield maximum reduction in parasitemia (parasitemia, <0.1%) in the malaria mouse model. Interestingly, the concentration of KAE609 needed to inhibit 50% of parasite (*P. berghei*) *in vitro* (IC_{50} = 26 nM or 10 ng /mL, Table 20) is significantly lower than the one needed to reduce parasitemia by 50% *in vivo* (C_{max} = 260 ng/mL) as derived from C_{max}/TRE (Table 25). The difference could be due to the limitations of the *in vitro* experimental setting, which does not capture reinvasion. Also, parasites are exposed to a constant concentration of the compound over time *in vitro* (static system), whereas *in vivo* (dynamic system) the exposure varies with time, according to the pharmacokinetics of the compound. In addition, the protein binding might differ in the two systems (Zeitlinger et al., 2011). KAE609 and other spiroindolone analogs showed very high plasma protein binding in mice (≥ 99%) (Table 20). It is challenging to accurately measure free fraction accurately for highly protein bound compounds (Weiss and Gatlik, 2014). For our analysis, we used total plasma concentrations when analyzing the PK-PD relationship, similarly to what was reported for other drug candidates such as bedaquiline (Rouan et al., 2012). Considering the relationship between *in vitro* potency and concentration achieved in mice, compounds with a C_{max}/TRE ≥ 30, AUC_{0-48}/TRE ≥ 587 and $T_{>TRE}$ of 100% would likely be efficacious and would be prioritized for further studies.

The use of murine models in drug discovery for both PK and PD assessment of antimalarial test compounds is widespread (Charman et al., 2011; Jimenez-Diaz et al., 2013; Patel et al., 2013; Rottmann et al., 2010). These models can generate robust PK-PD data that can be used for dose optimization. This has been reported for dihydroartemisinin (DHA) (Gibbons et al., 2007), piperaquine (Moore et al., 2008) and chloroquine (Moore et al., 2011). The data reported in this thesis were generated in either uninfected CD-1 mice (PK) or NMRI mice (PD). Surprisingly, for KAE609 significant strain differences were observed, yielding to a 4-fold higher exposure in NMRI mice compared to that in CD-1 mice. No significant difference between infected and uninfected NMRI mice was observed; these results are consistent with published reports showing no impact of malaria infection on the PK of antimalarial agents (Batty et al., 2008; Moore et al., 2008; Moore et al., 2011). The reasons for the observed strain difference are yet to be understood. A two-compartment pharmacokinetic model with nonlinear elimination was chosen to fit to the plasma concentration versus time data of KAE609 generated in NMRI mice (infected and uninfected) at 5.3 mg/kg. Preliminary analysis of i.v PK data for KAE609 in CD-1 mice showed that a two compartment model better describes the data than a one compartment model. The parameters and diagnostic plots are given in the below Table 26, Figure 38 and Figure 39. The nonlinear behavior for KAE609 was previously observed in the dose proportionality studies in CD-1 mice (Table 21, Figure 40). The nonlinear mixed-effects modeling provides a good solution for modeling sparse datasets and has been well established in preclinical and clinical situation (Bouzom et al., 2000). The concentration time data obtained from different population

(infected and uninfected NMRI mice) were fitted simultaneously using this method. The estimated model parameters were used to simulate the PK profiles of KAE609 at any of the doses and regimens administered in the dose fractionation study.

In conclusion, all spiroindolone analogs studied displayed good dose-response relationship in the *P. berghei* murine model. KAE609 exhibits a trend favoring time or exposure over threshold as most important determinant of reduction in parasitemia. Furthermore, our results suggest that for KAE609 and, supposedly, for its analogs, dosing regimens covering $T_{>TRE}$ of 100%, $AUC_{0\text{-}48}$/TRE of 587 and C_{max}/TRE of 30 are likely to result in maximum reduction in parasitemia (<0.1%) in the *P. berghei* mouse model of malaria. Based on the present results, the optimization campaign of leads belonging to the same chemical class could be guided by a PK-PD driven strategy. Compounds could be characterized in terms of their potency and *in vivo* pharmacokinetics. PK-PD indices could be estimated and compared to those derived here for KAE609. Compounds showing promising properties (i.e., matching the indices of KAE609) could be prioritized and efficacy studies designed in an informed manner in order to maximize the reduction in parasitemia. A similar approach could be used as guide for designing clinical studies.

Table 26. PK parameter estimates for i.v. profile of KAE609 from one and two compartment models

Parameters	1 compartment estimate (% CV)	2 compartment estimate (% CV)
V	1063 (33%)	485 (26%)
CL	347 (26%)	608 (9%)
V2	-	1832 (14%)
CLD2	-	2048 (29%)
Correlation	0.69	1.00
AIC	13.5	-3.8

V, central volume of distribution; CL, clearance; V2, peripheral volume of distribution, CLD2, intercompartmental clearance; AIC, Akaike information criterion

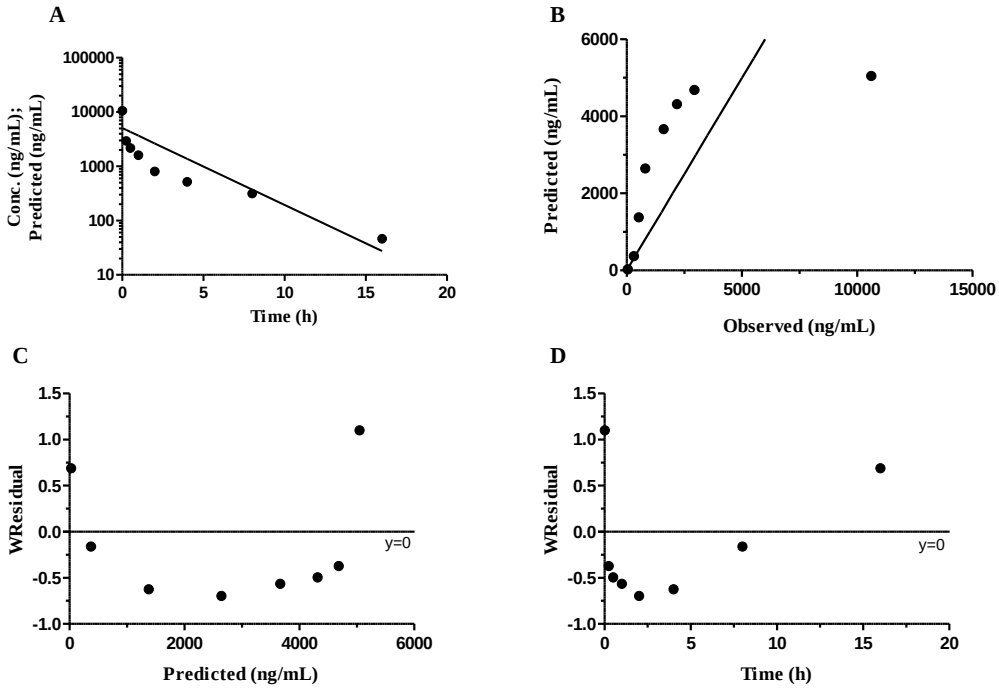

Figure 38. One-compartment analysis after i.v. administration of KAE609 in CD-1 mice

(A) Observed and predicted concentration versus time; (B) Predicted versus observed concentration; (C) Weighted residuals versus predicted concentration; (D) Weighed residuals versus time. Poor fit of observed and predicted concentrations; bias in predictions, as observed data points are deviating to some extent from line of identity.

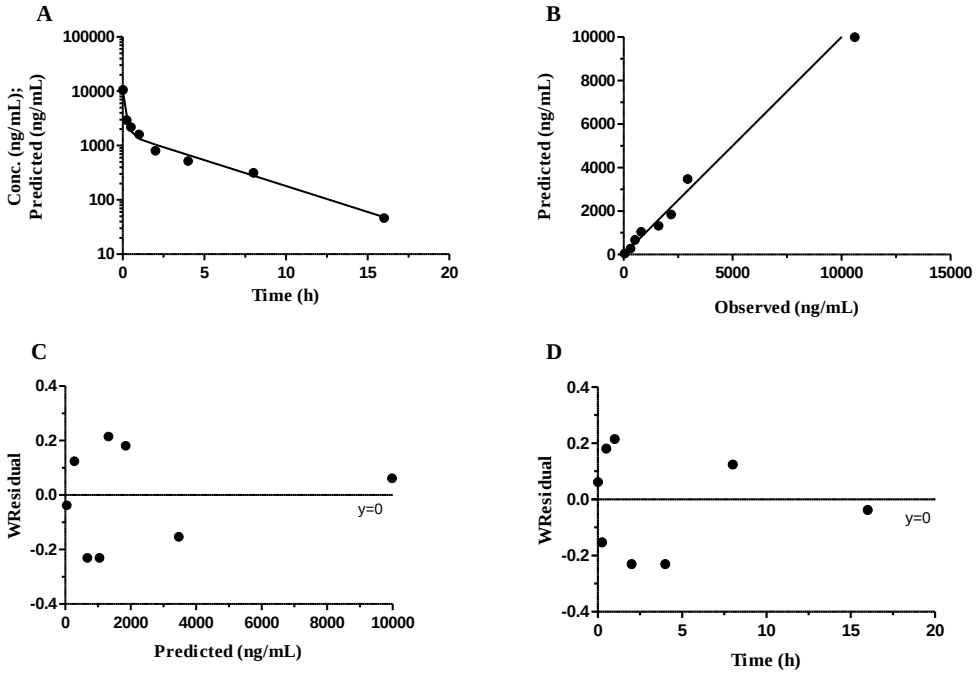

Figure 39. Two-compartment analysis after i.v. administration of KAE609 in CD-1 mice
(A) Observed and predicted concentration versus time; (B) Predicted versus observed concentration; (C) Weighted residuals versus predicted concentration; (D) Weighed residuals versus time. Good fit of observed and predicted concentrations; unbiased predictions, as observed & predicted data points are close to line of identity.

Assuming similar PK-PD relationships, regardless of the parasite species, the PK-PD indices (as TRE the human relevant 2* *P. falciparum* IC_{99} is to be considered) derived in the present study could be applied to the clinical situation. Our results support a recent clinical phase II study with KAE609 demonstrating positive results with a 3-day dosing regimen of 30 mg daily clearing parasitemia in *P. vivax* and *P. falciparum* malaria patients (White et al., 2014). The average PK parameters from the two cohorts were C_{max} of 855 ng/mL, AUC of 14300 ng·h/mL and % $T_{>TRE}$ of 100% of the treatment period (2* *P. falciparum* IC_{99} = 1 ng/mL = TRE).

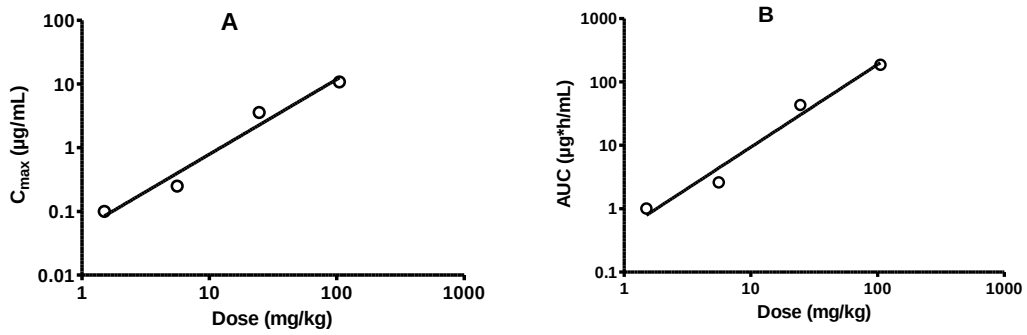

Figure 40. Dose proportionality for KAE609 in CD-1 mouse

Dose linearity tests on C_{max} and AUC_{0-24} were carried out by the regression of log-transformed data (power regression model) (Hummel et al. 2009; Smith et al. 2000). Doses (1.5 – 105 mg/kg) and PK parameters (C_{max} and AUC_{0-24}) were log-transformed, and correlation coefficient (R^2), slope, and 95% confidence intervals of slope were calculated using the GraphPad Prism version 5.02 for windows (GraphPad software, San Diego, California USA). The system was considered to be linear when $R^2 \sim 1$, Slope 95% $CI_{lower} \geq 0.8$, and $CI_{upper} \leq 1.25$ (Hummel et al. 2009; Smith et al. 2000). (A) Dose vs C_{max} ($R^2 = 0.97$, Slope = 1.18, 95% $CI_{lower} = 0.52$ and $CI_{upper} = 1.83$); (B) Dose vs AUC_{0-24} ($R^2 = 0.97$, Slope = 1.30, 95% $CI_{lower} = 0.65$ and $CI_{upper} = 1.96$). Based on the above observations, KAE609 shows nonlinear behavior in CD-1 mouse between the doses studied.

Such parameters are comparable to the ones derived for KAE609 in the *P. berghei* murine malaria (C_{max} of 1440 ng/mL, AUC of 28176 ng·h/mL and % $T_{>TRE}$ of 100% (2* *P. berghei* IC_{99} = 48 ng/mL = TRE). This demonstrates that PK-PD indices required for reduction in parasitemia were similar between mouse and human models. Overall, our results could be used to prioritize analogs within the same class of compounds and contribute to the design of efficacy studies, thereby facilitating early drug discovery and development programs.

Chapter 6. Conclusions and Future directions

6.1 Conclusions

It is vital to select the most promising drug candidates to progress into development. This will help minimizing late-stage failures and thus reduce the overall cost, time and resources involved. Moreover, the animal pharmacology studies are lengthy and resource intensive, hence there is a need to have a prioritization process in place to limit the number of compounds selected. For this purpose, it would be of interest to investigate early on in the drug discovery cycle the *in silico – in vitro – in vivo* correlations and understand the pharmacokinetic-pharmacodynamics relationships to guide lead optimization programs.

Chapter 1 gives an overview of literatures on the drug discovery of the two therapeutic areas (tuberculosis and malaria), with discussion on the desirable properties of the ideal drug candidates, current drug discovery pipeline, efficacy of combination therapy and challenges encountered in the development of each of these therapeutic agents. In addition, various strategies adopted in drug discovery are highlighted. Drug discovery aims to deliver a candidate that shows efficacy, exposure and tolerability in a relevant animal model and in man. *In silico* and *in vitro* assays are employed in lead finding and optimization, attempting to predict the *in vivo* properties. Empirical rules have been established for diverse set of compounds from different therapeutic areas. Further, in the antibacterial field, PK-PD relationship and drivers are known for specific classes and individual compounds, but not for all. There is a lack of systematic *in silico – in vitro – in vivo* correlation analysis and concentration – effect (PK-PD) relationship analysis for anti-mycobacterial and anti-malarial compounds.

Chapter 2 describes the rationale, hypotheses and objectives of the work. We formulated two hypotheses and the main objective of the first study was to establish the relationship between physicochemical and pharmacokinetic properties by studying *in silico – in vitro – in vivo* correlations for standard anti-TB compounds. In the second study, we attempted to understand the PK-PD relationship for nitroimidazole and spiroindolone analogs with the aim to extend it to new compounds of the same class. To our knowledge such analysis is novel and has never been reported before. The outcome will be used to prioritize new drug candidates, thereby facilitating the lead optimization and possibly expedite the drug discovery process.

The currently used first line anti-mycobacterial drugs in the market were discovered during 1950s and 1960s. Noteworthy, TB drug development has met limited success with only two new drugs approved over the last 40 years. In chapter 3, we have comprehensively determined and compiled physicochemical parameters, *in vitro* and *in vivo* pharmacokinetic properties of 36 anti-mycobacterials, most of which are in clinical use against TB. Analysis of physicochemical properties, *in vitro* PK and *in vivo* PK has been undertaken to identify the relationship that could potentially serve as guide for medicinal chemists and pharmacologists to select new promising candidates in discovery phase. Anti-TB drugs displayed a wide range of physicochemical properties. However, majority of the anti-TB compounds followed empirical rules (Lipinski, Veber, Egan and Gleeson) with few exceptions (natural products). Acceptable solubility, permeability and plasma protein binding are displayed by molecules with molecular weight < 400 and cLogP <4. Good

solubility, permeability and metabolic stability were found to be important prerequisites for high oral bioavailability. Further, lipophilicity appeared to be one of the most important physicochemical parameter that will not only influence various PK properties but also contribute to developability challenges. This finding agrees with previous studies in different therapeutic area. The novelty of this work is that, to our knowledge, it is the first comprehensive summary and analysis of physicochemical properties, *in vitro* PK and *in vivo* PK for standard anti-mycobacterial drugs. Our hope is that this standardized data set represents a useful reference for the TB drug discovery community. The understanding of the impact of such individual properties and their interplay on the PK of the drug candidates is key for lead optimization in TB drug discovery programs.

In chapter 4, a panel of closely related potent bicyclic 4-nitroimidazoles was profiled in both *in vivo* PK and efficacy studies. Lung PK parameters correlated well with *in vivo* efficacy than plasma PK parameters. Total lung $T_{>MIC}$ correlated better than C_{max}/MIC or AUC/MIC. Interestingly, V_{ss} also showed positive correlation with *in vivo* efficacy. Over all, our findings show that the efficacy of all bicyclic 4-nitroimidazole analogs is most likely driven by lung PK. Generally, tuberculosis efficacy studies are lengthy. It takes approximately 10 to 12 weeks to obtain single PD readout. Alternatively, V_{ss} and lung distribution can be generated from single dose pharmacokinetic studies. A simple surrogate would be useful during the lead optimization to prioritize candidates for resource intensive efficacy studies. For bicyclic 4-nitroimidazoles, efficacy correlated better with concentration in lungs, consistent with V_{ss} and differential lung to plasma distributions. The

results of this analysis could potentially be exploited to prioritize new analogs for efficacy studies based on *in vitro* potency, volume of distribution and lung concentration. This process will reduce the overall turnaround time and expedite drug discovery programs.

Spiroindolones, a new class of compounds, were found to be active against malarial parasites. KAE609 is a compound of the spiroindolone class currently in clinical development for the treatment of *P. falciparum* and *P. vivax* malaria. This compound exhibited promising therapeutic effects in preclinical studies. Understanding the PK-PD relationship of KAE609 will be valuable for the lead optimization and the selection of back-up compounds belonging to the same chemical class. In chapter 5, we report the PK-PD analysis done for spiroindolones. All analogs studied displayed good dose-response relationship in the *P. berghei* murine model. KAE609 was identified as the most potent analog exhibiting a trend that favors percentage of the time the concentration of KAE609 over threshold or exposure over threshold as most important determinant of reduction in parasitemia. Furthermore, the results suggest that for KAE609, and supposedly for its analogs, dosing regimens covering $T_{>TRE}$ of 100%, $AUC_{0\text{-}48}$/TRE of 587 and C_{max}/TRE of 30 are likely to result in maximum reduction in parasitemia (<0.1%) in the *P. berghei* mouse model of malaria. We propose that this information could be used to prioritize back-up compounds and to design efficacy studies, thereby facilitating early drug discovery and lead optimization programs.

Assuming a conserved mechanism of action across a compound class, the PK-PD correlations can be extended from one compound to new members of the same class. We suggest here to prioritize potential back-up compounds

based on *in vitro* potency and *in vivo* PK, before conducting labor-intensive *in vivo* efficacy studies. Such approach would be very useful to reduce attrition rate and increase the chance of success during drug discovery and preclinical development specifically in the anti-mycobacterial and anti-malarial fields.

The work presented in this thesis evaluated ISIVIVC and PK-PD relationships. The findings indicate that new lead compounds foreseen as chemotherapy against tuberculosis must not only show good *in vitro* activity but also have good physicochemical and pharmacokinetic properties. Most importantly, our investigations showed that volume of distribution and lung PK could be used as surrogate markers for progression of promising compounds into lengthy efficacy studies that are critical for lead optimization in TB drug discovery programs. Further, PK-PD analysis done for KAE609 led to the identification of indices related to the compound's efficacy in a mouse malaria model. The same PK-PD indices could be used to identify promising back-up candidates belonging to the same chemical class. To the best of our knowledge, this is the first comprehensive report about ISIVIVC for anti-mycobacterial compounds; PK-PD analysis for a compound class (nitroimidazole and spiroindolone analogs) and further dose fractionation analysis of a novel anti-malarial compound (KAE609).

The work reported in this thesis represents the attempt to develop an understanding of ISIVIVC and PK-PD correlations in early drug discovery programs to avoid late stage failures. In conclusion, our results could contribute to drug discovery programs in the field of tuberculosis and malaria. Furthermore, the same strategy could be extended broadly beyond specific

compound classes and therapeutic areas aiding successful lead optimization and drug discovery programs.

6.2 Future directions

The *in vivo* efficacy of bicyclic 4-nitroimidazols correlated with total lung $T_{>MIC}$. Our results differ from the ones reported for PA-824 where *in vivo* efficacy correlated well with the time during which the free drug concentrations in plasma were above the MIC ($fT_{>MIC}$) (Ahmad et al., 2011). In their study, PA-824 results were obtained from extensive dose fractionation experiment, whereas the analysis reported here are from single dosing regimen with multiple bicyclic 4-nitroimidazole analogs. Hence, further investigations are warranted to confirm the hypothesis of similar PK-PD driver existing across the compound class by conducting dose fractionation studies for additional nitroimidazole analogs. In addition, total concentrations in lungs were used for PK-PD analysis of bicyclic 4-nitroimidazoles. Additional work is necessary to assess their free concentration in lungs and consider it for PK-PD analysis.

Classical dose fractionation study was done only for KAE609. The other compounds were characterized in dose-response studies. Additional investigations would be recommended to confirm the hypothesis that a similar PK-PD driver exists across the compound class. In addition, NMRI mouse PK data was available only for KAE609. PK in NMRI mice for other spiroindolone analogs would be useful to establish the relationship between *in vitro* potency and PK. Moreover, the PK-PD relationship for KAE609 was analyzed considering parasitemia reduction as pharmacodynamic readout. The

relationship with cure as alternative pharmacodynamic readout is not yet understood. Further efforts need to be made in this direction in the future.

REFERENCES

2014. Stan Development Team. 2014. Stan: A C++ Library for Probability and Sampling, Version 2.1. http://mc-stan.org/.

Ahmad, Z., Peloquin, C.A., Singh, R.P., Derendorf, H., Tyagi, S., Ginsberg, A., Grosset, J.H., and Nuermberger, E.L., 2011. PA-824 exhibits time-dependent activity in a murine model of tuberculosis. Antimicrob.Agents Chemother. 55, 239-245.

Alanine, A., Nettekoven, M., Roberts, E., and Thomas, A.W., 2003. Lead generation--enhancing the success of drug discovery by investing in the hit to lead process. Comb.Chem.High Throughput.Screen. 6, 51-66.

Ambrose, P.G., Bhavnani, S.M., Rubino, C.M., Louie, A., Gumbo, T., Forrest, A., and Drusano, G.L., 2007. Pharmacokinetics-pharmacodynamics of antimicrobial therapy: it's not just for mice anymore. Clin.Infect.Dis. 44, 79-86.

Andes, D. and Craig, W.A., 2002. Animal model pharmacokinetics and pharmacodynamics: a critical review. Int.J.Antimicrob.Agents 19, 261-268.

Andries, K., Gevers, T., and Lounis, N., 2010. Bactericidal potencies of new regimens are not predictive of their sterilizing potencies in a murine model of tuberculosis. Antimicrob.Agents Chemother. 54, 4540-4544.

Andries, K., Verhasselt, P., Guillemont, J., Gohlmann, H.W., Neefs, J.M., Winkler, H., Van, G.J., Timmerman, P., Zhu, M., Lee, E., Williams, P., de, C.D., Huitric, E., Hoffner, S., Cambau, E., Truffot-Pernot, C., Lounis, N., and Jarlier, V., 2005. A diarylquinoline drug active on the ATP synthase of Mycobacterium tuberculosis. Science 307, 223-227.

Ashley, E.A., Pinoges, L., Turyakira, E., Dorsey, G., Checchi, F., Bukirwa, H., van, d.B., I, Zongo, I., Urruta, P.P., van, H.M., Balkan, S., Taylor, W.R., Olliaro, P., and Guthmann, J.P., 2008. Different methodological approaches to the assessment of in vivo efficacy of three artemisinin-based combination antimalarial treatments for the treatment of uncomplicated falciparum malaria in African children. Malar.J. 7, 154.

Avdeef, A., 2005. The rise of PAMPA. Expert.Opin.Drug Metab Toxicol. 1, 325-342.

Avdeef, A., Bendels, S., Di, L., Faller, B., Kansy, M., Sugano, K., and Yamauchi, Y., 2007. PAMPA-critical factors for better predictions of absorption. J.Pharm.Sci. 96, 2893-2909.

Bakshi, R.P., Nenortas, E., Tripathi, A.K., Sullivan, D.J., and Shapiro, T.A., 2013. Model system to define pharmacokinetic requirements for antimalarial drug efficacy. Sci.Transl.Med. 5, 205ra135.

Baldwin, J., Michnoff, C.H., Malmquist, N.A., White, J., Roth, M.G., Rathod, P.K., and Phillips, M.A., 2005. High-throughput screening for potent and selective inhibitors of Plasmodium falciparum dihydroorotate dehydrogenase. J.Biol.Chem. 280, 21847-21853.

Balganesh, T.S., Alzari, P.M., and Cole, S.T., 2008. Rising standards for tuberculosis drug development. Trends Pharmacol.Sci. 29, 576-581.

Balimane, P.V. and Chong, S., 2005. Cell culture-based models for intestinal permeability: a critique. Drug Discov.Today 10, 335-343.

Banker, M.J., Clark, T.H., and Williams, J.A., 2003. Development and validation of a 96-well equilibrium dialysis apparatus for measuring plasma protein binding. J.Pharm.Sci. 92, 967-974.

Barbour, A., Scaglione, F., and Derendorf, H., 2010. Class-dependent relevance of tissue distribution in the interpretation of anti-infective pharmacokinetic/pharmacodynamic indices. Int.J.Antimicrob.Agents 35, 431-438.

Barnes, K.I., Watkins, W.M., and White, N.J., 2008. Antimalarial dosing regimens and drug resistance. Trends Parasitol. 24, 127-134.

Barry, C.E., Cherian, J., Chio, I., Keller, T., Manjunatha, U.H., Nayyar, A., and Young, H., 2011. Organic compounds. US Patent WO 2011/087995.

Barry, C.E., III, Boshoff, H.I., Dartois, V., Dick, T., Ehrt, S., Flynn, J., Schnappinger, D., Wilkinson, R.J., and Young, D., 2009. The spectrum of latent tuberculosis: rethinking the biology and intervention strategies. Nat.Rev.Microbiol. 7, 845-855.

Batty, K.T., Gibbons, P.L., Davis, T.M., and Ilett, K.F., 2008. Pharmacokinetics of dihydroartemisinin in a murine malaria model. Am.J.Trop.Med.Hyg. 78, 641-642.

Blaser, A., Palmer, B.D., Sutherland, H.S., Kmentova, I., Franzblau, S.G., Wan, B., Wang, Y., Ma, Z., Thompson, A.M., and Denny, W.A., 2012. Structure-activity relationships for amide-, carbamate-, and urea-linked analogues of the tuberculosis drug (6S)-2-nitro-6-{[4-(trifluoromethoxy)benzyl]oxy}-6,7-dihydro-5H-imidazo[2,1-b][1, 3]oxazine (PA-824). J.Med.Chem. 55, 312-326.

Bleicher, K.H., Bohm, H.J., Muller, K., and Alanine, A.I., 2003. Hit and lead generation: beyond high-throughput screening. Nat.Rev.Drug Discov. 2, 369-378.

Boshoff, H.I. and Barry, C.E., III, 2005. Tuberculosis - metabolism and respiration in the absence of growth. Nat.Rev.Microbiol. 3, 70-80.

Bouzom, F., Laveille, C., Merdjan, H., and Jochemsen, R., 2000. Use of nonlinear mixed effect modeling for the meta-analysis of preclinical

pharmacokinetic data: application to S 20342 in the rat. J.Pharm.Sci. 89, 603-613.

Brennan, P.J. and Young, D.B., 2008. Tuberculosis, Handbook of Anti-Tuberculosis Agents, Global Alliance for TB Drug Development. 88 ed., pp. 85-170.

Brennan, P.J., Young, D.B., and Robertson B.D, 2008. Tuberculosis. Handbook of Anti-Tuberculosis Agents, Global Alliance for TB Drug Development. Amsterdam: Elservier. 88 ed., pp. 85-170.

Brunner, M., Derendorf, H., and Muller, M., 2005. Microdialysis for in vivo pharmacokinetic/pharmacodynamic characterization of anti-infective drugs. Curr.Opin.Pharmacol. 5, 495-499.

Brunner, R., Aissaoui, H., Boss, C., Bozdech, Z., Brun, R., Corminboeuf, O., Delahaye, S., Fischli, C., Heidmann, B., Kaiser, M., Kamber, J., Meyer, S., Papastogiannidis, P., Siegrist, R., Voss, T., Welford, R., Wittlin, S., and Binkert, C., 2012. Identification of a new chemical class of antimalarials. J.Infect.Dis. 206, 735-743.

Brunton, L.L., Chabner, B.A., and Knollmann, B.C., 2010. Goodman & Gilman's The Pharmacological Basis of Therapeutics, 12th Edition, McGraw-Hill.

Budha, N.R., Lee, R.E., and Meibohm, B., 2008. Biopharmaceutics, pharmacokinetics and pharmacodynamics of antituberculosis drugs. Curr.Med.Chem. 15, 809-825.

Burman, W., Dooley, K.E., and Nuermberger, E.L., 2011. The Rifamycins: Renewed Interest in an Old Drug Class. Chapter 3 Donald RP, Van Helden PD (eds): Antituberculosis Chemotherapy. Prog Respir Res. Basel, Karger. 40. 40 ed., pp. 18-24.

Burrows, J.N., Burlot, E., Campo, B., Cherbuin, S., Jeanneret, S., Leroy, D., Spangenberg, T., Waterson, D., Wells, T.N., and Willis, P., 2014. Antimalarial drug discovery - the path towards eradication. Parasitology 141, 128-139.

Charman, S.A., Arbe-Barnes, S., Bathurst, I.C., Brun, R., Campbell, M., Charman, W.N., Chiu, F.C., Chollet, J., Craft, J.C., Creek, D.J., Dong, Y., Matile, H., Maurer, M., Morizzi, J., Nguyen, T., Papastogiannidis, P., Scheurer, C., Shackleford, D.M., Sriraghavan, K., Stingelin, L., Tang, Y., Urwyler, H., Wang, X., White, K.L., Wittlin, S., Zhou, L., and Vennerstrom, J.L., 2011. Synthetic ozonide drug candidate OZ439 offers new hope for a single-dose cure of uncomplicated malaria. Proc.Natl.Acad.Sci.U.S.A 108, 4400-4405.

Chaurasia, C.S., Muller, M., Bashaw, E.D., Benfeldt, E., Bolinder, J., Bullock, R., Bungay, P.M., DeLange, E.C., Derendorf, H., Elmquist, W.F., Hammarlund-Udenaes, M., Joukhadar, C., Kellogg, D.L., Jr., Lunte, C.E., Nordstrom, C.H., Rollema, H., Sawchuk, R.J., Cheung, B.W., Shah, V.P.,

Stahle, L., Ungerstedt, U., Welty, D.F., and Yeo, H., 2007. AAPS-FDA workshop white paper: microdialysis principles, application and regulatory perspectives. Pharm.Res. 24, 1014-1025.

Cherian, J., Choi, I., Nayyar, A., Manjunatha, U.H., Mukherjee, T., Lee, Y.S., Boshoff, H.I., Singh, R., Ha, Y.H., Goodwin, M., Lakshminarayana, S.B., Niyomrattanakit, P., Jiricek, J., Ravindran, S., Dick, T., Keller, T.H., Dartois, V., and Barry, C.E., III, 2011. Structure-activity relationships of antitubercular nitroimidazoles. 3. Exploration of the linker and lipophilic tail of ((s)-2-nitro-6,7-dihydro-5H-imidazo[2,1-b][1,3]oxazin-6-yl)-(4-trifluoromethoxybe nzyl)amine (6-amino PA-824). J.Med.Chem. 54, 5639-5659.

Chierakul, N., Klomsawat, D., Chulavatnatol, S., and Chindavijak, B., 2001. Intrapulmonary pharmacokinetics of ofloxacin in drug-resistant tuberculosis. Int.J.Tuberc.Lung Dis. 5, 278-282.

Conte, J.E., Jr., Golden, J.A., Duncan, S., McKenna, E., and Zurlinden, E., 1999. Intrapulmonary concentrations of pyrazinamide. Antimicrob.Agents Chemother. 43, 1329-1333.

Conte, J.E., Jr., Golden, J.A., Kipps, J., Lin, E.T., and Zurlinden, E., 2001. Effects of AIDS and gender on steady-state plasma and intrapulmonary ethambutol concentrations. Antimicrob.Agents Chemother. 45, 2891-2896.

Conte, J.E., Jr., Golden, J.A., Kipps, J., and Zurlinden, E., 2002a. Intrapulmonary pharmacokinetics of linezolid. Antimicrob.Agents Chemother. 46, 1475-1480.

Conte, J.E., Jr., Golden, J.A., McQuitty, M., Kipps, J., Duncan, S., McKenna, E., and Zurlinden, E., 2002b. Effects of gender, AIDS, and acetylator status on intrapulmonary concentrations of isoniazid. Antimicrob.Agents Chemother. 46, 2358-2364.

Conte, J.E., Jr., Golden, J.A., McQuitty, M., Kipps, J., Lin, E.T., and Zurlinden, E., 2000. Single-dose intrapulmonary pharmacokinetics of rifapentine in normal subjects. Antimicrob.Agents Chemother. 44, 985-990.

Cooper, C.B., 2013. Development of Mycobacterium tuberculosis whole cell screening hits as potential antituberculosis agents. J.Med.Chem. 56, 7755-7760.

Coteron, J.M., Marco, M., Esquivias, J., Deng, X., White, K.L., White, J., Koltun, M., El, M.F., Kokkonda, S., Katneni, K., Bhamidipati, R., Shackleford, D.M., Angulo-Barturen, I., Ferrer, S.B., Jimenez-Diaz, M.B., Gamo, F.J., Goldsmith, E.J., Charman, W.N., Bathurst, I., Floyd, D., Matthews, D., Burrows, J.N., Rathod, P.K., Charman, S.A., and Phillips, M.A., 2011. Structure-guided lead optimization of triazolopyrimidine-ring substituents identifies potent Plasmodium falciparum dihydroorotate dehydrogenase inhibitors with clinical candidate potential. J.Med.Chem. 54, 5540-5561.

Cox, E. and Laessig, K., 2014. FDA approval of bedaquiline--the benefit-risk balance for drug-resistant tuberculosis. N.Engl.J.Med. 371, 689-691.

Craig, W.A., 1998. Pharmacokinetic/pharmacodynamic parameters: rationale for antibacterial dosing of mice and men. Clin.Infect.Dis. 26, 1-10.

Craig, W.A., 2001. Does the dose matter? Clin.Infect.Dis. 33 Suppl 3, S233-S237.

D'Alessandro, U., 2009. Existing antimalarial agents and malaria-treatment strategies. Expert.Opin.Pharmacother. 10, 1291-1306.

Dartois, V., 2014. The path of anti-tuberculosis drugs: from blood to lesions to mycobacterial cells. Nat.Rev.Microbiol. 12, 159-167.

Dartois, V. and Barry, C.E., 2010. Clinical pharmacology and lesion penetrating properties of second- and third-line antituberculous agents used in the management of multidrug-resistant (MDR) and extensively-drug resistant (XDR) tuberculosis. Curr.Clin.Pharmacol. 5, 96-114.

Dartois, V. and Barry, C.E., III, 2013. A medicinal chemists' guide to the unique difficulties of lead optimization for tuberculosis. Bioorg.Med.Chem.Lett. 23, 4741-4750.

Davies, G.R. and Nuermberger, E.L., 2008. Pharmacokinetics and pharmacodynamics in the development of anti-tuberculosis drugs. Tuberculosis.(Edinb.) 88 Suppl 1, S65-S74.

Davis, A.M., Webborn, P.J., and Salt, D.W., 2000. Robust assessment of statistical significance in the use of unbound/intrinsic pharmacokinetic parameters in quantitative structure-pharmacokinetic relationships with lipophilicity. Drug Metab Dispos. 28, 103-106.

Denny, W.A. and Palmer, B.D., 2010. The nitroimidazooxazines (PA-824 and analogs): structure-activity relationship and mechanistic studies. Future.Med.Chem. 2, 1295-1304.

Desjardins, R.E., Canfield, C.J., Haynes, J.D., and Chulay, J.D., 1979. Quantitative assessment of antimalarial activity in vitro by a semiautomated microdilution technique. Antimicrob.Agents Chemother. 16, 710-718.

Deye, G.A., Gettayacamin, M., Hansukjariya, P., Im-erbsin, R., Sattabongkot, J., Rothstein, Y., Macareo, L., Fracisco, S., Bennett, K., Magill, A.J., and Ohrt, C., 2012. Use of a rhesus Plasmodium cynomolgi model to screen for anti-hypnozoite activity of pharmaceutical substances. Am.J.Trop.Med.Hyg. 86, 931-935.

Di, L. and Kerns, E.H., 2003. Profiling drug-like properties in discovery research. Curr.Opin.Chem.Biol. 7, 402-408.

Diacon, A.H., Dawson, R., du, B.J., Narunsky, K., Venter, A., Donald, P.R., van, N.C., Erondu, N., Ginsberg, A.M., Becker, P., and Spigelman, M.K.,

2012a. A phase II dose-ranging trial of the early bactericidal activity of PA-824. Antimicrob.Agents Chemother.

Diacon, A.H., Dawson, R., Hanekom, M., Narunsky, K., Maritz, S.J., Venter, A., Donald, P.R., van, N.C., Whitney, K., Rouse, D.J., Laurenzi, M.W., Ginsberg, A.M., and Spigelman, M.K., 2010. Early bactericidal activity and pharmacokinetics of PA-824 in smear-positive tuberculosis patients. Antimicrob.Agents Chemother. 54, 3402-3407.

Diacon, A.H., Dawson, R., Hanekom, M., Narunsky, K., Venter, A., Hittel, N., Geiter, L.J., Wells, C.D., Paccaly, A.J., and Donald, P.R., 2011. Early bactericidal activity of delamanid (OPC-67683) in smear-positive pulmonary tuberculosis patients. Int.J.Tuberc.Lung Dis. 15, 949-954.

Diacon, A.H., Dawson, R., von Groote-Bidlingmaier, F., Symons, G., Venter, A., Donald, P.R., van, N.C., Everitt, D., Winter, H., Becker, P., Mendel, C.M., and Spigelman, M.K., 2012b. 14-day bactericidal activity of PA-824, bedaquiline, pyrazinamide, and moxifloxacin combinations: a randomised trial. Lancet 380, 986-993.

Diacon, A.H., Pym, A., Grobusch, M.P., de los Rios, J.M., Gotuzzo, E., Vasilyeva, I., Leimane, V., Andries, K., Bakare, N., De, M.T., Haxaire-Theeuwes, M., Lounis, N., Meyvisch, P., De, P.E., van Heeswijk, R.P., and Dannemann, B., 2014. Multidrug-resistant tuberculosis and culture conversion with bedaquiline. N.Engl.J.Med. 371, 723-732.

Dickson, M. and Gagnon, J.P., 2004a. Key factors in the rising cost of new drug discovery and development. Nat.Rev.Drug Discov. 3, 417-429.

Dickson, M. and Gagnon, J.P., 2004b. The cost of new drug discovery and development. Discov.Med. 4, 172-179.

Diehl, K.H., Hull, R., Morton, D., Pfister, R., Rabemampianina, Y., Smith, D., Vidal, J.M., and van, d., V, 2001. A good practice guide to the administration of substances and removal of blood, including routes and volumes. J.Appl.Toxicol. 21, 15-23.

Ding, X.C., Ubben, D., and Wells, T.N., 2012. A framework for assessing the risk of resistance for anti-malarials in development. Malar.J. 11, 292.

Djukic, M., Munz, M., Sorgel, F., Holzgrabe, U., Eiffert, H., and Nau, R., 2012. Overton's rule helps to estimate the penetration of anti-infectives into patients' cerebrospinal fluid. Antimicrob.Agents Chemother. 56, 979-988.

Dondorp, A.M., Nosten, F., Yi, P., Das, D., Phyo, A.P., Tarning, J., Lwin, K.M., Ariey, F., Hanpithakpong, W., Lee, S.J., Ringwald, P., Silamut, K., Imwong, M., Chotivanich, K., Lim, P., Herdman, T., An, S.S., Yeung, S., Singhasivanon, P., Day, N.P., Lindegardh, N., Socheat, D., and White, N.J., 2009. Artemisinin resistance in Plasmodium falciparum malaria. N.Engl.J.Med. 361, 455-467.

Dow, G.S., Gettayacamin, M., Hansukjariya, P., Imerbsin, R., Komcharoen, S., Sattabongkot, J., Kyle, D., Milhous, W., Cozens, S., Kenworthy, D., Miller, A., Veazey, J., and Ohrt, C., 2011. Radical curative efficacy of tafenoquine combination regimens in Plasmodium cynomolgi-infected Rhesus monkeys (Macaca mulatta). Malar.J. 10, 212.

Drusano, G.L., 2004. Antimicrobial pharmacodynamics: critical interactions of 'bug and drug'. Nat.Rev.Microbiol. 2, 289-300.

Drusano, G.L., 2007. Pharmacokinetics and pharmacodynamics of antimicrobials. Clin.Infect.Dis. 45 Suppl 1, S89-S95.

Duijkers, I.J., Klipping, C., Boerrigter, P.J., Machielsen, C.S., De Bie, J.J., and Voortman, G., 2002. Single dose pharmacokinetics and effects on follicular growth and serum hormones of a long-acting recombinant FSH preparation (FSH-CTP) in healthy pituitary-suppressed females. Hum.Reprod. 17, 1987-1993.

Durairaj, C., Shah, J.C., Senapati, S., and Kompella, U.B., 2009. Prediction of vitreal half-life based on drug physicochemical properties: quantitative structure-pharmacokinetic relationships (QSPKR). Pharm.Res. 26, 1236-1260.

Dye, C. and Williams, B.G., 2010. The population dynamics and control of tuberculosis. Science 328, 856-861.

Egan, W.J., Merz, K.M., Jr., and Baldwin, J.J., 2000. Prediction of drug absorption using multivariate statistics. J.Med.Chem. 43, 3867-3877.

England, K., Boshoff, H.I., Arora, K., Weiner, D., Dayao, E., Schimel, D., Via, L.E., and Barry, C.E., III, 2012. Meropenem-clavulanic acid shows activity against Mycobacterium tuberculosis in vivo. Antimicrob.Agents Chemother. 56, 3384-3387.

Ferl, G.Z., Zhang, X., Wu, H.M., Kreissl, M.C., and Huang, S.C., 2007. Estimation of the 18F-FDG input function in mice by use of dynamic small-animal PET and minimal blood sample data. J.Nucl.Med. 48, 2037-2045.

Ferreira, P.E., Culleton, R., Gil, J.P., and Meshnick, S.R., 2013. Artemisinin resistance in Plasmodium falciparum: what is it really? Trends Parasitol. 29, 318-320.

Fidock, D.A., Rosenthal, P.J., Croft, S.L., Brun, R., and Nwaka, S., 2004. Antimalarial drug discovery: efficacy models for compound screening. Nat.Rev.Drug Discov. 3, 509-520.

Franke-Fayard, B., Trueman, H., Ramesar, J., Mendoza, J., van der Keur, M., van der Linden, R., Sinden, R.E., Waters, A.P., and Janse, C.J., 2004. A Plasmodium berghei reference line that constitutively expresses GFP at a high level throughout the complete life cycle. Mol.Biochem.Parasitol. 137, 23-33.

Franzblau, S.G., DeGroote, M.A., Cho, S.H., Andries, K., Nuermberger, E., Orme, I.M., Mdluli, K., Angulo-Barturen, I., Dick, T., Dartois, V., and

Lenaerts, A.J., 2012. Comprehensive analysis of methods used for the evaluation of compounds against Mycobacterium tuberculosis. Tuberculosis.(Edinb.) 92, 453-488.

Fung, E.N., Chen, Y.H., and Lau, Y.Y., 2003. Semi-automatic high-throughput determination of plasma protein binding using a 96-well plate filtrate assembly and fast liquid chromatography-tandem mass spectrometry. J.Chromatogr.B Analyt.Technol.Biomed.Life Sci. 795, 187-194.

Gabrielsson, J., Dolgos, H., Gillberg, P.G., Bredberg, U., Benthem, B., and Duker, G., 2009. Early integration of pharmacokinetic and dynamic reasoning is essential for optimal development of lead compounds: strategic considerations. Drug Discov.Today 14, 358-372.

Gabrielsson, J. and Weiner, D., 2006. Pharmacokinetic-Pharmacodynamic Data Analysis: Concepts and Applications (4th edn), Swedish Pharmaceutical Press ISBN 13 978 91 9765 100 4.

Gaonkar, S., Jayaram, R., Lakshminarayana, S., Bharath, S., Shandil, R., and Balasubramanian, V., 2006. Moxifloxacin: Time Course of Effect in an Aeroson Infection Model of Tuberculosis. Intersci Conf Antimicrob Agents Chemother (abstract no. A-1563).

Gautam, A., Ahmed, T., Batra, V., and Paliwal, J., 2009. Pharmacokinetics and pharmacodynamics of endoperoxide antimalarials. Curr.Drug Metab 10, 289-306.

German, P.I. and Aweeka, F.T., 2008. Clinical pharmacology of artemisinin-based combination therapies. Clin.Pharmacokinet. 47, 91-102.

Giao, P.T. and de Vries, P.J., 2001. Pharmacokinetic interactions of antimalarial agents. Clin.Pharmacokinet. 40, 343-373.

Gibbons, P.L., Batty, K.T., Barrett, P.H., Davis, T.M., and Ilett, K.F., 2007. Development of a pharmacodynamic model of murine malaria and antimalarial treatment with dihydroartemisinin. Int.J.Parasitol. 37, 1569-1576.

Gillespie, S.H., Crook, A.M., McHugh, T.D., Mendel, C.M., Meredith, S.K., Murray, S.R., Pappas, F., Phillips, P.P., and Nunn, A.J., 2014. Four-month moxifloxacin-based regimens for drug-sensitive tuberculosis. N.Engl.J.Med. 371, 1577-1587.

Ginsberg, A.M., 2010. Drugs in development for tuberculosis. Drugs 70, 2201-2214.

Ginsberg, A.M., Laurenzi, M.W., Rouse, D.J., Whitney, K.D., and Spigelman, M.K., 2009. Safety, tolerability, and pharmacokinetics of PA-824 in healthy subjects. Antimicrob.Agents Chemother. 53, 3720-3725.

Giuliano, C., Jairaj, M., Zafiu, C.M., and Laufer, R., 2005. Direct determination of unbound intrinsic drug clearance in the microsomal stability assay. Drug Metab Dispos. 33, 1319-1324.

Gleeson, M.P., 2008. Generation of a set of simple, interpretable ADMET rules of thumb. J.Med.Chem. 51, 817-834.

Gler, M.T., Skripconoka, V., Sanchez-Garavito, E., Xiao, H., Cabrera-Rivero, J.L., Vargas-Vasquez, D.E., Gao, M., Awad, M., Park, S.K., Shim, T.S., Suh, G.Y., Danilovits, M., Ogata, H., Kurve, A., Chang, J., Suzuki, K., Tupasi, T., Koh, W.J., Seaworth, B., Geiter, L.J., and Wells, C.D., 2012. Delamanid for multidrug-resistant pulmonary tuberculosis. N.Engl.J.Med. 366, 2151-2160.

Gonzalez, D., Schmidt, S., and Derendorf, H., 2013. Importance of relating efficacy measures to unbound drug concentrations for anti-infective agents. Clin.Microbiol.Rev. 26, 274-288.

Greenwood, B. and Mutabingwa, T., 2002. Malaria in 2002. Nature 415, 670-672.

Grosset, J. and Ji, B., 1998. Experimental chemotherapy of mycobacterial diseases.

Grzegorzewicz, A.E., Pham, H., Gundi, V.A., Scherman, M.S., North, E.J., Hess, T., Jones, V., Gruppo, V., Born, S.E., Kordulakova, J., Chavadi, S.S., Morisseau, C., Lenaerts, A.J., Lee, R.E., McNeil, M.R., and Jackson, M., 2012. Inhibition of mycolic acid transport across the Mycobacterium tuberculosis plasma membrane. Nat.Chem.Biol. 8, 334-341.

Healy, D.P., Polk, R.E., Garson, M.L., Rock, D.T., and Comstock, T.J., 1987. Comparison of steady-state pharmacokinetics of two dosage regimens of vancomycin in normal volunteers. Antimicrob.Agents Chemother. 31, 393-397.

Held, J., Kreidenweiss, A., and Mordmuller, B., 2013. Novel approaches in antimalarial drug discovery. Expert.Opin.Drug Discov. 8, 1325-1337.

Hirabayashi, H., Sawamoto, T., Fujisaki, J., Tokunaga, Y., Kimura, S., and Hata, T., 2001. Relationship between physicochemical and osteotropic properties of bisphosphonic derivatives: rational design for osteotropic drug delivery system (ODDS). Pharm.Res. 18, 646-651.

Holdiness, M.R., 1984. Clinical pharmacokinetics of the antituberculosis drugs. Clin.Pharmacokinet. 9, 511-544.

Hoshen, M.B., Stein, W.D., and Ginsburg, H., 2002. Mathematical modelling of malaria chemotherapy: combining artesunate and mefloquine. Parasitology 124, 9-15.

Hoshen, M.B., Stein, W.D., and Ginsburg, H.D., 2001. Pharmacokinetic-pharmacodynamic modelling of the antimalarial activity of mefloquine. Parasitology 123, 337-346.

Hugonnet, J.E., Tremblay, L.W., Boshoff, H.I., Barry, C.E., III, and Blanchard, J.S., 2009. Meropenem-clavulanate is effective against extensively drug-resistant Mycobacterium tuberculosis. Science 323, 1215-1218.

Hummel, J., McKendrick, S., Brindley, C., and French, R., 2009. Exploratory assessment of dose proportionality: review of current approaches and proposal for a practical criterion. Pharm.Stat. 8, 38-49.

Jayaram, R., Gaonkar, S., Kaur, P., Suresh, B.L., Mahesh, B.N., Jayashree, R., Nandi, V., Bharat, S., Shandil, R.K., Kantharaj, E., and Balasubramanian, V., 2003. Pharmacokinetics-pharmacodynamics of rifampin in an aerosol infection model of tuberculosis. Antimicrob.Agents Chemother. 47, 2118-2124.

Jayaram, R., Shandil, R.K., Gaonkar, S., Kaur, P., Suresh, B.L., Mahesh, B.N., Jayashree, R., Nandi, V., Bharath, S., Kantharaj, E., and Balasubramanian, V., 2004. Isoniazid pharmacokinetics-pharmacodynamics in an aerosol infection model of tuberculosis. Antimicrob.Agents Chemother. 48, 2951-2957.

Jimenez-Diaz, M.B., Viera, S., Ibanez, J., Mulet, T., Magan-Marchal, N., Garuti, H., Gomez, V., Cortes-Gil, L., Martinez, A., Ferrer, S., Fraile, M.T., Calderon, F., Fernandez, E., Shultz, L.D., Leroy, D., Wilson, D.M., Garcia-Bustos, J.F., Gamo, F.J., and Angulo-Barturen, I., 2013. A new in vivo screening paradigm to accelerate antimalarial drug discovery. PLoS.One. 8, e66967.

Jindani, A., Harrison, T.S., Nunn, A.J., Phillips, P.P., Churchyard, G.J., Charalambous, S., Hatherill, M., Geldenhuys, H., McIlleron, H.M., Zvada, S.P., Mungofa, S., Shah, N.A., Zizhou, S., Magweta, L., Shepherd, J., Nyirenda, S., van Dijk, J.H., Clouting, H.E., Coleman, D., Bateson, A.L., McHugh, T.D., Butcher, P.D., and Mitchison, D.A., 2014. High-dose rifapentine with moxifloxacin for pulmonary tuberculosis. N.Engl.J.Med. 371, 1599-1608.

Jiricek, J., Patel, S., Keller, T., Barry, C.E., and Dowd, C.S., 2007. Nitroimidazole compounds. US Patent WO 2007/075872.

John, G.K., Douglas, N.M., von, S.L., Nosten, F., Baird, J.K., White, N.J., and Price, R.N., 2012. Primaquine radical cure of Plasmodium vivax: a critical review of the literature. Malar.J. 11, 280.

Kaneko, T., Cooper, C., and Mdluli, K., 2011. Challenges and opportunities in developing novel drugs for TB. Future.Med.Chem. 3, 1373-1400.

Karbwang, J., Na, B.K., Thanavibul, A., Back, D.J., Bunnag, D., and Harinasuta, T., 1994. Pharmacokinetics of mefloquine alone or in combination with artesunate. Bull.World Health Organ 72, 83-87.

Kariv, I., Cao, H., and Oldenburg, K.R., 2001. Development of a high throughput equilibrium dialysis method. J.Pharm.Sci. 90, 580-587.

Kerns, E.H. and Di, L., 2003. Pharmaceutical profiling in drug discovery. Drug Discov.Today 8, 316-323.

Kiem, S. and Schentag, J.J., 2008. Interpretation of antibiotic concentration ratios measured in epithelial lining fluid. Antimicrob.Agents Chemother. 52, 24-36.

Kim, P., Kang, S., Boshoff, H.I., Jiricek, J., Collins, M., Singh, R., Manjunatha, U.H., Niyomrattanakit, P., Zhang, L., Goodwin, M., Dick, T., Keller, T.H., Dowd, C.S., and Barry, C.E., III, 2009a. Structure-activity relationships of antitubercular nitroimidazoles. 2. Determinants of aerobic activity and quantitative structure-activity relationships. J.Med.Chem. 52, 1329-1344.

Kim, P., Zhang, L., Manjunatha, U.H., Singh, R., Patel, S., Jiricek, J., Keller, T.H., Boshoff, H.I., Barry, C.E., III, and Dowd, C.S., 2009b. Structure-activity relationships of antitubercular nitroimidazoles. 1. Structural features associated with aerobic and anaerobic activities of 4- and 5-nitroimidazoles. J.Med.Chem. 52, 1317-1328.

Kjellsson, M.C., Via, L.E., Goh, A., Weiner, D., Low, K.M., Kern, S., Pillai, G., Barry, C.E., III, and Dartois, V., 2012. Pharmacokinetic evaluation of the penetration of antituberculosis agents in rabbit pulmonary lesions. Antimicrob.Agents Chemother. 56, 446-457.

Kmentova, I., Sutherland, H.S., Palmer, B.D., Blaser, A., Franzblau, S.G., Wan, B., Wang, Y., Ma, Z., Denny, W.A., and Thompson, A.M., 2010. Synthesis and Structure-Activity Relationships of Aza- and Diazabiphenyl Analogues of the Antitubercular Drug (6S)-2-Nitro-6-{[4-(trifluoromethoxy)benzyl]oxy}-6,7-dihydro-5H-imidazo[2,1-b][1, 3]oxazine (PA-824). J.Med.Chem.

Knudsen, J.D., Fuursted, K., Raber, S., Espersen, F., and Frimodt-Moller, N., 2000. Pharmacodynamics of glycopeptides in the mouse peritonitis model of Streptococcus pneumoniae or Staphylococcus aureus infection. Antimicrob.Agents Chemother. 44, 1247-1254.

Kola, I. and Landis, J., 2004. Can the pharmaceutical industry reduce attrition rates? Nat.Rev.Drug Discov. 3, 711-715.

Kondreddi, R.R., Jiricek, J., Rao, S.P., Lakshminarayana, S.B., Camacho, L.R., Rao, R., Herve, M., Bifani, P., Ma, N.L., Kuhen, K., Goh, A., Chatterjee, A.K., Dick, T., Diagana, T.T., Manjunatha, U.H., and Smith, P.W., 2013. Design, synthesis, and biological evaluation of indole-2-carboxamides: a promising class of antituberculosis agents. J.Med.Chem. 56, 8849-8859.

Koul, A., Arnoult, E., Lounis, N., Guillemont, J., and Andries, K., 2011. The challenge of new drug discovery for tuberculosis. Nature 469, 483-490.

Kuhen, K.L., Chatterjee, A.K., Rottmann, M., Gagaring, K., Borboa, R., Buenviaje, J., Chen, Z., Francek, C., Wu, T., Nagle, A., Barnes, S.W., Plouffe, D., Lee, M.C., Fidock, D.A., Graumans, W., van, d., V, van Gemert, G.J., Wirjanata, G., Sebayang, B., Marfurt, J., Russell, B., Suwanarusk, R., Price, R.N., Nosten, F., Tungtaeng, A., Gettayacamin, M., Sattabongkot, J., Taylor,

J., Walker, J.R., Tully, D., Patra, K.P., Flannery, E.L., Vinetz, J.M., Renia, L., Sauerwein, R.W., Winzeler, E.A., Glynne, R.J., and Diagana, T.T., 2014. KAF156 is an antimalarial clinical candidate with potential for use in prophylaxis, treatment, and prevention of disease transmission. Antimicrob.Agents Chemother. 58, 5060-5067.

Kurabachew, M., Lu, S.H., Krastel, P., Schmitt, E.K., Suresh, B.L., Goh, A., Knox, J.E., Ma, N.L., Jiricek, J., Beer, D., Cynamon, M., Petersen, F., Dartois, V., Keller, T., Dick, T., and Sambandamurthy, V.K., 2008. Lipiarmycin targets RNA polymerase and has good activity against multidrug-resistant strains of Mycobacterium tuberculosis. J.Antimicrob.Chemother. 62, 713-719.

Langhorne, J., Buffet, P., Galinski, M., Good, M., Harty, J., Leroy, D., Mota, M.M., Pasini, E., Renia, L., Riley, E., Stins, M., and Duffy, P., 2011. The relevance of non-human primate and rodent malaria models for humans. Malar.J. 10, 23.

Lenaerts, A.J., Gruppo, V., Marietta, K.S., Johnson, C.M., Driscoll, D.K., Tompkins, N.M., Rose, J.D., Reynolds, R.C., and Orme, I.M., 2005. Preclinical testing of the nitroimidazopyran PA-824 for activity against Mycobacterium tuberculosis in a series of in vitro and in vivo models. Antimicrob.Agents Chemother. 49, 2294-2301.

Leong, F.J., Li, R., Jain, J.P., Lefevre, G., Magnusson, B., Diagana, T.T., and Pertel, P., 2014a. A first-in-human randomized, double-blind, placebo-controlled, single- and multiple-ascending oral dose study of novel antimalarial Spiroindolone KAE609 (Cipargamin) to assess its safety, tolerability, and pharmacokinetics in healthy adult volunteers. Antimicrob.Agents Chemother. 58, 6209-6214.

Leong, F.J., Zhao, R., Zeng, S., Magnusson, B., Diagana, T.T., and Pertel, P., 2014b. A first-in-human randomized, double-blind, placebo-controlled, single- and multiple-ascending oral dose study of novel Imidazolopiperazine KAF156 to assess its safety, tolerability, and pharmacokinetics in healthy adult volunteers. Antimicrob.Agents Chemother. 58, 6437-6443.

Lienhardt, C., Raviglione, M., Spigelman, M., Hafner, R., Jaramillo, E., Hoelscher, M., Zumla, A., and Gheuens, J., 2012. New drugs for the treatment of tuberculosis: needs, challenges, promise, and prospects for the future. J.Infect.Dis. 205 Suppl 2, S241-S249.

Lin, J.H., 2006. Tissue distribution and pharmacodynamics: a complicated relationship. Curr.Drug Metab 7, 39-65.

Lipinski, C.A., Lombardo, F., Dominy, B.W., and Feeney, P.J., 2001. Experimental and computational approaches to estimate solubility and permeability in drug discovery and development settings. Adv.Drug Deliv.Rev. 46, 3-26.

Liu, P., Muller, M., and Derendorf, H., 2002. Rational dosing of antibiotics: the use of plasma concentrations versus tissue concentrations. Int.J.Antimicrob.Agents 19, 285-290.

Ma, Z., Lienhardt, C., McIlleron, H., Nunn, A.J., and Wang, X., 2010. Global tuberculosis drug development pipeline: the need and the reality. Lancet 375, 2100-2109.

Manjunatha, U.H., Boshoff, H., Dowd, C.S., Zhang, L., Albert, T.J., Norton, J.E., Daniels, L., Dick, T., Pang, S.S., and Barry, C.E., III, 2006. Identification of a nitroimidazo-oxazine-specific protein involved in PA-824 resistance in Mycobacterium tuberculosis. Proc.Natl.Acad.Sci.U.S.A 103, 431-436.

Marino, A.M., Yarde, M., Patel, H., Chong, S., and Balimane, P.V., 2005. Validation of the 96 well Caco-2 cell culture model for high throughput permeability assessment of discovery compounds. Int.J.Pharm. 297, 235-241.

Matsumoto, M., Hashizume, H., Tomishige, T., Kawasaki, M., Tsubouchi, H., Sasaki, H., Shimokawa, Y., and Komatsu, M., 2006. OPC-67683, a nitro-dihydro-imidazooxazole derivative with promising action against tuberculosis in vitro and in mice. PLoS.Med. 3, e466.

Meister, S., Plouffe, D.M., Kuhen, K.L., Bonamy, G.M., Wu, T., Barnes, S.W., Bopp, S.E., Borboa, R., Bright, A.T., Che, J., Cohen, S., Dharia, N.V., Gagaring, K., Gettayacamin, M., Gordon, P., Groessl, T., Kato, N., Lee, M.C., McNamara, C.W., Fidock, D.A., Nagle, A., Nam, T.G., Richmond, W., Roland, J., Rottmann, M., Zhou, B., Froissard, P., Glynne, R.J., Mazier, D., Sattabongkot, J., Schultz, P.G., Tuntland, T., Walker, J.R., Zhou, Y., Chatterjee, A., Diagana, T.T., and Winzeler, E.A., 2011. Imaging of Plasmodium liver stages to drive next-generation antimalarial drug discovery. Science 334, 1372-1377.

Merle, C.S., Fielding, K., Sow, O.B., Gninafon, M., Lo, M.B., Mthiyane, T., Odhiambo, J., Amukoye, E., Bah, B., Kassa, F., N'Diaye, A., Rustomjee, R., de Jong, B.C., Horton, J., Perronne, C., Sismanidis, C., Lapujade, O., Olliaro, P.L., and Lienhardt, C., 2014. A four-month gatifloxacin-containing regimen for treating tuberculosis. N.Engl.J.Med. 371, 1588-1598.

Miotto, O., Almagro-Garcia, J., Manske, M., Macinnis, B., Campino, S., Rockett, K.A., Amaratunga, C., Lim, P., Suon, S., Sreng, S., Anderson, J.M., Duong, S., Nguon, C., Chuor, C.M., Saunders, D., Se, Y., Lon, C., Fukuda, M.M., Amenga-Etego, L., Hodgson, A.V., Asoala, V., Imwong, M., Takala-Harrison, S., Nosten, F., Su, X.Z., Ringwald, P., Ariey, F., Dolecek, C., Hien, T.T., Boni, M.F., Thai, C.Q., Amambua-Ngwa, A., Conway, D.J., Djimde, A.A., Doumbo, O.K., Zongo, I., Ouedraogo, J.B., Alcock, D., Drury, E., Auburn, S., Koch, O., Sanders, M., Hubbart, C., Maslen, G., Ruano-Rubio, V., Jyothi, D., Miles, A., O'Brien, J., Gamble, C., Oyola, S.O., Rayner, J.C., Newbold, C.I., Berriman, M., Spencer, C.C., McVean, G., Day, N.P., White, N.J., Bethell, D., Dondorp, A.M., Plowe, C.V., Fairhurst, R.M., and Kwiatkowski, D.P., 2013. Multiple populations of artemisinin-resistant Plasmodium falciparum in Cambodia. Nat.Genet. 45, 648-655.

MMV, 2014. http://www.mmv.org/.

Moehrle, J.J., Duparc, S., Siethoff, C., van Giersbergen, P.L., Craft, J.C., Arbe-Barnes, S., Charman, S.A., Gutierrez, M., Wittlin, S., and Vennerstrom, J.L., 2013. First-in-man safety and pharmacokinetics of synthetic ozonide OZ439 demonstrates an improved exposure profile relative to other peroxide antimalarials. Br.J.Clin.Pharmacol. 75, 524-537.

Moore, B.R., Batty, K.T., Andrzejewski, C., Jago, J.D., Page-Sharp, M., and Ilett, K.F., 2008. Pharmacokinetics and pharmacodynamics of piperaquine in a murine malaria model. Antimicrob.Agents Chemother. 52, 306-311.

Moore, B.R., Page-Sharp, M., Stoney, J.R., Ilett, K.F., Jago, J.D., and Batty, K.T., 2011. Pharmacokinetics, pharmacodynamics, and allometric scaling of chloroquine in a murine malaria model. Antimicrob.Agents Chemother. 55, 3899-3907.

Moreno, A., Badell, E., Van, R.N., and Druilhe, P., 2001. Human malaria in immunocompromised mice: new in vivo model for chemotherapy studies. Antimicrob.Agents Chemother. 45, 1847-1853.

Mouton, J.W., Dudley, M.N., Cars, O., Derendorf, H., and Drusano, G.L., 2005. Standardization of pharmacokinetic/pharmacodynamic (PK/PD) terminology for anti-infective drugs: an update. J.Antimicrob.Chemother. 55, 601-607.

Mouton, J.W., Theuretzbacher, U., Craig, W.A., Tulkens, P.M., Derendorf, H., and Cars, O., 2008. Tissue concentrations: do we ever learn? J.Antimicrob.Chemother. 61, 235-237.

Muller, M., dela, P.A., and Derendorf, H., 2004. Issues in pharmacokinetics and pharmacodynamics of anti-infective agents: distribution in tissue. Antimicrob.Agents Chemother. 48, 1441-1453.

Murray, C.J., Rosenfeld, L.C., Lim, S.S., Andrews, K.G., Foreman, K.J., Haring, D., Fullman, N., Naghavi, M., Lozano, R., and Lopez, A.D., 2012. Global malaria mortality between 1980 and 2010: a systematic analysis. Lancet 379, 413-431.

Na-Bangchang, K. and Karbwang, J., 2009. Current status of malaria chemotherapy and the role of pharmacology in antimalarial drug research and development. Fundam.Clin.Pharmacol. 23, 387-409.

Nagle, A., Wu, T., Kuhen, K., Gagaring, K., Borboa, R., Francek, C., Chen, Z., Plouffe, D., Lin, X., Caldwell, C., Ek, J., Skolnik, S., Liu, F., Wang, J., Chang, J., Li, C., Liu, B., Hollenbeck, T., Tuntland, T., Isbell, J., Chuan, T., Alper, P.B., Fischli, C., Brun, R., Lakshminarayana, S.B., Rottmann, M., Diagana, T.T., Winzeler, E.A., Glynne, R., Tully, D.C., and Chatterjee, A.K., 2012. Imidazolopiperazines: lead optimization of the second-generation antimalarial agents. J.Med.Chem. 55, 4244-4273.

Navaratnam, V., Mansor, S.M., Sit, N.W., Grace, J., Li, Q., and Olliaro, P., 2000. Pharmacokinetics of artemisinin-type compounds. Clin.Pharmacokinet. 39, 255-270.

Newton, P.N., Barnes, K.I., Smith, P.J., Evans, A.C., Chierakul, W., Ruangveerayuth, R., and White, N.J., 2006. The pharmacokinetics of intravenous artesunate in adults with severe falciparum malaria. Eur.J.Clin.Pharmacol. 62, 1003-1009.

NITD, 2014. http://www.nibr.com/research/developing_world/NITD/.

Noedl, H., Se, Y., Schaecher, K., Smith, B.L., Socheat, D., and Fukuda, M.M., 2008. Evidence of artemisinin-resistant malaria in western Cambodia. N.Engl.J.Med. 359, 2619-2620.

Nuermberger, E. and Grosset, J., 2004. Pharmacokinetic and pharmacodynamic issues in the treatment of mycobacterial infections. Eur.J.Clin.Microbiol.Infect.Dis. 23, 243-255.

Nuermberger, E., Rosenthal, I., Tyagi, S., Williams, K.N., Almeida, D., Peloquin, C.A., Bishai, W.R., and Grosset, J.H., 2006. Combination chemotherapy with the nitroimidazopyran PA-824 and first-line drugs in a murine model of tuberculosis. Antimicrob.Agents Chemother. 50, 2621-2625.

Nuermberger, E.L., Yoshimatsu, T., Tyagi, S., O'Brien, R.J., Vernon, A.N., Chaisson, R.E., Bishai, W.R., and Grosset, J.H., 2004. Moxifloxacin-containing regimen greatly reduces time to culture conversion in murine tuberculosis. Am.J.Respir.Crit Care Med. 169, 421-426.

Nwaka, S. and Ridley, R.G., 2003. Virtual drug discovery and development for neglected diseases through public-private partnerships. Nat.Rev.Drug Discov. 2, 919-928.

O'Shea, R. and Moser, H.E., 2008. Physicochemical properties of antibacterial compounds: implications for drug discovery. J.Med.Chem. 51, 2871-2878.

Obach, R.S., 1999. Prediction of human clearance of twenty-nine drugs from hepatic microsomal intrinsic clearance data: An examination of in vitro half-life approach and nonspecific binding to microsomes. Drug Metab Dispos. 27, 1350-1359.

Obach, R.S., Lombardo, F., and Waters, N.J., 2008. Trend analysis of a database of intravenous pharmacokinetic parameters in humans for 670 drug compounds. Drug Metab Dispos. 36, 1385-1405.

Olliaro, P.L. and Yuthavong, Y., 1999. An overview of chemotherapeutic targets for antimalarial drug discovery. Pharmacol.Ther. 81, 91-110.

Onajole, O.K., Pieroni, M., Tipparaju, S.K., Lun, S., Stec, J., Chen, G., Gunosewoyo, H., Guo, H., Ammerman, N.C., Bishai, W.R., and Kozikowski, A.P., 2013. Preliminary structure-activity relationships and biological evaluation of novel antitubercular indolecarboxamide derivatives against drug-

susceptible and drug-resistant Mycobacterium tuberculosis strains. J.Med.Chem. 56, 4093-4103.

Palmer, B.D., Thompson, A.M., Sutherland, H.S., Blaser, A., Kmentova, I., Franzblau, S.G., Wan, B., Wang, Y., Ma, Z., and Denny, W.A., 2010. Synthesis and structure-activity studies of biphenyl analogues of the tuberculosis drug (6S)-2-nitro-6-{[4-(trifluoromethoxy)benzyl]oxy}-6,7-dihydro-5H-imidazo[2,1-b][1, 3]oxazine (PA-824). J.Med.Chem. 53, 282-294.

Patel, K., Batty, K.T., Moore, B.R., Gibbons, P.L., Bulitta, J.B., and Kirkpatrick, C.M., 2013. Mechanism-based model of parasite growth and dihydroartemisinin pharmacodynamics in murine malaria. Antimicrob.Agents Chemother. 57, 508-516.

Peters, W., Howells, R.E., Portus, J., Robinson, B.L., Thomas, S., and Warhurst, D.C., 1977. The chemotherapy of rodent malaria, XXVII. Studies on mefloquine (WR 142,490). Ann.Trop.Med.Parasitol. 71, 407-418.

Peters, W., Robinson, B.L., and Ellis, D.S., 1987. The chemotherapy of rodent malaria. XLII. Halofantrine and halofantrine resistance. Ann.Trop.Med.Parasitol. 81, 639-646.

Pethe, K., Bifani, P., Jang, J., Kang, S., Park, S., Ahn, S., Jiricek, J., Jung, J., Jeon, H.K., Cechetto, J., Christophe, T., Lee, H., Kempf, M., Jackson, M., Lenaerts, A.J., Pham, H., Jones, V., Seo, M.J., Kim, Y.M., Seo, M., Seo, J.J., Park, D., Ko, Y., Choi, I., Kim, R., Kim, S.Y., Lim, S., Yim, S.A., Nam, J., Kang, H., Kwon, H., Oh, C.T., Cho, Y., Jang, Y., Kim, J., Chua, A., Tan, B.H., Nanjundappa, M.B., Rao, S.P., Barnes, W.S., Wintjens, R., Walker, J.R., Alonso, S., Lee, S., Kim, J., Oh, S., Oh, T., Nehrbass, U., Han, S.J., No, Z., Lee, J., Brodin, P., Cho, S.N., Nam, K., and Kim, J., 2013. Discovery of Q203, a potent clinical candidate for the treatment of tuberculosis. Nat.Med. 19, 1157-1160.

Pethe, K., Sequeira, P.C., Agarwalla, S., Rhee, K., Kuhen, K., Phong, W.Y., Patel, V., Beer, D., Walker, J.R., Duraiswamy, J., Jiricek, J., Keller, T.H., Chatterjee, A., Tan, M.P., Ujjini, M., Rao, S.P., Camacho, L., Bifani, P., Mak, P.A., Ma, I., Barnes, S.W., Chen, Z., Plouffe, D., Thayalan, P., Ng, S.H., Au, M., Lee, B.H., Tan, B.H., Ravindran, S., Nanjundappa, M., Lin, X., Goh, A., Lakshminarayana, S.B., Shoen, C., Cynamon, M., Kreiswirth, B., Dartois, V., Peters, E.C., Glynne, R., Brenner, S., and Dick, T., 2010. A chemical genetic screen in Mycobacterium tuberculosis identifies carbon-source-dependent growth inhibitors devoid of in vivo efficacy. Nat.Commun. 1, 57.

Posner, G.H., Paik, I.H., Sur, S., McRiner, A.J., Borstnik, K., Xie, S., and Shapiro, T.A., 2003. Orally active, antimalarial, anticancer, artemisinin-derived trioxane dimers with high stability and efficacy. J.Med.Chem. 46, 1060-1065.

Price, R.N., Hasugian, A.R., Ratcliff, A., Siswantoro, H., Purba, H.L., Kenangalem, E., Lindegardh, N., Penttinen, P., Laihad, F., Ebsworth, E.P., Anstey, N.M., and Tjitra, E., 2007. Clinical and pharmacological determinants

of the therapeutic response to dihydroartemisinin-piperaquine for drug-resistant malaria. Antimicrob.Agents Chemother. 51, 4090-4097.

Prideaux, B., Dartois, V., Staab, D., Weiner, D.M., Goh, A., Via, L.E., Barry, C.E., III, and Stoeckli, M., 2011. High-sensitivity MALDI-MRM-MS imaging of moxifloxacin distribution in tuberculosis-infected rabbit lungs and granulomatous lesions. Anal.Chem. 83, 2112-2118.

Proost, J.H., Roggeveld, J., Wierda, J.M., and Meijer, D.K., 1997. Relationship between chemical structure and physicochemical properties of series of bulky organic cations and their hepatic uptake and biliary excretion rates. J.Pharmacol.Exp.Ther. 282, 715-726.

Rao, S.P., Lakshminarayana, S.B., Kondreddi, R.R., Herve, M., Camacho, L.R., Bifani, P., Kalapala, S.K., Jiricek, J., Ma, N.L., Tan, B.H., Ng, S.H., Nanjundappa, M., Ravindran, S., Seah, P.G., Thayalan, P., Lim, S.H., Lee, B.H., Goh, A., Barnes, W.S., Chen, Z., Gagaring, K., Chatterjee, A.K., Pethe, K., Kuhen, K., Walker, J., Feng, G., Babu, S., Zhang, L., Blasco, F., Beer, D., Weaver, M., Dartois, V., Glynne, R., Dick, T., Smith, P.W., Diagana, T.T., and Manjunatha, U.H., 2013. Indolcarboxamide is a preclinical candidate for treating multidrug-resistant tuberculosis. Sci.Transl.Med. 5, 214ra168.

Rawlins, M.D., 2004. Cutting the cost of drug development? Nat.Rev.Drug Discov. 3, 360-364.

Remuinan, M.J., Perez-Herran, E., Rullas, J., Alemparte, C., Martinez-Hoyos, M., Dow, D.J., Afari, J., Mehta, N., Esquivias, J., Jimenez, E., Ortega-Muro, F., Fraile-Gabaldon, M.T., Spivey, V.L., Loman, N.J., Pallen, M.J., Constantinidou, C., Minick, D.J., Cacho, M., Rebollo-Lopez, M.J., Gonzalez, C., Sousa, V., Angulo-Barturen, I., Mendoza-Losana, A., Barros, D., Besra, G.S., Ballell, L., and Cammack, N., 2013. Tetrahydropyrazolo[1,5-a]pyrimidine-3-carboxamide and N-benzyl-6',7'-dihydrospiro[piperidine-4,4'-thieno[3,2-c]pyran] analogues with bactericidal efficacy against Mycobacterium tuberculosis targeting MmpL3. PLoS.One. 8, e60933.

Rhoades, E.R., Frank, A.A., and Orme, I.M., 1997. Progression of chronic pulmonary tuberculosis in mice aerogenically infected with virulent Mycobacterium tuberculosis. Tuber.Lung Dis. 78, 57-66.

Rosenthal, I.M., Tasneen, R., Peloquin, C.A., Zhang, M., Almeida, D., Mdluli, K.E., Karakousis, P.C., Grosset, J.H., and Nuermberger, E.L., 2012. Dose-ranging comparison of rifampin and rifapentine in two pathologically distinct murine models of tuberculosis. Antimicrob.Agents Chemother. 56, 4331-4340.

Rottmann, M., McNamara, C., Yeung, B.K., Lee, M.C., Zou, B., Russell, B., Seitz, P., Plouffe, D.M., Dharia, N.V., Tan, J., Cohen, S.B., Spencer, K.R., Gonzalez-Paez, G.E., Lakshminarayana, S.B., Goh, A., Suwanarusk, R., Jegla, T., Schmitt, E.K., Beck, H.P., Brun, R., Nosten, F., Renia, L., Dartois, V., Keller, T.H., Fidock, D.A., Winzeler, E.A., and Diagana, T.T., 2010. Spiroindolones, a potent compound class for the treatment of malaria. Science 329, 1175-1180.

Rouan, M.C., Lounis, N., Gevers, T., Dillen, L., Gilissen, R., Raoof, A., and Andries, K., 2012. Pharmacokinetics and pharmacodynamics of TMC207 and its N-desmethyl metabolite in a murine model of tuberculosis. Antimicrob.Agents Chemother. 56, 1444-1451.

Scaglione, F., Mouton, J.W., Mattina, R., and Fraschini, F., 2003. Pharmacodynamics of levofloxacin and ciprofloxacin in a murine pneumonia model: peak concentration/MIC versus area under the curve/MIC ratios. Antimicrob.Agents Chemother. 47, 2749-2755.

Scaglione, F. and Paraboni, L., 2006. Influence of pharmacokinetics/pharmacodynamics of antibacterials in their dosing regimen selection. Expert.Rev.Anti.Infect.Ther. 4, 479-490.

Schuck, E.L. and Derendorf, H., 2005. Pharmacokinetic/pharmacodynamic evaluation of anti-infective agents. Expert.Rev.Anti.Infect.Ther. 3, 361-373.

Shandil, R.K., Jayaram, R., Kaur, P., Gaonkar, S., Suresh, B.L., Mahesh, B.N., Jayashree, R., Nandi, V., Bharath, S., and Balasubramanian, V., 2007. Moxifloxacin, ofloxacin, sparfloxacin, and ciprofloxacin against Mycobacterium tuberculosis: evaluation of in vitro and pharmacodynamic indices that best predict in vivo efficacy. Antimicrob.Agents Chemother. 51, 576-582.

Siefert, H.M., Domdey-Bette, A., Henninger, K., Hucke, F., Kohlsdorfer, C., and Stass, H.H., 1999a. Pharmacokinetics of the 8-methoxyquinolone, moxifloxacin: a comparison in humans and other mammalian species. J.Antimicrob.Chemother. 43 Suppl B, 69-76.

Siefert, H.M., Kohlsdorfer, C., Steinke, W., and Witt, A., 1999b. Pharmacokinetics of the 8-methoxyquinolone, moxifloxacin: tissue distribution in male rats. J.Antimicrob.Chemother. 43 Suppl B, 61-67.

Silber, H.E., Burgener, C., Letellier, I.M., Peyrou, M., Jung, M., King, J.N., Gruet, P., and Giraudel, J.M., 2010. Population pharmacokinetic analysis of blood and joint synovial fluid concentrations of robenacoxib from healthy dogs and dogs with osteoarthritis. Pharm.Res. 27, 2633-2645.

Singh, R., Manjunatha, U., Boshoff, H.I., Ha, Y.H., Niyomrattanakit, P., Ledwidge, R., Dowd, C.S., Lee, I.Y., Kim, P., Zhang, L., Kang, S., Keller, T.H., Jiricek, J., and Barry, C.E., III, 2008. PA-824 kills nonreplicating Mycobacterium tuberculosis by intracellular NO release. Science 322, 1392-1395.

Sinou, V., Taudon, N., Mosnier, J., Aglioni, C., Bressolle, F.M., and Parzy, D., 2008. Pharmacokinetics of artesunate in the domestic pig. J.Antimicrob.Chemother. 62, 566-574.

Slatter, J.G., Adams, L.A., Bush, E.C., Chiba, K., Daley-Yates, P.T., Feenstra, K.L., Koike, S., Ozawa, N., Peng, G.W., Sams, J.P., Schuette, M.R., and Yamazaki, S., 2002. Pharmacokinetics, toxicokinetics, distribution,

metabolism and excretion of linezolid in mouse, rat and dog. Xenobiotica 32, 907-924.

Smith, B.P., Vandenhende, F.R., DeSante, K.A., Farid, N.A., Welch, P.A., Callaghan, J.T., and Forgue, S.T., 2000. Confidence interval criteria for assessment of dose proportionality. Pharm.Res. 17, 1278-1283.

Smith, D.A., Di, L., and Kerns, E.H., 2010. The effect of plasma protein binding on in vivo efficacy: misconceptions in drug discovery. Nat.Rev.Drug Discov. 9, 929-939.

Smith, D.A., Jones, B.C., and Walker, D.K., 1996. Design of drugs involving the concepts and theories of drug metabolism and pharmacokinetics. Med.Res.Rev. 16, 243-266.

Smith, P.W., Diagana, T.T., and Yeung, B.K., 2014. Progressing the global antimalarial portfolio: finding drugs which target multiple Plasmodium life stages. Parasitology 141, 66-76.

Soman, A., Honeybourne, D., Andrews, J., Jevons, G., and Wise, R., 1999. Concentrations of moxifloxacin in serum and pulmonary compartments following a single 400 mg oral dose in patients undergoing fibre-optic bronchoscopy. J.Antimicrob.Chemother. 44, 835-838.

Spillman, N.J., Allen, R.J., McNamara, C.W., Yeung, B.K., Winzeler, E.A., Diagana, T.T., and Kirk, K., 2013. Na(+) regulation in the malaria parasite Plasmodium falciparum involves the cation ATPase PfATP4 and is a target of the spiroindolone antimalarials. Cell Host.Microbe 13, 227-237.

Steingart, K.R., Jotblad, S., Robsky, K., Deck, D., Hopewell, P.C., Huang, D., and Nahid, P., 2011. Higher-dose rifampin for the treatment of pulmonary tuberculosis: a systematic review. Int.J.Tuberc.Lung Dis. 15, 305-316.

Stella, V.J. and Rajewski, R.A., 1997. Cyclodextrins: their future in drug formulation and delivery. Pharm.Res. 14, 556-567.

Stover, C.K., Warrener, P., VanDevanter, D.R., Sherman, D.R., Arain, T.M., Langhorne, M.H., Anderson, S.W., Towell, J.A., Yuan, Y., McMurray, D.N., Kreiswirth, B.N., Barry, C.E., and Baker, W.R., 2000. A small-molecule nitroimidazopyran drug candidate for the treatment of tuberculosis. Nature 405, 962-966.

Svensson, U.S., Alin, H., Karlsson, M.O., Bergqvist, Y., and Ashton, M., 2002. Population pharmacokinetic and pharmacodynamic modelling of artemisinin and mefloquine enantiomers in patients with falciparum malaria. Eur.J.Clin.Pharmacol. 58, 339-351.

Talisuna, A.O., Bloland, P., and D'Alessandro, U., 2004. History, dynamics, and public health importance of malaria parasite resistance. Clin.Microbiol.Rev. 17, 235-254.

TB Alliance, 2014. http://www.tballiance.org/pipeline/pipeline.php.

Theuretzbacher, U., 2007. Tissue penetration of antibacterial agents: how should this be incorporated into pharmacodynamic analyses? Curr.Opin.Pharmacol. 7, 498-504.

Thompson, A.M., Sutherland, H.S., Palmer, B.D., Kmentova, I., Blaser, A., Franzblau, S.G., Wan, B., Wang, Y., Ma, Z., and Denny, W.A., 2011. Synthesis and structure-activity relationships of varied ether linker analogues of the antitubercular drug (6S)-2-nitro-6-{[4-(trifluoromethoxy)benzyl]oxy}-6,7-dihydro-5h-imidazo[2,1-b][1, 3]oxazine (PA-824). J.Med.Chem. 54, 6563-6585.

Trager, W. and Jensen, J.B., 1976. Human malaria parasites in continuous culture. Science 193, 673-675.

Tsuji, A., Tamai, I., Hirooka, H., and Terasaki, T., 1987. Beta-lactam antibiotics and transport via the dipeptide carrier system across the intestinal brush-border membrane. Biochem.Pharmacol. 36, 565-567.

Tyagi, S., Nuermberger, E., Yoshimatsu, T., Williams, K., Rosenthal, I., Lounis, N., Bishai, W., and Grosset, J., 2005. Bactericidal activity of the nitroimidazopyran PA-824 in a murine model of tuberculosis. Antimicrob.Agents Chemother. 49, 2289-2293.

Udwadia, Z.F., Amale, R.A., Ajbani, K.K., and Rodrigues, C., 2012. Totally drug-resistant tuberculosis in India. Clin.Infect.Dis. 54, 579-581.

Vaddady, P.K., Lee, R.E., and Meibohm, B., 2010. In vitro pharmacokinetic/pharmacodynamic models in anti-infective drug development: focus on TB. Future.Med.Chem. 2, 1355-1369.

van de Waterbeemd, H., Smith, D.A., and Jones, B.C., 2001. Lipophilicity in PK design: methyl, ethyl, futile. J.Comput.Aided Mol.Des 15, 273-286.

van De, W.H., Smith, D.A., Beaumont, K., and Walker, D.K., 2001. Property-based design: optimization of drug absorption and pharmacokinetics. J.Med.Chem. 44, 1313-1333.

van, I.J., Aarnoutse, R.E., Donald, P.R., Diacon, A.H., Dawson, R., Plemper van, B.G., Gillespie, S.H., and Boeree, M.J., 2011. Why Do We Use 600 mg of Rifampicin in Tuberculosis Treatment? Clin.Infect.Dis. 52, e194-e199.

Veber, B., Vallee, E., Desmonts, J.M., Pocidalo, J.J., and Azoulay-Dupuis, E., 1993. Correlation between macrolide lung pharmacokinetics and therapeutic efficacy in a mouse model of pneumococcal pneumonia. J.Antimicrob.Chemother. 32, 473-482.

Veber, D.F., Johnson, S.R., Cheng, H.Y., Smith, B.R., Ward, K.W., and Kopple, K.D., 2002. Molecular properties that influence the oral bioavailability of drug candidates. J.Med.Chem. 45, 2615-2623.

Vennerstrom, J.L., Dong, Y., Andersen, S.L., Ager, A.L., Jr., Fu, H., Miller, R.E., Wesche, D.L., Kyle, D.E., Gerena, L., Walters, S.M., Wood, J.K.,

Edwards, G., Holme, A.D., McLean, W.G., and Milhous, W.K., 2000. Synthesis and antimalarial activity of sixteen dispiro-1,2,4, 5-tetraoxanes: alkyl-substituted 7,8,15,16-tetraoxadispiro[5.2.5. 2]hexadecanes. J.Med.Chem. 43, 2753-2758.

Via, L.E., Lin, P.L., Ray, S.M., Carrillo, J., Allen, S.S., Eum, S.Y., Taylor, K., Klein, E., Manjunatha, U., Gonzales, J., Lee, E.G., Park, S.K., Raleigh, J.A., Cho, S.N., McMurray, D.N., Flynn, J.L., and Barry, C.E., III, 2008. Tuberculous granulomas are hypoxic in guinea pigs, rabbits, and nonhuman primates. Infect.Immun. 76, 2333-2340.

Wallis, R.S., Jakubiec, W.M., Kumar, V., Silvia, A.M., Paige, D., Dimitrova, D., Li, X., Ladutko, L., Campbell, S., Friedland, G., Mitton-Fry, M., and Miller, P.F., 2010. Pharmacokinetics and whole-blood bactericidal activity against Mycobacterium tuberculosis of single doses of PNU-100480 in healthy volunteers. J.Infect.Dis. 202, 745-751.

Warner, D.F. and Mizrahi, V., 2014. Shortening treatment for tuberculosis--to basics. N.Engl.J.Med. 371, 1642-1643.

Warrell, D.A., Watkins, W.M., and Winstanley, P.A., 1993. Treatment and prevention of malaria. pp. 268-312.

Wayne, L.G. and Hayes, L.G., 1996. An in vitro model for sequential study of shiftdown of Mycobacterium tuberculosis through two stages of nonreplicating persistence. Infect.Immun. 64, 2062-2069.

Weiss, H.M. and Gatlik, E., 2014. Equilibrium gel filtration to measure plasma protein binding of very highly bound drugs. J.Pharm.Sci. 103, 752-759.

Wells, T.N., Alonso, P.L., and Gutteridge, W.E., 2009. New medicines to improve control and contribute to the eradication of malaria. Nat.Rev.Drug Discov. 8, 879-891.

White, N.J., 1997. Assessment of the pharmacodynamic properties of antimalarial drugs in vivo. Antimicrob.Agents Chemother. 41, 1413-1422.

White, N.J., 2002. The assessment of antimalarial drug efficacy. Trends Parasitol. 18, 458-464.

White, N.J., 2004. Antimalarial drug resistance. J.Clin.Invest 113, 1084-1092.

White, N.J., 2013. Pharmacokinetic and pharmacodynamic considerations in antimalarial dose optimization. Antimicrob.Agents Chemother.

White, N.J., Pongtavornpinyo, W., Maude, R.J., Saralamba, S., Aguas, R., Stepniewska, K., Lee, S.J., Dondorp, A.M., White, L.J., and Day, N.P., 2009. Hyperparasitaemia and low dosing are an important source of anti-malarial drug resistance. Malar.J. 8, 253.

White, N.J., Pukrittayakamee, S., Phyo, A.P., Rueangweerayut, R., Nosten, F., Jittamala, P., Jeeyapant, A., Jain, J.P., Lefevre, G., Li, R., Magnusson, B.,

Diagana, T.T., and Leong, F.J., 2014. Spiroindolone KAE609 for falciparum and vivax malaria. N.Engl.J.Med. 371, 403-410.

White, N.J., Stepniewska, K., Barnes, K., Price, R.N., and Simpson, J., 2008. Simplified antimalarial therapeutic monitoring: using the day-7 drug level? Trends Parasitol. 24, 159-163.

WHO, 2012a. Global Tuberculosis Report. World Health Organization, Geneva, Switzerland. *www.who.int/iris/bitstream/10665/75938/1/9789241564502_eng.pdf*.

WHO, 2012b. Multidrug and extensively drug-resistant TB (M/XDR-TB): 2010 global report on surveillance and response. World Health Organization, Geneva, Switzerland. Report no.: WHO/HTM/TB/2010.3.

WHO, 2012c. World Malaria Report (2012). World Health Organization, Geneva, Switzerland. (http://www.who.int/malaria/publications/world_malaria_report_2012/en/).

WHO, 2013. http://www.who.int/tb/features_archive/gtb_report_2013/en/.

WHO, 2014a. http://www.who.int/topics/infectious_diseases/en/.

WHO, 2014b. http://www.who.int/topics/malaria/en/.

Wohnsland, F. and Faller, B., 2001. High-throughput permeability pH profile and high-throughput alkane/water log P with artificial membranes. J.Med.Chem. 44, 923-930.

Wongsrichanalai, C., Pickard, A.L., Wernsdorfer, W.H., and Meshnick, S.R., 2002. Epidemiology of drug-resistant malaria. Lancet Infect.Dis. 2, 209-218.

Wright, D.H., Brown, G.H., Peterson, M.L., and Rotschafer, J.C., 2000. Application of fluoroquinolone pharmacodynamics. J.Antimicrob.Chemother. 46, 669-683.

Yeung, B.K., Zou, B., Rottmann, M., Lakshminarayana, S.B., Ang, S.H., Leong, S.Y., Tan, J., Wong, J., Keller-Maerki, S., Fischli, C., Goh, A., Schmitt, E.K., Krastel, P., Francotte, E., Kuhen, K., Plouffe, D., Henson, K., Wagner, T., Winzeler, E.A., Petersen, F., Brun, R., Dartois, V., Diagana, T.T., and Keller, T.H., 2010. Spirotetrahydro beta-carbolines (spiroindolones): a new class of potent and orally efficacious compounds for the treatment of malaria. J.Med.Chem. 53, 5155-5164.

Yokokawa, F., Wang, G., Chan, W.L., Ang, S.H., Wong, J., Ma, I., Rao, S.P., Manjunatha, U., Lakshminarayana, S.B., Herve, M., Kounde, C., Tan, B.H., Thayalan, P., Ng, S.H., Nanjundappa, M., Ravindran, S., Gee, P., Tan, M., Wei, L., Goh, A., Chen, P.Y., Lee, K.S., Zhong, C., Wagner, T., Dix, I., Chatterjee, A.K., Pethe, K., Kuhen, K., Glynne, R., Smith, P., Bifani, P., and Jiricek, J., 2013. Discovery of tetrahydropyrazolopyrimidine carboxamide derivatives as potent and orally active antitubercular agents. ACS Med.Chem.Lett. 4, 451-455.

Yu, S., Li, S., Yang, H., Lee, F., Wu, J.T., and Qian, M.G., 2005. A novel liquid chromatography/tandem mass spectrometry based depletion method for measuring red blood cell partitioning of pharmaceutical compounds in drug discovery. Rapid Commun.Mass Spectrom. 19, 250-254.

Yuthavong, Y., Tarnchompoo, B., Vilaivan, T., Chitnumsub, P., Kamchonwongpaisan, S., Charman, S.A., McLennan, D.N., White, K.L., Vivas, L., Bongard, E., Thongphanchang, C., Taweechai, S., Vanichtanankul, J., Rattanajak, R., Arwon, U., Fantauzzi, P., Yuvaniyama, J., Charman, W.N., and Matthews, D., 2012. Malarial dihydrofolate reductase as a paradigm for drug development against a resistance-compromised target. Proc.Natl.Acad.Sci.U.S.A 109, 16823-16828.

Zeitlinger, M.A., Derendorf, H., Mouton, J.W., Cars, O., Craig, W.A., Andes, D., and Theuretzbacher, U., 2011. Protein binding: do we ever learn? Antimicrob.Agents Chemother. 55, 3067-3074.

Zhou, L., Yang, L., Tilton, S., and Wang, J., 2007. Development of a high throughput equilibrium solubility assay using miniaturized shake-flask method in early drug discovery. J.Pharm.Sci. 96, 3052-3071.

Ziglam, H.M., Baldwin, D.R., Daniels, I., Andrew, J.M., and Finch, R.G., 2002. Rifampicin concentrations in bronchial mucosa, epithelial lining fluid, alveolar macrophages and serum following a single 600 mg oral dose in patients undergoing fibre-optic bronchoscopy. J.Antimicrob.Chemother. 50, 1011-1015.

APPENDIX

Appendix 1. Determination of *in vitro* anti-TB activity

Mtb H37Rv (ATCC #27294) was maintained in Middlebrook 7H9 broth supplemented with 0.05% Tween 80 and 10% ADS (5% Albumin, 2% Dextrose and 0.81% Sodium chloride) supplement. The compounds dissolved in 90% DMSO were two-fold serially diluted in duplicates and spotted by mosquito HTS liquid handler (TTP LabTech, Hertfordshire, UK) to 384-well clear plates, resulting in 10 dilutions of each compound. A volume of 50 µL of Mtb culture (final OD_{600} of 0.02) was added to each well, and the plates were incubated at 37 °C for 5 days. OD_{600} values were recorded using a Spectramax M2 spectrophotometer, and MIC_{50} curves were plotted using Graph Pad Prism 5 software.

Appendix 2. Optimized LC-MS/MS conditions for standard anti-TB compounds

Sl. No.	Drugs	Actual mass (amu)	Optimized mass (amu)	Parent Daughter Transition	Cone voltage (V)	Collision energy (eV)	Ionization mode	λ_{max} wavelength (nm)
1	Isoniazid	137.059	137.08	138.08 > 121.34	25	15	ESP+	256
2	Rifampicin	822.405	822.52	823.52 > 791.25	25	15	ESP+	313
3	Pyrazinamide	123.043	122.99	123.99 > 80.94	25	15	ESP+	259
4	Ethambutol	204.184	204.43	205.43 > 116.32	25	15	ESP+	300
5	Streptomcin	581.26	581.69	582.69 > 263.75	50	35	ESP+	309
6	Kanamycin	484.238	484.69	485.69 > 162.45	30	25	ESP+	305
7	Amikacin	585.286	585.75	586.75 > 163.35	30	35	ESP+	330
8	PAS	153.043	153.09	152.09 > 107.26	25	15	ESP-	265
9	Cycloserine	102.043	101.9	102.90 > 74.91	15	5	ESP+	308
10	Ethionamide	166.056	166.18	167.18 > 107.26	35	25	ESP+	267
11	Rifabutin	846.442	846.61	847.61 > 815.33	40	25	ESP+	264
12	Rifapentine	876.452	876.61	877.61 > 845.32	30	25	ESP+	310
13	Moxifloxacin	401.175	401.56	402.56 > 110.24	40	25	ESP+	233
14	Levofloxacin	361.144	361.56	362.56 > 261.57	30	25	ESP+	267
15	Gatifloxacin	375.159	375.56	376.56 > 261.61	35	25	ESP+	249
17	Ofloxacin	361.144	361.56	362.56 > 261.61	35	25	ESP+	308
18	Sparfloxacin	392.166	392.62	393.62 > 292.63	30	25	ESP+	279
19	Capreomycin	654.331	652.33	653.33 > 491.08	40	35	ESP+	269
20	Thioacetazone	236.073	236.37	237.37 > 120.29	25	25	ESP+	268
21	Linezolid	337.144	337.5	338.50 > 296.69	35	15	ESP+	243
22	Prothionamide	180.072	180.26	181.26 > 121.33	35	25	ESP+	231
23	Clarithromycin	747.477	747.77	748.77 >	20	25	ESP+	210

				158.05				
24	Amoxicillin	365.105	365.02	366.02 > 113.87	20	15	ESP+	226
25	Clavulanate	237.004	196.13	197.13 > 149.01	30	25	ESP+	266
26	Meropenem	383.151	330.06	331.06 > 220.14	25	15	ESP+	272
27	Clofazimine	472.122	472.62	473.62 > 431.58	50	35	ESP+	268
28	Metronidazole	171.064	171.24	172.24 > 82.28	25	25	ESP+	301
29	Thioridazine	370.154	370.62	371.62 > 126.43	35	25	ESP+	258
30	Mefloquine	378.117	378.62	379.62 > 82.35	45	45	ESP+	269
31	Vancomycin	1447.43	724.33	725.33 > 143.92	25	15	ESP+	269
34	PA-824	359.073	359.43	360.43 > 175.42	35	25	ESP+	311
35	TMC-207	554.157	556.62	557.62 > 58.01	30	45	ESP+	300

Appendix 3. MRM transitions for bicyclic 4-nitroimidazole analogs

Sl. No.	Compound ID	Molecular weight	Parent Daughter Transition
1	PA-824	359.26	360.2 > 175.1
2	NI-622	471.4	472.3 > 245.1
3	NI-644	459.36	457.2 > 230.2
4	Amino-824	358.28	359.2 > 175.1
5	AminoEthyl-824	372.31	373.3 > 244.2
6	NI-135	392.05	393 > 209.1
7	NI-147	374.08	375 > 191
8	NI-136	376.08	377 > 193.1
9	NI-176	404.11	405.1 > 193.2
10	NI-269	386.12	387.1 > 175.1
11	NI-182	386.12	387.1 > 175.1
12	NI-145	387.1	388.4 > 175.1
13	NI-297	462.42	463.5 > 251.1
14	NI-302	386.12	386.3 > 227.3

Appendix 4. Determination of *in vitro* antimalarial activity

Isolates of *P. falciparum* were maintained using standard methods (Trager and Jensen, 1976) in an atmosphere of 93% N_2, 4% CO_2, 3% O_2 at 37 °C in complete medium (CM) (10.44 g/liter RPMI 1640, 5.94 g/liter Hepes, 5 g/liter Albumax II, 50 mg/liter hypoxanthine, 2.1 g/liter sodium bicarbonate and 100 mg/liter neomycin). Human erythrocytes served as host cells. *In vitro* antimalarial activity was measured using the [^{3}H]-hypoxanthine incorporation assay (Desjardins et al., 1979) with strain NF54 of *P. falciparum* (obtained from Hoffmann-LaRoche Ltd). The compounds were dissolved in dimethyl sulfoxide (DMSO) at a concentration of 10 mM, diluted in hypoxanthine-free culture medium and titrated in duplicates over a 64 fold range in 96-well plates. Infected erythrocytes (0.3% final parasitemia and 1.25% final hematocrit) were added to the wells. After 16 h incubation, 0.25 μCi of [^{3}H]-hypoxanthine was added per well, and plates were incubated for an additional 8 h (in contrast to the conventional 48-h plus 24-h assay) to enable direct comparison with the *in vitro* (*ex vivo) P. berghei* assay (see below). The parasites were harvested onto glass fiber filters, and radioactivity was counted using a Betaplate liquid scintillation counter (Wallac, Zurich, Switzerland).

For *in vitro* (*ex vivo) P. berghei* maturation assays (Brunner et al., 2012), heparinized blood from infected mice (*P. berghei* GFP ANKA malaria strain $PbGFP_{CON}$, a donation from A. P. Waters and C. J. Janse, Leiden University, Leiden, the Netherlands) (Franke-Fayard et al. 2004) was washed with 9 mL of hypoxanthine-free culture medium and diluted with hypoxanthine-free culture medium and red blood cells (RBCs) from uninfected mice to a hematocrit of 5% and a parasitemia of 0.3%. Serial

compound dilutions were prepared in DMSO and distributed as described above. The infected erythrocytes (0.3% final parasitemia and 2.5% final hematocrit) were added into the wells. After the plates were incubated for 16 h, 0.25 μCi of [^{3}H]-hypoxanthine was added per well, and plates were incubated for an additional 8 h. The parasites were harvested, and the *in vitro (ex vivo) P. berghei* $IC_{50,}$ $IC_{90,}$ and IC_{99} values were determined as described above.

Appendix 5. NONMEM code for dose-response relationship

$PROB Dose-response spiroindolones, all single dose [mg/kg]

```
; PRBC = parasitized RBCs [%] (P.RBC.100)
; DOSE = Dose [mg/kg]  (DOSE)
; CMPD = compound  (CPD)
; ID   = individual study (STDY)
; UID  = unique identifier, compound and study (CMPD.STDY)
; LOGD = IDV Log10 Dose (mg/kg) (LOG DOSE)
; DV   = LOG10 parasitemia (log% parasitemia)
; Equation from graphpad prism help (dose finding)
; Y=Bottom + (Top-Bottom)/(1+10^((X-LogIC50)*HillSlope))

$DATA  Spiroindolones.NMRI.Mice.Dose.Response.csv IGNORE=@
$PRED
  TVTP = THETA(1)
  BASE = TVTP*EXP(ETA(1))

  TVBT = THETA(2)
  MIN = TVBT*EXP(ETA(2))

  TVI9 = THETA(3)
  ID90 = TVI9*EXP(ETA(3))

  TVHS = THETA(4)
  SLP = TVHS*EXP(ETA(4))

TRF90 = (1/0.90-1)**(1/SLP)
TRF95 = (1/0.95-1)**(1/SLP)
TRF99 = (1/0.99-1)**(1/SLP)

ID50=TRF90*ID90
ID95=ID50/TRF95
ID99=ID50/TRF99
IPRED =MIN + (BASE-MIN)/((1+10**((LOGD-
LOG10(ID50))*SLP)))**TRT
; TRT yields exact baseline estimation (0, 1 switch)

Y = IPRED + EPS(1)

  IRES  = DV-IPRED
  IWRES = IRES   ; for xpose

$THETA
(0, 1.5)   ; BASE
(-2,-1,0)   ; MIN
(0,40)   ; ID90
(0.5,5,10) ; SLP
```

$OMEGA
0.1 ; BASE
0 FIX ; MIN
0 FIX ; ID90
0.1 ; SLP

$SIGMA 0.1

$EST MAX=9990 SIG=3 PRINT=5 METHOD=1 INTER LAPLACE NOABORT

$COV

1NONLINEAR MIXED EFFECTS MODEL PROGRAM (NONMEM) DOUBLE PRECISION NONMEM VERSION VI LEVEL 2.0
DEVELOPED AND PROGRAMMED BY STUART BEAL AND LEWIS SHEINER

MINIMUM VALUE OF OBJECTIVE FUNCTION: -101.131

Appendix 6. NONMEM code for PK modeling

```
$PROB 2-cmt model - KAE609_Mouse_PPK.nmctl

; COMPOUND 1: KAE609
; TRT=0 healthy, TRT=1 Malaria

$SUBROUTINES ADVAN6 TRANS1 TOL=5
$MODEL NCOMPARTMENTS=3
COMP=(DEPOT)
COMP=(CENTRAL)
COMP=(PERI1)

$PK
TVVM = THETA(1)*EXP(ETA(1))
TVKM = THETA(2)*EXP(ETA(2))
TVVC = THETA(3)*EXP(ETA(3))
TVVP = THETA(4)*EXP(ETA(4))
TVQ  = THETA(5)*EXP(ETA(5))
TVKA = THETA(6)*EXP(ETA(6))

VMAX=TVVM
KM = TVKM
VC = TVVC
VP = TVVP
Q =  TVQ
KA = TVKA

S2 = VC/1000

$DES
CP = A(2)/S2
CL = VMAX/(KM+CP)
K10 = CL/VC
K12 = Q/VC
K21 = Q/VP

DADT(1) = -KA*A(1)
DADT(2) = KA*A(1)-K10*A(2)-K12*A(2)+K21*A(3)
DADT(3) = K12*A(2)-K21*A(3)

;###################################################
; Karlsson parameterization (THETAs for $ERROR)
;###################################################
$ERROR
IPRED=F         ;  individual-specific prediction
IRES=DV-IPRED    ;  individual-specific residual
DEL=0
IF (IPRED.EQ.0) DEL=1
IWRES=IRES/(IPRED+DEL) ; for XPOSE (expected input)
```

```
Y = IPRED*(1+EPS(1))+EPS(2)

;#####################################################
$SIGMA 0.1 10 ;(1 is BLOQ)
;#####################################################
; starting values for NPD fits
; TH8: RACE on F1
$THETA (0,200) (0,1000) (0,2) (0,2) (0,1) (0,0.6)
$OMEGA 0 FIX 0 FIX 0 FIX 0 FIX 0 FIX 0 FIX

$EST METHOD=1 INTER MAXEVAL=9990 NOABORT PRINT=5
LAPLACE MSFO=program.nmmsf
$COV

1NONLINEAR MIXED EFFECTS MODEL PROGRAM (NONMEM)
DOUBLE PRECISION NONMEM    VERSION VI LEVEL 2.0
 DEVELOPED AND PROGRAMMED BY STUART BEAL AND LEWIS
SHEINER

MINIMUM VALUE OF OBJECTIVE FUNCTION   : 489.256
```